



## Special Feature

## Noble metal nanoparticles for water purification: A critical review

T. Pradeep\*, Anshup

Department of Chemistry and Sophisticated Analytical Instrument Facility, Indian Institute of Technology Madras, Chennai 600 036, India

## ARTICLE INFO

Available online 1 April 2009

## Keywords:

Water purification  
Nanotechnology  
Noble metals  
Nanoparticles  
Pesticides  
Heavy metal ions  
Micro-organisms  
Drinking water

## ABSTRACT

Water is one of the essential enablers of life on earth. Beginning with the origin of the earliest form of life in seawater, it has been central to the evolution of human civilizations. Noble metals have been similarly associated with the prosperity of human civilizations through their prominent use in jewellery and medical applications. The most important reason for the use of noble metals is the minimal reactivity at the bulk scale, which can be explained by a number of concepts such as electrochemical potential, relativistic contraction, molecular orbital theory, etc. Recently, water quality has been associated with the development index of society. A number of chemical and biological contaminants have endangered the quality of drinking water. An overview of important events during last 200 years in the area of drinking water purification is presented. Realizing the molecular nature of contamination in drinking water, significant progress has been made to utilize the chemistry of nanomaterials for water purification. This article summarizes recent efforts in the area of noble metal nanoparticle synthesis and the origin of their reactivity at the nanoscale. The application of noble metal nanoparticle based chemistry for drinking water purification is summarized for three major types of contaminants: halogenated organics including pesticides, heavy metals and microorganisms. Recent efforts for the removal, as well as ultralow concentration detection of such species, using noble metal nanoparticles are summarized. Important challenges during the commercialization of nano-based products are highlighted through a case study of pesticide removal using noble metal nanoparticles. Recent efforts in drinking water purification using other forms of nanomaterials are also summarized. The article concludes with recent investigations on the issue of nanotoxicity and its implications for the future.

© 2009 Elsevier B.V. All rights reserved.

Take up one idea. Make that one idea your life – think of it, dream of it, live on that idea. Let the brain, muscles, nerves, every part of your body, be full of that idea, and just leave every other idea alone. This is the way to success, that is the way great spiritual giants are produced.

- Swami Vivekananda, World's most-respected Vedanta thinker, 1863–1902

Vedanta Philosophy: Lectures by Swami Vivekananda, Kessinger Publishing, USA, 1996, Page 70.

## 1. Introduction

The theme of this review is water, one of the essential companions of life on earth. During the phases of creation, evolution and continuity of life on earth, water remained as its most vital component. The molecular as well as macromolecular functions of making life possible are carried out using water. The earliest form of life appeared in sea

water about 3.5 billion years ago and was transferred to land only 380 million years ago. Despite this transfer to land, an ocean, in terms of fluidic composition, continues to exist within us. Similarly, keeping a very high proportion of living organisms' body weight as water (~70%), Nature has iterated the vitality of water for life. It is very appropriate to say that existence of life on Earth is largely owed to the presence of water. It is vital to us, both as a universal solvent as well as being an important component of metabolic processes within the body. Clean and fresh water is essential for the existence of life. The evolution of civilization has always revolved around water. The Nile was the lifeline of the Egyptian civilization. The Indus Valley civilization flourished on the banks of the Indus river. There is no aspect of our life that is not touched by water. Water is one of the clear signs of prosperity, health, serenity, beauty, artistry, purity and many other attributes. Leonardo Da Vinci had described water as "*the vehicle of nature*" ("*vetturale di natura*").

For time immemorial, Nature has made noble metals part of our daily life. In being a part of numerous applications such as jewellery, currencies, photographic films and electrical conductors; noble metals have made a mark for themselves as being our own household materials. This is a very important milestone for our societal progress – the reason being we spent sufficient time in making sure that what is being used by us, should be friendly to us. This has become a fundamental question

\* Corresponding author. Tel.: +91 44 2257 4208 (direct) 2257 5938/5942 (lab and students); fax: +91 44 2257 0545/0509/4202.

E-mail address: [pradeep@iitm.ac.in](mailto:pradeep@iitm.ac.in) (T. Pradeep).

URL: <http://www.dstuns.iitm.ac.in/pradeep-research-group.php> (T. Pradeep).

while we are discovering newer materials every day. With noble metals, perhaps we know the answer.

Gold and silver belong to the family of “metals of antiquity”, having their history with mankind dating back to 6000 BC and 4000 BC, respectively. Gold's brilliance, intrinsic beauty and ability to preserve its shine for long periods made it the most documented metal in the human history. While there are no clear-cut references for the discovery of gold, it has always been associated with the gods, with immortality, and with wealth across the human civilizations.

The earliest evidence for the use of gold in jewellery comes from Sumer civilization (southern Iraq, 3000 BC). The use of gold as jewellery continued through different civilizations thereafter (tomb of King Tutankhaman [Egypt, 1300 BC], gold ornaments from Indus valley [Mohenjadar, 3000 BC] and royal crowns from the Tilia tepe treasure [Scythian, 100 BC]). Another milestone in the history of noble metals was reached around 700 BC when Lydian merchants produced the first coins through use of gold–silver alloys called ‘*electrum*’. The use of noble metals for currency was further developed by the Roman Empire (100 AD) [1].

It was suggested that the use of gold, in the form of *swarna bhasma* (meaning, gold ash), for medicinal purposes started during the Vedic period (1000 BC–600 BC) in ancient India [2]. References also exist in the Chinese literature about the medicinal properties of gold and it was thought to act as the elixir of life [3]. The medicinal uses of gold were promoted after the work of Paracelsus (15th century) who first prepared gold colloid solution in modern times. The purple solution of gold was called *Aurum Potable* and it was strongly believed that this would impart rejuvenation to the human body, as historically gold was equated with the sun (“*tears of the sun*”). Antonii described the medical uses of colloidal gold in 1618, in the reportedly first documented literature on colloidal gold [4]. This was followed by an effort from Johann Kunckels, a German chemist, to explore the medicinal properties of the *pink-solution* of gold (1676) [5]. A few other subsequent efforts followed, highlighting the stable dispersion of gold [6–10]. The unusual color of metallic gold caught the attention of many researchers. As a consequence of the work accomplished so far on gold, Michael Faraday attempted a novel synthetic route to prepare colloidal gold in 1857 (Fig. 1) [11]. He synthesized a dark red solution of colloidal gold by the reduction of an aqueous solution of chloroauric acid using phosphorus in CS<sub>2</sub>. He realized that stability of colloidal gold against aggregation can be achieved using stabilizing agents. He also noticed the reversible color changes driven by mechanical compression (blue–purple → green) of thin films prepared with colloidal gold [12]. In 1890, the distinguished German bacteriologist Robert Koch discovered the use of gold cyanide for bacteriostatic action against *tubercle bacillus*, the causative agent for tuberculosis. Later, it was found that *tubercle bacillus* is also responsible for rheumatoid arthritis. This led to further investigations in modern medicinal uses of gold [16–18].

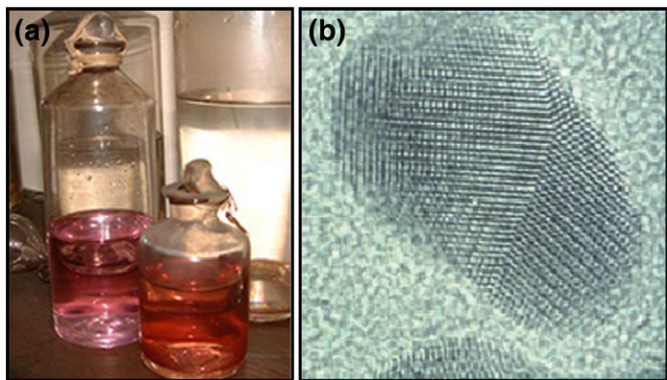


Fig. 1. (a) Faraday's colloidal suspension of gold [14]. (b) High resolution transmission electron microscopic image of individual colloidal gold particles (at a magnification of  $10^7\times$ ), prepared according to Faraday's recipe [15].

Silver has been equally popular for domestic use since the ancient times. As gold was associated with sun due to its color, the white brightness of silver became associated with the moon. The distinct optical properties of silver defined its name: the word silver is of Gothic origin meaning shiny white and the Latin name *argentum* originates from an Aryan root which means white and shining.

From the historical times, utensils were fabricated with silver lining. Silver vessels were utilized for the preservation of perishable items as well as for disinfection of water. The writings of Herodotus suggested that Cyrus the Great (Persia, 550–529 BC) consumed water boiled in silver vessels [19]. The account also mentions the use of silver as a precious booty, during the time of Pausanias (Sparta, 5th century BC). Silver was widely used as a disinfectant and anti-spoilage agent, across many civilizations (Greece, Rome, Phoenicia, Macedonia) [20]. Hippocrates, the Father of medicine, promoted the use of silver for early healing of wounds [20]. Alexander the Great (335 BC) was advised by Aristotle to store water in silver vessels and boil prior to use [21]. Evidence exists for the use of silver nitrate as an anti-bacterial agent, in the Roman pharmacopeias.

During the late 13th century, Lanfranc utilized silver tubes for introduction of food beyond fistula [22]. Thereafter, Paracelsus (1493–1541) pioneered the use of metals for medical applications. He linked silver with the development of brain activities in his hermetic and alchemical writings. During the mid-19th century, Joseph Lister and Marion Sims promoted the use of silver wire sutures, in order to reduce the incidences of septic complications [22]. During the late 18th century, Crede, a German obstetrician, popularized the use of prophylactic 1% silver nitrate eye solution for the prevention of ophthalmia neonatorum [23]. Pioneering work in the study of anti-bacterial properties was carried out by Ravelin (1869) and von Nageli (1893) [20]. It was reported that even at low concentrations of  $9.2\times 10^{-9}$  and  $5.5\times 10^{-6}$  M, silver salt was toxic to *Spirogyra* and *Aspergillus niger* spores, respectively [20]. The term “*oligodynamic*” was coined to represent the activity even at low concentrations. A landmark work in the chemistry of silver was accomplished by Carey Lea in the late 19th century [24,25]. Silver colloid was first prepared through the reduction of silver nitrate using ferrous sulfate and consequent protection of colloidal particles with citrate ions [24,25]. A number of researchers worked on the anti-bacterial properties of silver salts: In the early 20th century, a porous metallic mesh of silver was prepared (“*Katadyn silver*”) and was utilized as an anti-bacterial water filter. The popularity of silver salts continued to grow through the development of new silver salts; e.g., silver sulfadiazine, silver citrate, silver lactate, etc. A number of products based on silver were also commercialized throughout the 20th century (Katadyn, Argyrol, Movidyn, Tetrasil, Alagon, etc.) [26]. Attempts were also made to immobilize silver in zerovalent form on activated carbon and subsequently use it for disinfection of water [27].

As illustrated from the historical perspective, the properties of gold and silver have been used continuously for a number of applications. Till a century ago, the applications were largely restricted to their medicinal value. A few applications of noble metals based catalysis were also studied in the last century such as silver based catalysis of methanol to formaldehyde [28] and ethylene to ethylene oxide [29]. Till recently, all of these applications have been based on properties of macroscopic form of the noble metals. Excellent review articles have been written on each subject area [16,30–36] and these are not part of the present review.

The origin of chemical reactivity for metals is related to their standard reduction potentials. Metals are usually electropositive and have a tendency to lose electrons depending on the corresponding ionization energy. Reduction potential is thus correlated with the electropositive nature of the metals i.e. a metal with high electropositive nature is likely to exist as an ion in the solution phase and thus is a strong reducing agent. Based on the reduction potential, metals usually belong to two groups: d-block metals belong to the moderately reducing group ( $\text{Cd}^{2+}|\text{Cd} = -0.40\text{ V}$ ,  $\text{Fe}^{2+}|\text{Fe} = -0.44\text{ V}$ ) whereas s-block metals belong to the strongly reducing group ( $\text{Li}^{+}|\text{Li} = -3.05\text{ V}$ ,  $\text{Na}^{+}|\text{Na} = -2.71\text{ V}$ ).

**Table 1**

Overview of the basic properties of noble metals and a comparison with other transition metals.

a	b	c	d	e	f	g	h	i	j	k	l
Copper	FCC	1090	887	2.2	78	947	114	1440	5727	596	50
Gold	FCC	1337	3129	2.5	223	890	174	2450	19,300	446	320
Silver	FCC	1235	2435	1.9	126	731	165	25	10,490	631	430
Platinum	FCC	2041	4098	2.3	205	870	177	392	21,090	94	72
Palladium	FCC	1828	3236	2.2	54	804	169	37	12,023	95	72
Mercury	RH	234	630	2.0	0	1,007	171	–	13,534	10	8
Ruthenium	FCC	2607	4423	2.2	101	710	178	2160	12,370	132	120
Rhodium	FCC	2237	3968	2.3	110	720	173	1100	12,450	222	150
Rhenium	FCC	3459	5869	1.9	15	760	188	1320	21,020	52	48
Osmium	FCC	3306	5285	2.2	106	840	185	3920	22,610	105	88
Iridium	FCC	2739	4701	2.2	151	880	180	1670	22,650	189	150
Avg (NM)	–	2010	3515	2	106	833	170	1451	15,751	234	137
Avg (TM)	–	2277	4021	1.7	45	690	182	865	9027	77	61

Column headers: (a) Noble metal, (b) Lattice structure, (c) Melting point in K, (d) Boiling point in K, (e) Electronegativity, (f) Electron affinity in kJ/mol, (g) Ionization energy in kJ/mol, (h) Radius in pm, (i) Hardness in MPa, (j) Density in kg/m<sup>3</sup>, (k) Electrical conductivity in mho/cm, and (l) Thermal conductivity in W/mK. (Abbreviations – FCC: Face-centered cubic, RH: Rhombohedral, NM: Noble metals, TM: Transition metals).

However, there are exceptions to this rule: Gold ( $\text{Au}^{3+}|\text{Au} = 1.5 \text{ V}$ ), Silver ( $\text{Ag}^{+}|\text{Ag} = 0.80 \text{ V}$ ), Mercury ( $\text{Hg}^{2+}|\text{Hg} = 0.87 \text{ V}$ ), Platinum ( $\text{Pt}^{2+}|\text{Pt} = 1.2 \text{ V}$ ) and Palladium ( $\text{Pd}^{2+}|\text{Pd} = 0.83 \text{ V}$ ). The category of metals exhibiting the exception, thus, can exist in the metallic state, without any oxidative effects of oxygen or water ( $\text{O}_2|\text{OH}^- = 0.40 \text{ V}$ ). This property of existing in the metallic state renders the noble metals highly inactive for any chemical reactions. The nobility of certain transition metals is discussed in the next section.

## 2. Origin of nobility in certain transition metals

A summary of physical properties exhibited by noble metals is presented in Table 1. Some of the surprises for noble metals are: high conductivity, extreme hardness, large density and high electron affinity.

The factors affecting the standard oxidation potential of metals can be understood by the Born-Haber cycle:

$$E_{\text{oxidation}} = \Delta H_s + \Delta H_h + \text{IE}$$

where,

- Sublimation of a solid metal ( $\Delta H_s$ )
- Hydration of a gaseous ion ( $\Delta H_h$ )
- Ionization of a gaseous metal atom (IE).

Transition metals usually have high melting points leading to a high energy of sublimation. Similarly, owing to filling of the d-band, the transition metal atoms are usually smaller in size (Table 1) and thus have higher ionization energies (Table 1). This explains the lower oxidation potential of transition metals with respect to s-block.

The noble nature of certain transition metals is explained using the relativistic contraction concept [37]. The Dirac-Fock equation [38] was solved for all atoms with atomic number less than 120 [39]. The explanation for relativistic contraction arises due to the special theory of relativity which imposes a limit on the maximum speed of particles. As the particle accelerates to a velocity nearer to the speed of light, a correction in the mass is required and is calculated as follows:

$$m = m_0 / \sqrt{[1 - (v/c)^2]}.$$

Here  $m$  is the corrected mass,  $m_0$  is the rest mass,  $v$  is the velocity of the particle and  $c$  is the speed of light.

According to non-relativistic quantum mechanics, the average radial velocity of the electron in 1 s shell is  $\langle v_r \rangle / c = Z\alpha$ , where  $Z$  is the atomic number and  $\alpha$  is the fine structure constant ( $\alpha \approx 1/137$ ). The effect of the relativistic contraction is explained using the example of mercury. The atomic number of mercury is 80, i.e.  $v_r/c = 80/137 = 0.58$ ; thus the radial velocity of 1 s electron is 58% of the velocity of light.

Based on the relativistic mass equation, the calculated electron mass in the 1 s shell of a mercury atom is  $m = 1.23 m_e$ , where  $m_e$  is the rest mass of the electron. Thus, in the relativistic calculation, the mass of the electron increases significantly. Assuming Bohr's model for calculating the shell radius, the radius of the 1 s shell correspondingly contracts significantly ( $a_0 = 4\pi\epsilon_0\hbar^2/m_e^2 = 5.1 \times 10^{-11} \text{ m}$ ). In the case of mercury, the relativistic radius is around 81% of the non-relativistic radius. Similarly, the other s shells, up to the valence shell, undergo relativistic contraction. A similar nature of contraction is experienced by p-shells, but to a lesser degree. The contrary effect is felt by d and f-shells. The relativistic contractions of s and p orbitals lead to more effective nuclear screening. It leads to a reduction in the attraction between the nucleus and the electrons in the d and f shells.

Based on the concepts of relativistic contraction/expansion, the relativistic contraction of the 6 s shell in elements was studied (Fig. 2(a)). The first phase of continuous increase in contraction (decreasing curve profile) is due to filling of 4f and 5d shells. An interesting feature appears for gold ( $[\text{Kr}]5d^{10}6s^1$ ): the pronounced local maximum, which is not found until reaching fermium ( $Z = 100$ ). This pronounced contraction is reflected in the noble characteristics exhibited by gold.

Recently, there have been further efforts to explain the origin of nobility in certain transition metals by the molecular orbital (MO)

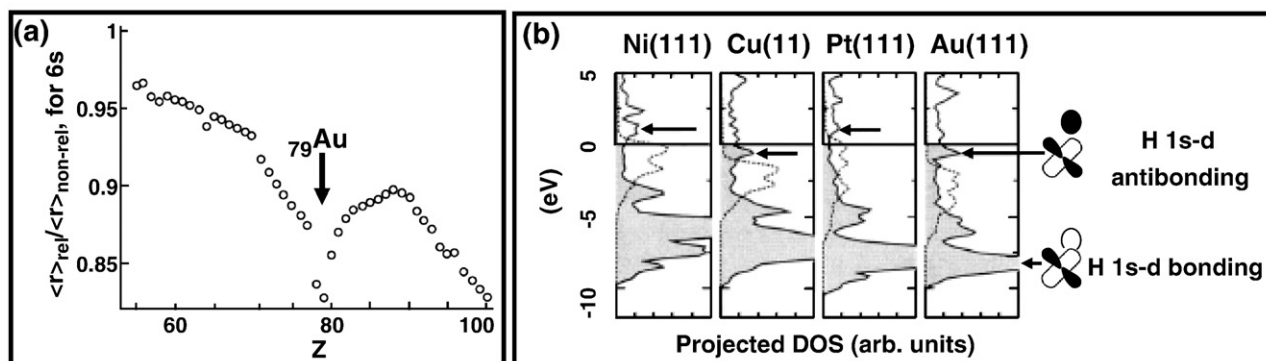


**Fig. 2.** (a) The relativistic contraction of the 6s shell in the elements Cs ( $Z = 55$ ) to Fm ( $Z = 100$ ) [37]. (b) The density of one-electron states (DOS) (solid lines) for H atomically chemisorbed on the (111) surface of Ni, Cu, Pt and Au [40]. The DOS is projected onto the atomic H 1s state. The surface d bands DOS (dashed lines) of the four clean metal surfaces are shown for comparison. The dominant features are the H 1s-metal d bonding resonances at energies; between  $-5$  and  $-10$  eV. Also prominent are the H 1s-metal d anti-bonding DOS peaks (indicated by arrows) directly above the metal d bands. These anti-bonding states cause repulsion in Cu and Au, where they are filled. As indicated by the grey-shading, only states below the Fermi energy (which is the energy zero in all cases) are filled.



theory, widely used to explain the concepts of bonding. The underlying principle in MO theory is that stability of a structure is reached after attaining the noble gas configuration. This helps to explain the formation of covalent bonds (and resultant sharing of p-shell electrons) in p-block elements as a method of attaining stability.

Applying a similar concept, 'n' metal atoms can be visualized to share the valence shell electrons, leading to the formation of  $M_n$  species. However, due to the electropositive nature of metals, the valence electrons are delocalized in the metal lattice. Therefore, the valence electrons are shared across all the metal atoms present. From MO theory, we know that sharing of electrons between 'n' atoms lead to the formation of 'n' bonding and 'n' anti-bonding orbitals. MO theory states that overlapping of electronic states of two atoms leads to orbital orthogonalization (Pauli's exclusion). From an energy standpoint, formation of the bonding orbital is positively favored (due to its symmetric nature) whereas the formation of anti-bonding orbital is negatively favored (due to its anti-symmetric nature). In case both bonding and anti-bonding orbitals are occupied, the energy required for orthogonalization will render the bond formation energetically hindered. In the case of metals, the highest occupied molecular orbital (HOMO) is called the Fermi level at absolute zero temperature. The spacing,  $\delta$ , between the adjacent energy levels in a band is given by the approximate relationship,  $\delta \approx E_F/n$ , where  $E_F$  is the Fermi level energy and n is the number of atoms in the particle. It is important to quickly point out that properties differ at the nano scale vs. bulk scale: In case of bulk material as  $n \rightarrow \infty$ ,  $\delta$  becomes negligible leading to the formation of conduction and valence bands in metals whenever  $\delta$  is smaller than the thermal energy. However, as one restricts n, the discrete nature of energy levels starts to appear leading to dramatic changes in the properties at smaller size.

With the above understanding, let us briefly look at the density of one-electron states for different transition metals. The density of states (DOS) of a quantum-mechanical system is defined as the number of states at each energy level that are available to be occupied. To illustrate it with an example: the density of states for energy levels between the valence and conduction bands of an insulator is zero.

The nobility of certain transition metals is explained through the dissociation of  $H_2$  on the surface of four transition metals (Fig. 2(b)) [40]. It has to be understood that amongst all the transition metals, differences in properties arise largely due to the valence d-band structure. Thus, the interaction between an adsorbate and a transition metal surface can be described as a two-state problem (adsorbate state and valence d-band) leading to the formation of bonding and anti-bonding states. Thus, an upshift of d states should increase the adsorbate-metal interaction, as it would lead to the formation of an anti-bonding orbital closer to the Fermi level. The strong features appearing between  $-5$  and  $-10$  eV represent the formation of a bonding orbital through the interaction of hydrogen 1s with the metal d band, and this formation is shown by all the metals considered. However, the difference arises in the anti-bonding DOS peak as appearing for Au and Cu vs. other metals. In the case of Au and Cu, the anti-bonding DOS peaks appear below the Fermi energy level, leading to the formation of a H 1s-metal d anti-bonding orbital. The formation of an anti-bonding orbital in turn leads to a drastic reduction in the stability of metal-hydrogen compounds (hydrides). Therefore, the metal-hydrogen bond is highly unstable in the case of Au. On the contrary, for other metals, the anti-bonding DOS peak appears above the Fermi energy level, leading to an empty anti-bonding orbital. From the DOS peak intensity for anti-bonding orbitals and metal d band, it can be interpreted that Au-H bond is highly unstable even vis-à-vis Cu-H. This leads to nobility of certain transition metals.

While the first evidence of existence of non-macroscopic properties for gold appeared many centuries ago (The Lycurgus Cup [41]), the first explanation was offered by Faraday in 1857. Faraday attributed the origin of the wine-red color of gold solutions to the colloidal nature of gold particles, which interact differently with light vis-à-vis

metallic gold. Mie was the first to provide an explanation for the dependence of color on the metal particle size [42]. This led to the understanding of the phenomenon called surface plasmon resonance (discussed elsewhere in the article). The next major thrust to explore the properties of nanomaterials in general, came from Richard Feynman's oft-repeated talk – *There is plenty of room at the bottom* [43].

There are two more exciting discoveries that furthered the interest in nanoscale properties: (a) the size dependence of the melting point of gold discovered by Buffat and Borel [44] (melting point of 4 nm gold crystals is 700 K while the bulk value is 1337 K) and (b) the variation in the reduction potentials of metals with size (reduction potential for  $Au^{3+}|Au$  (atom) =  $-1.5$  V,  $Ag^+|Ag$  (atom) =  $-1.80$  V [45,46]).

The objective of this review article is to provide a consolidated view of the research efforts accomplished so far, in the area of noble metal nanoparticles for drinking water purification. The article begins with a review of challenges in drinking water purification. Thereafter, noble metal nanoparticle based chemistry is discussed in detail: various synthesis protocols, origin of reactivity, methods for nanoparticle deposition on supports and novel reactions feasible at the nanoscale. Through a case study – nanoparticles based chemistry for removal of pesticides from drinking water – some of the challenges associated with the commercialization of novel technologies in the market are highlighted. Thereafter, a few of the other nanomaterial-based approaches for drinking water purification are summarized. A brief overview of nanomaterial based commercialized technologies is presented. The article is summarized with a review of the environmental implications of use of noble metal nanoparticles at the commercial scale.

### 3. Drinking water purification – challenges

With the evolution of human civilization, our understanding of pure drinking water underwent dramatic changes. In early civilizations, the commonly practiced measure for purity was the taste of the water. Water was recognized as a symbol for the origin of life and for its medicinal value; it was not designated as a carrier of diseases. In the 17th century, Anton van Leeuwenhoek's discovery of the microscope started to change the perception of purity: We were empowered to see beyond the suspended particles e.g., the tiny material particles to the micro-organisms. Following the discoveries of Louis Pasteur (study of micro-organism based diseases) and John Snow (linking of cholera spread in London with the quality of water), our understanding of pure drinking water was changed [47]. Interestingly, the first governmental act was passed in 1852 and was titled, Metropolis Water Act of 1852. Access to pure water was being recognized as a right to every human being.

The era of water purification had begun.

During the course of over 150 years, our understanding of water quality, its effects on health and methods for water purification has undergone a sea-change. A chronological view of some of the important milestones in water purification is described in Table 2. A number of important events had happened prior to this period which significantly influenced the course of the last 150 years. The historical records suggest that the importance of pure water was emphasized even during ancient civilizations. Early Sanskrit writings outlined several methods for purifying water such as crude sand and charcoal filters (*Sushruta Samhita*). The first recorded use of ion-exchange appears in the Old Testament of the Holy Bible [48]. Ancient civilizations started the use of aqueducts for creating efficient water transport networks (Indus valley, Greek, Roman and American civilizations). Hippocrates, the father of medicine, linked the importance of water to overall well-being of the human health. In early 1600s, Sir Francis Bacon scientifically tested the idea of a sand filter for desalination in 1627.

The severity of pure drinking water scarcity has to be looked at from two aspects: first, the quantity of available water and second, the

**Table 2**

Important milestones in the history of water purification (1800–2007) from the perspective of noble metal nanoparticles in water treatment (compiled from multiple sources on the World Wide Web).

Year	Milestone
1804	Setup of world's first city-wide municipal water treatment plant (Scotland, sand-filter technology)
1810	Discovery of chlorine as a disinfectant (H. Davy)
1852	Formulation of Metropolis Water Act (England)
1879	Formulation of Germ Theory (L. Pasteur)
1902	Use of chlorine as a disinfectant in drinking water supply (calcium hypochlorite, Belgium)
1906	Use of ozone as a disinfectant (France)
1908	Use of chlorine as a disinfectant in municipal supply, New Jersey
1914	Federal regulation of drinking water quality (USPHS)
1916	Use of UV treatment in municipal supplies
1935	Discovery of synthetic ion exchange resin (B. A. Adams, E. L. Holmes)
1948	Nobel Prize to Paul Hermann Muller (insecticidal properties of DDT)
1959	Discovery of synthetic reverse osmosis membrane (S. Yuster, S. Loeb, S. Sourirajan)
1962	<i>Silent Spring</i> published, first report on harmful effects of DDT (R. Carson)
1965	World's first commercial RO plant launched
1974	Reports on carcinogenic by-products of disinfection with chlorine Formulation of Safe Drinking Water Act (USEPA)
1975	Development of carbon block for drinking water purification
1994	Report on use of zerovalent iron for degradation of halogenated organics (R. W. Gillham, S. F. O'Hannesin)
1997	Report on use of zerovalent iron nanoparticles for degradation of halogenated organics (C-B. Wang, W.-X. Zhang)
1998	Drinking Water Directive applied in EU
2000	Adoption of Millennium Declaration during the UN Millennium Summit (UN Millennium Development Goals)
2003	Report on use of noble metal nanoparticles for the degradation of pesticides (A.S. Nair, R. T. Tom, T. Pradeep)
2004	Stockholm Convention, banning the use of persistent organic pollutants
2007	Launch of noble metal nanoparticle-based domestic water purifier (T. Pradeep, A. S. Nair, Eureka Forbes Limited)

quality of drinking water. As a part of "Millennium Development Goals 2015" adopted in 2000, the United Nations has set a goal of reducing by half the number of people without sustainable access to safe drinking water [49].

We need to clearly realize that due to climatic changes, the perennial availability of water through surface and ground water resources is becoming a big challenge [50]. Therefore, it becomes natural that to have universal access to drinking water, we need to economically extract water from the sea. Even though the cost of reverse osmosis based seawater desalination has fallen by almost one-third in the last 30 years [51], we are still far away from being economical. In this context, the statement by John F. Kennedy (former US president, 1961) is worth recalling: *If we could ever competitively, at a cheap rate, get fresh water from saltwater, this would be in the long-range interests of humanity which could really dwarf any other scientific accomplishments* [52].

The second part of the problem arises as an effect of brisk industrialization accomplished globally. Economic growth has led to significant improvement in the economic status of human life; however it has also been coupled with many environmental issues which have largely been ignored, primarily due to unavailability of economic solutions.

Many bodies such as USEPA, WHO, and EU (see list of acronyms and their definitions at the end of the article) have played a key role in developing regulations for many toxic species found in drinking water. Looking at some of the information provided by such bodies (Fig. 3), a few conclusions can be drawn.

- Most of the regulated chemicals fall in the organohalogen group
- Organochlorine pesticides and halogenated organics continue to remain on the USEPA radar for future regulative activity
- The other major contributors to the list are metals, inorganic salts and micro-organisms

- Regulatory coverage of the USEPA for safe drinking water has increased over four times since its inception (in 1974), with revisions in maximum limits for many contaminants

To provide a larger overview of the extent of the drinking water contamination, a consolidated summary of major contaminants is outlined in Table 3. It is quite clear that drinking water contamination has reached global levels in terms of the size of the population impacted. A number of contaminants such as lead and pesticides are affecting water supplies globally due to their widespread use; pollutants of geochemical origin such as arsenic and fluoride are currently found in selected countries. In addition, the biggest class of contaminants affecting drinking water is microorganisms. Every year, 1.8 million people die from diarrheal diseases (including cholera); 90% are children under five, mostly in developing countries. Worldwide, 1 billion people lack access to safe drinking water, 2.4 billion to adequate sanitation. Improved water supply reduces diarrhea morbidity by 6% to 25%; improved sanitation reduces it by 32%. However, improving quality is a difficult task in areas where the risk of contamination is high. For example, one drop of oil can render up to 25 l of water unfit for drinking.

To understand the application of noble metal nanoparticles for drinking water purification, it is imperative to have a larger appreciation of the problem. A case study, about the origin of pesticide contamination and its historical ramifications, is briefly described here.

A review of commonly used pesticides, their structures and health effects is presented in Table 4. It is quite evident that many such pesticides contain highly toxic recalcitrant groups and hence are extremely difficult to break through normal synthetic routes of degradation. In the early 1960s, society had just begun to see the harmful effects of pesticides on human health and its long-term impacts on the food cycle. There is no denial of the importance of the fact that commercial use of pesticides created food-security across the globe. Similarly, the use of dichlorodiphenyltrichloroethane (DDT) to control malaria helped save a large number of lives. However, the long-term impact of the incessant use slowly started to reveal the scale of environmental contamination. In India, the first incidence of such effects happened in one of its states, Kerala in 1958, where over 100 people died after consuming wheat flour contaminated with parathion [59]. A few years ago, the US FDA had expressed interest to review the fears expressed by the public about the increasing content

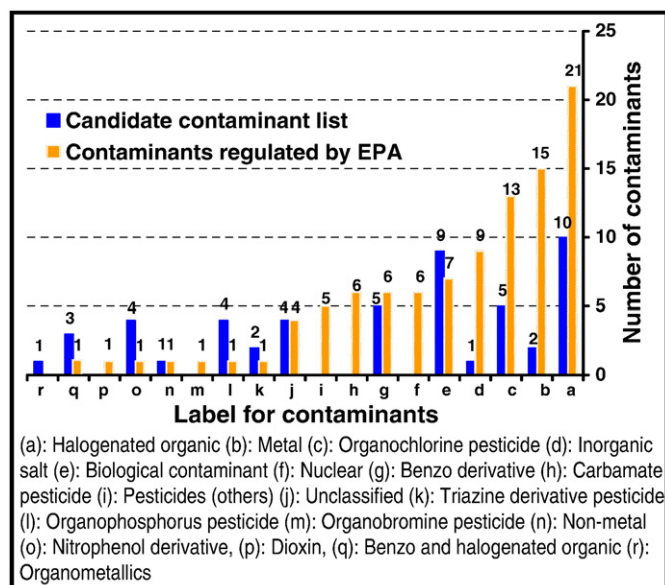


Fig. 3. Category-wise distribution of contaminants regulated by USEPA and future contaminants (USEPA CCL 2005) [53].

**Table 3**  
Review of major drinking water contaminants, their health impacts and a few associated events (compiled from multiple sources on the World Wide Web).

Major pollutant	Origin	Permissible limits	Affected countries	Population at risk	Health effects	Specific incidents
Pesticides	- Farming, effluents, home use	DDT: 1 ppb; Carbofuran: 40 ppb; Simazine: 4 ppb	US, Kenya, Egypt, India, European Union, Africa, China, Australia	Poisoning: 28 million agricultural workers in the developing countries. ~ 18,000 deaths	Cancer, cardiovascular/reproductive/neurological disorders, liver/kidney problems	Pesticide contamination in soft drinks, the Union Carbide Bhopal tragedy (India)
Halogenated organics	Chlorination, effluents, home insecticide	CCl <sub>4</sub> : 5 ppb; TCE: 5 ppb; THMs: 80 ppb	Japan, Central Asia, Arabian Peninsula, Sweden, Poland, Germany, USA, Egypt, China	~180 million people in US consume chloraminated water	CCl <sub>4</sub> : High toxicity to liver and kidney, carcinogenic. TCE: Lung/liver tumor	25 million pounds of TCE were released into the U.S. environment by manufacturing plants in 1995
Fluoride	- Geological origin, mineral weathering, coal mining	- 2 ppm	Asia, Mexico, Australia, Argentina, Africa, New Zealand	62 million (India)	Dental and skeletal fluorosis, Muscle fibre regeneration, nervous system malfunction	In 1999, a union of 1200 scientists, doctors and lawyers announced their opposition to water fluoridation (USA)
Arsenic	- Geological origin	10 ppb	Bangladesh, India, China, Pakistan, Nepal, Myanmar, Vietnam	65 million (Asia)	High blood pressure, glucosuria, hyperpigmentation, keratoses, cancer	1 in 100 people (Conc: 0.05 mg/l) and 10 in 100 people (Conc: 0.5 mg/l) die due to cancer in long-term
Mercury	- Industrial pollution, dental filling, Food (fish)	- 2 ppb	Indonesia, China, Africa, Philippines, Japan, Kazakhstan, USA, Brazil, Australia, Taiwan, EU	~630,000 infants are born with high Hg content in the blood every year (USEPA)	Neurotoxicant, tremors, respiratory failure, gastrointestinal failures, and kidney damage	- ~30% of the mercury in US comes from abroad e.g., China -Unilever plant, Kodaikanal (India). Minamata, Niigata (Japan), River Nura (Kazakhstan).
Lead	- Old piping lines, mineral weathering, paint	15 ppb	Egypt, EU, USA, Thailand, China, Cambodia	>300,000 US children and 65% of Shanghai children have high lead concentration	Delays in physical/mental development, Kidney problem, high blood pressure	- Incidence of Gout due to leaded wine and rum - Use of lead in paints and discharge in environment - Use of lead in paints and discharge in environment

of pesticides in food. It is important to note that during this period inorganic pesticides were dominant in use and the use of organic pesticides had just begun [60].

It was one of the important decisions to list pesticides as a separate chemical additive in the Federal Economic Poisons Act (USA). A similar important decision was reached through the Miller Bill which established the pesticide residue tolerances in food crops [61]. The first study on large-scale environmental impact of pesticides published in 1962 [62], brought significant change in the legislative views on the use of pesticides and the subsequent harmful effects. A report published by the US President's Science Advisory Committee Panel recognized the trade-offs involved in the use of pesticides for agricultural activities.

The report clearly acknowledged two facts: pesticides have contributed to increasing the agricultural output to a large scale; however, their variety, toxicity and environmental persistence may significantly affect human health and the effect need not be limited to only people engaged in agriculture [63]. Over a period of time, it became clear that due to the lack of proper training on the controlled use of pesticides, their release in the environment was much larger in magnitude. From the context of the developing world, this problem was even more severe. Over a period of time, scientific investigations established how such harmful chemicals are slowly entering in the natural food cycle. It is important to highlight that over the same time period, the capability to detect pesticides at ultra-low concentrations got greatly enhanced. Thereafter, many lines of research investigations happened on the degradation of pesticides using micro-organisms, photo-degradation [64] and chemical adsorption [65]. The first scientific report on the degradation of pesticides using micro-organisms appeared in 1985 [66].

The current situation is not comforting: the global utilization of pesticides amounts to 5.05 billion metric tons (Year: 2001) valued at \$31.76 billion [67,68]. The per hectare consumption of agrochemicals in India is 570 g compared to 2500 g in USA, 3000 g in Europe and 12,000 g in Japan. Though low consumption in India vis-à-vis other developed economies point to low overall consumption, there are many areas in India where the use of pesticides has been excessively high. Many of the organic pesticides are highly stable in the en-

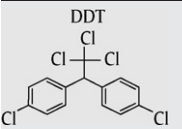
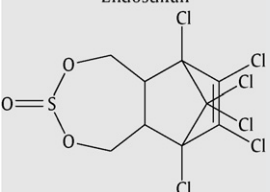
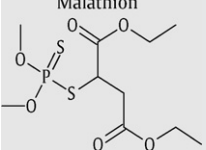
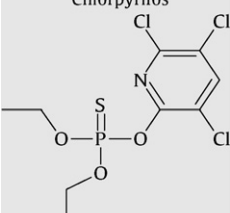
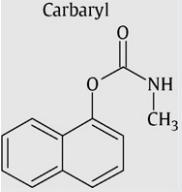
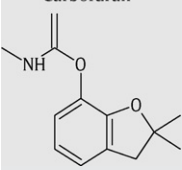
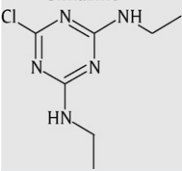
vironment and highly insoluble in water (e.g., the solubility of endosulfan is 2 ppm). However, the dispersions used are of much higher in concentration leading to saturation solubility. The other most common pesticides such as chlorpyrifos, malathion and DDT are similar; applied concentrations are very large and solubility fairly low. As a result, pesticide levels detected in the surface waters of India vary from ppt to ppm levels. Similarly, an additional issue arises due to conformational isomers and derivatives of pesticides, which in some cases are more stable, toxic and highly soluble; e.g., Endosulfan is a mixture of stereo isomers, designated as "α-endosulfan" and "β-endosulfan". Amongst the two, α-Endosulfan is the more thermodynamically stable, and β-endosulfan slowly and irreversibly undergoes isomeric conversion. While there are no nationwide details available on pesticide contamination in drinking water, regional surveys conducted across India definitely point towards high pesticide contamination in drinking water [69–71]. In villages, where endosulfan was aerially sprayed for 25 years, it caused hitherto unknown effects, including genetic deformations [72]. It is also imperative to realize that with rising populations in many developing countries, the use of pesticides and other agrochemicals is projected to increase proportionately to ensure food security for the people. The impact of the problem is also likely to be felt in the developed countries due to the extreme persistence of certain organic compounds and continued commercial use of large numbers of chemicals. An excellent review article discusses the aspect of persistence and scale of consumption of a number of organic compounds in the US market [73]. The problem outlined above will intensify as water resources are limited and available water becomes increasingly contaminated by anthropogenic reasons, other than those mentioned. Without quality drinking water, all developmental programs become only proposals and practical improvement in human development becomes a distant dream. It is in this context that newer technologies for cleaner and affordable water must be investigated.

#### 4. Need for nanomaterials in water purification

In the course of our evolving understanding of the effect of water quality on health, standards for drinking water have been revised several

**Table 4**

Information about a representative group of organic pesticides (compiled from multiple sources on the World Wide Web).

Pesticide	Type	Toxicity	Application	Health effects	Environmental half-life
 DDT	OC	MH	Very effective against insects, domestic insects and mosquitoes	Chronic liver damage, endocrine and reproductive disorders, immuno-suppression, cytogenic effects	28 days (river water) [55] 2–15 years (soil) [55,56]
 Endosulfan	OC	MH	Broad spectrum control against insect pests	Affects kidney, fetus, reproductive system and liver. Mutagenic	Unsterile seawater: $\alpha$ form: 4.9 days, $\beta$ form: 2.2 days [57] 50 days (soil) [56]
 Malathion	OP	SH	Controls aphids thrips, red spider mites and leafhoppers	Carcinogen. Mutagenic. Neurological disorders, allergy, immuno-depressant	<1 week (water) [56] 1–25 days (soil) [56]
 Chlorpyrifos	OP	MH	Controls domestic pests	Neurobehavioral disorders e.g., persistent headaches, blurred vision, memory, concentration	35–78 days (water) [57] 60–120 days (soil) [56]
 Carbofuryl	C	MH	Controls pests of fruits, vegetables and cotton	Mutagenic. Affects kidney, nervous system. Produces N-nitrocarbofuryl, a carcinogen	10 days (water) [57] 7–28 days (soil) [57]
 Carbofuran	C	HH	Broad spectrum control against insects and mites	Cholinesterase inhibitor affecting nervous system function	8.2 weeks (water) [57] 30–120 days (soil) [57]
 Simazine	TD	–	Controls weeds in maize, sugarcane, citrus, coffee, tea	Cancer of testes	30 days (water) [56] 28–149 days (soil) [58]

Acronyms: OC – Organochlorine, OP – Organophosphorus, C – Carbamate, TD – Triazine derivative; HH – Highly hazardous, MH – Moderately hazardous, SH – Slightly hazardous (Definitions based on WHO classification [54]).

times. For example, the allowed limits for well-known contaminants were revised periodically (e.g., lead), the definition of contaminant is becoming specific (e.g., maximum concentration of organic residues vs. pesticides) and newer contaminants (e.g., RDX) are being brought under regulation [68,74]. In this course of evolution, it is likely that the contaminant concentrations will reach molecular limits; i.e. the level at which they pose risks could become a few molecules/ions/atoms per glass of drinking water consumed. This can be understood from the examples of arsenic and lead (Fig. 4). The recommended maximum value for arsenic in drinking water, as per the WHO International standards, has been reduced from 200 ppb to 10 ppb, through a number

of revisions during the last 50 years. During the same period, the allowed concentration for lead in drinking water was reduced from 100 ppb to 10 ppb. The same is reflected in the case of revisions in drinking water norms by other agencies such as USEPA (1976–2001: reduction in allowed lindane concentration from 4 ppb to 0.2 ppb, reduction in allowed arsenic concentration from 50 ppb to 10 ppb, reduction in allowed lead concentration from 50 ppb to 15 ppb).

As a result, the technology to remove these contaminants must also reach molecular limits. There must be highly efficient molecular capturing agents which would grab them during single encounter events. The other equally important requirements of such a solution are:



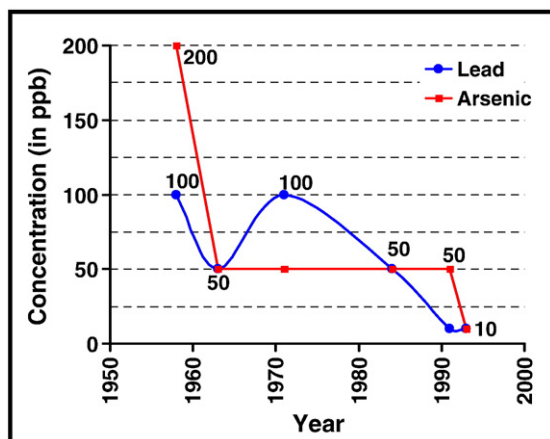


Fig. 4. Changes in maximum allowable concentration for lead and arsenic in drinking water, based on WHO advisory.

minimum electricity, economical feasibility and environmental friendliness. Importantly, the chemistry should be effective even at parts per billion concentrations. In most chemical processes we see around us, the concentrations involved are sufficiently large such that the encounters between the reacting partners are numerous. On the contrary, at a dilution of  $10^9$ , the encounters also get reduced proportionately. Traditional approaches for the removal of such trace contaminants lead to further ecological damage in terms of waste generated; e.g., adsorption capacity of fluoride with conventional sorbents such as activated alumina is usually in the range of  $< 10$  mg/g [75]. Thus, a minimum of 6.5 kg of activated alumina is required for the design of a domestic purifier unit (with a capacity to purify 6500 l of water) catering to complete removal of 10 ppm fluoride. All of these pose numerous requirements, difficult to meet entirely.

Nature has beautifully incorporated a number of molecular technologies in different living bodies [68]. Think of watermelons, storing high quality water in a highly efficient fashion. Considering the feed water, the quality of water saved in tender coconuts is phenomenal. This occurs after a series of filtration and transportation events, in which everything unwanted is rejected. An example of the mediated-transport is exhibited through the flow of glucose across the erythrocyte membrane (Table 5). A similar example of such molecular transport is flow of water through widely-studied aquaporins, the water channels responsible for extremely fast flow through epithelial and renal cells. At least 10 human aquaporins have been identified; more than 200 members of the aquaporin family have been found in plants, microbes, invertebrates and vertebrates [76]. The water transport rate through a single aquaporin-1 channel, the first discovered member of aquaporin family, is of the order of  $10^9$  water molecules per second [77]. Surprisingly, the activation energy for the channel transport is nearly as low as the one associated with self-diffusion in bulk water. Even though the transport is enabled through the porous cavity in the aquaporin, which has size range similar to the water molecule, it is quite surprising that flow is extremely selective towards water and even ion flow is not enabled. This has been explained based on the passage of water through several consecutive gateways involving hydrophobic-hydrophilic interactions and electrostatic repulsion. The first main interaction site of water with aquaporin happens in the region containing Asparagine-Proline-Alanine (NPA) motifs. The presence of hydrophobic regions near the NPA motifs forces stronger interactions of water molecules. The second interaction site is formed due to aromatic side chains of phenylalanine and histidine along with positively charged arginine, which restrict the flow of positive ions. The hydrophobic phenylalanine side chain orients the water molecules such as to enforce strong hydrogen bonds to

arginine and histidine. The knowledge of aquaporins has been utilized for water purification [13] and in conjunction with the diverse properties of nanoparticles, a multifunctional system for drinking water purification may be developed [383].

It is also important to realize that due to the extraordinary diversity in the living system, Nature has developed a variety of methods for water purification; e.g., (a) In humans, more than 10 different aquaporins with specialized functionality are expressed in tissues as diverse as kidney, red blood cells, and brain [77]. (b) A number of flowering plants belonging to genus *Alyssum* exhibit extremely high heavy metal tolerance (3% of leaf dry mass) due to metal-chelation by free histidine [78]. (c) A number of bacteria and fungi are known to degrade toxic pesticides through oxidation, hydrolysis, reduction and immobilization [79,80].

A few of the examples available in Nature have been utilized for drinking water purification, a classic example being reverse osmosis membranes. Currently, reverse osmosis based desalination accounts for over 50% of the installed capacity. Various methods developed to control the pore dimensions have led to significant improvements in the cost of desalination [82,83]. The specific energy of desalination has been reduced from over  $10$  kWh/m<sup>3</sup> in 1980s to below  $4$  kWh/m<sup>3</sup>. However, the processes are still not the most energy efficient [84]; e.g., the theoretical minimum energy required for desalination with 50% recovery is  $0.97$  kWh/m<sup>3</sup>. While the currently pursued approaches for decreasing fouling [85] and improvement in pore size distribution [86] will improve the efficiency, an implementation of molecular transport mechanisms will help us in filtering water in the most energy efficient fashion. In addition to membrane research, a variety of approaches for drinking water purification are being pursued. It is thus far understood that due to the differences in the water quality across the world, there is no possibility of one solution catering to all situations. In the design of efficient molecular mechanisms for water purification, nanotechnology will continue to play a key role. A prominent amongst those approaches is the chemistry of noble metal nanoparticles, which is discussed in detail here.

It is vital to summarize a few of the advantages of nanomaterial chemistry with respect to conventional technologies (Table 6). Usually in cases of adsorption, surface sites of the adsorbent particles are more frequently utilized (as bulk diffusion is kinetically hindered in the absence of porous structure). The surface-to-volume ratio increases drastically with the reduction of the size of the adsorbent particle from bulk to nano dimensions. It leads to the availability of higher numbers of atoms/molecules on the surface for adsorption of contaminants. Accordingly the surface energy available with each adsorbent particle also increases significantly. This provides many advantages to drinking water purification:

- Effective contaminant removal even at low concentrations
- Less waste generation post-treatment as less quantity of nanomaterial will be required vis-à-vis its bulk form. This happens since more adsorbent atoms/molecules are present per unit mass of the adsorbent and thus are actively utilized for adsorption.
- Novel reactions can be accomplished at the nanoscale due to an increase in the number of surface atoms (i.e. surface energy), which is not possible with the analogous bulk material. An example of one such process is the use of noble metal nanoparticles for

Table 5  
Permeability coefficients of natural and synthetic membranes to D-Glucose and D-Mannitol at 25 °C [81].

Membrane preparation	Permeability coefficient (cm s <sup>-1</sup> )	
	D-Glucose	D-Mannitol
Synthetic lipid bilayer	$2.4 \times 10^{-10}$	$4.4 \times 10^{-11}$
Calculated non-mediated diffusion	$4 \times 10^{-9}$	$3 \times 10^{-9}$
Intact human erythrocyte	$2 \times 10^{-4}$	$5 \times 10^{-9}$



**Table 6**  
Review of conventional technologies utilized for drinking water purification.

	Reverse osmosis	Grannular activated carbon	UV-based filtration	Electro-dialysis	Distillation
Technology description	- Flow of water across semi-permeable membrane on application of pressure	- Adsorption of contaminants on porous surface	- Works on the generation of free radicals from UV lamp	- Charge separation on application of electric field	- Reduced pressure evaporation of water followed by condensation
Pros	- Removes TDS, heavy metals, fluoride, pesticides, micro-organisms	- Removes VOCs, pesticides, excess chlorine, color, odor - High throughput	- Broad-range micro-organism removal - High filtration capacity	- High TDS removal efficiency (-90%)	- Removes a broad range of contaminants - Reusable - Cost not proportional to TDS
Cons	- Low recovery - Brine disposal - High maintenance (membrane change in 3 years) - Pretreatment	- Doesn't remove: Microbial contamination, TDS, nitrates, fluorides, hardness	- Effectively degrades only micro-organisms - High costs	- Proportional increase in cost with TDS - Doesn't remove: pesticides, micro-organisms	- High initial investment - Regular maintenance - Volatile organics are not removed

the degradation of pesticides which can't be done by noble metals in their bulk form.

### 5. Noble metal nanoparticle based chemistry

The discovery of noble metal nanoparticle based chemistry has a fair amount of scientific history. The chemical synthesis of noble metal nanoparticles started with the pioneering work of Faraday [10]. Subsequent work by Turkevich [87] to develop a simple protocol, based on work by Hauser and Lynn [88], to synthesize colloidal gold, initiated the research on methods for nanoparticle synthesis. In addition to exploring the effect of temperature, reagent concentration and dilution, Turkevich also conducted detailed studies on the mechanism behind the nucleation and growth of gold colloid. Owing to the understanding developed by this work, it became the most-utilized method for noble metal nanoparticle synthesis. Recent efforts by different research groups to synthesize noble metal nanocrystals of different shapes and studies of their shape-dependent chemical properties have furthered the development of novel properties of noble metal nanomaterials [89].

The discovery of the novel chemistry of gold nanoparticles began with the work of Bond, Ozin and Haruta on nanoparticle assisted low-temperature oxidation of CO [90–92]. It was established that gold supported on various metal oxides is a useful candidate for alkene hydrogenation. A few interesting revelations arose from this research:

- Crystallite size plays a pivotal role in determining the extent of the reaction. The catalyst as prepared by co-precipitation resulted in much higher efficiency for CO oxidation vs. that achieved by the use of impregnation and reduction methods (the former method leads to the formation of 4 nm gold nanoparticle whereas the latter lead to formation of particles with size > 10 nm).
- The choice of metal oxide is equally important for high catalytic activity; e.g., oxidation efficiency was much higher in the case of Al<sub>2</sub>O<sub>3</sub> as a support vs. other supports such as Fe<sub>2</sub>O<sub>3</sub>, Co<sub>3</sub>O<sub>4</sub> and NiO. Metal oxide helps in dispersing gold nanoparticles in small sizes by promoting stronger interaction between gold precursor and support.

An important contribution to explaining the reactivity of nanoparticles came from the pioneering work of Henglein [93]. The change in the reactivity at the nanoscale was explained by the size-quantization effect. It was realized that the band structure in metals and semiconductors is not an atomic or molecular property but is attributed to the arrangement of atoms in a specific order in the crystal lattice. The traditional concept of valence and conduction band holds true only when there are sufficient number of atoms present, so as to organize themselves in a specific lattice arrangement. This can be understood from the fact that while the bulk form of gold organizes itself in a face-centered cubic arrangement, the Au<sub>32</sub> cluster is an empty icosahedron [94]. The effect of

the number of atoms in a lattice on chemical properties can be understood by changes in electrochemical properties. In the case of silver, when the number of atoms in the lattice is sufficiently large, the “bulk” potential of 0.799 V is reached. As the number of atoms is reduced, there is a dramatic reduction in the potential. The electrochemical potential for a free silver atom is measured to be – 1.8 V. In the intermittent size regime, the potential is between the two values, “bulk potential and “atom” potential.

Another important contribution towards the theoretical understanding of metallic nanoparticles was provided by Gustav Mie [42,95]. He studied the interaction of metal nanoparticles with electromagnetic radiation and explained the resultant scattering with the collective resonance of the conduction electrons of the metal nanoparticles. The relationship of Surface Plasmon Resonance (SPR), as it is famously referred to, with the nature of the metal and its environment was established using Maxwell's classical electromagnetic theory. The subsequent research to investigate the dependence of SPR on non-spherical metal nanostructures along with the variation of a variety of factors – the dielectric constant of the surrounding medium, the interaction between the surface stabilizer and the nanoparticle, adsorption of molecules on nanoparticle surface – was studied using the discrete dipole approximation [96]. It was also established that near the sharp tips of anisotropic structures, the electromagnetic field was enhanced by several orders of magnitude due to SPR and this contributed to the development of new protocols for the detection of species at ultra-low concentrations [97]. Theoretical studies conducted on noble metal clusters further investigated the structure and effect of various factors on the optical properties of clusters.

Several articles have been authored on the phenomenon of absorption and scattering of electromagnetic radiation [98–104]. The origin of brilliant color of noble metal nanoparticle solutions is attributed to SPR, and it has a correlation with the origin of reactivity at the nanoscale. A quick overview is highlighted here:

- The interaction of electron clouds in metal nanoparticles with electromagnetic light comprises two processes: absorption and scattering. The former dominates when the particle size is small, whereas the later becomes predominant in case of larger particles.
- In the case of interaction of small particles with electromagnetic radiation, the electron clouds displace to form a dipole charge distribution. An increase in the size of the particle leads to non-homogeneity and thus high-multipolar charge distribution.
- There are two forms of electronic transitions due to the interaction with electromagnetic light. Interband transitions occur from the occupied to the empty bulk bands. The energy required for this transition usually falls in the UV region of the electromagnetic spectrum. Intraband transitions occur due to an electronic transition at the Fermi level in incompletely filled bands, or when a filled band overlaps in energy with an empty band. The energy required for this transition usually falls in the visible-NIR region of

the electromagnetic spectrum i.e. intraband transitions lead to the formation of *free electrons*.

- At room temperature, the mean free path of the electron is usually of the order of a few nanometers. Thus, for small particles, a free electron can easily traverse from the bulk of the particle to the surface. This leads to effective dispersion of the electron across the surface of a nanoparticle.

With the above understanding, the chemical aspects of noble metal nanoparticles will be reviewed in detail.

### 5.1. Synthesis protocols

The seminal work of Faraday and Turkevich on metal nanoparticle synthesis and the mechanism behind the growth kinetics of nanoparticles, stimulated research on various synthetic protocols. It is appropriate to say that ongoing nano-research has largely been enabled due to the large number of synthetic protocols. As a result of this, many interesting size and shape dependent properties of nano-materials have been discovered.

Excellent review articles and books are available describing a multitude of synthetic protocols [89,105–122]. However, novel as well as improved methods are continuously being developed and it would be difficult to cover the entire spectrum of valuable activity in metal nanoparticle synthesis. Thus, here only selected contributions in the area of chemical synthesis of noble metal nanoparticles are discussed.

The usual method followed for metal nanoparticle synthesis is reduction of metal salts (precursors). During the reduction process, the growth kinetic parameters are controlled by a combination of low precursor concentration (increasing the diffusion distance), nature of solvent (higher solvent viscosity), slow acting reducing agent (reduced electrochemical gradient) and appropriate protection of the growth surface with a stabilizing agent (controlling surface reactivity). This enables the hindered diffusion of growth species from the solution to the nuclei and consequent formation of monodisperse nanoparticles.

As stated earlier, when the size of the particle is reduced to the nano level, the ratio of surface to bulk atoms increases thereby increasing the energy of the system as a whole, leading to a decrease in the system stability. Therefore, two nanoparticles have a natural tendency to be attracted to each other through van der Waals forces,

leading to agglomeration and corresponding reduction in the surface energy. The strength of the van der Waals forces for noble metals can be judged from the fact that the Hamaker constants [123] of gold and silver in water are  $4.5 \times 10^{-19}$  and  $4 \times 10^{-19}$  J, respectively, an order of magnitude higher than the values for polymeric lattices [124]. In this respect, it is important to understand the theoretical aspects behind the nanoparticle stability [112].

In addition to imparting stability to the nanoparticle system, the species present on the surface also play a role in surface functionalization. For example, in the case of dodecanethiol protected gold nanoparticle [125], the inherent nature of the stabilizing agent renders the nanoparticle system soluble in an organic solvent. Similar approaches for functionalization of noble metal nanoparticles have been developed using various other organic molecules (aliphatic and aromatic) containing a wide variety of functional groups; e.g., cyano ( $-\text{CN}$ ), mercapto ( $-\text{SH}$ ), carboxylic acid ( $-\text{COOH}$ ) and amino ( $-\text{NH}_2$ ) are known to have a high affinity for gold and thus are useful as surface protective functional groups [126–132]. Excellent review articles have appeared on the subject of surface functionalization of noble metal nanoparticles and the corresponding use in a wide variety of applications [133,134].

To enable the stabilization of a nanoparticle in a dispersant medium, sufficient repulsive forces have to be developed so as to counteract the van der Waals interaction. Two methods are usually followed: (i) develop surface charge on the nanoparticle surface (electrostatic stabilization, Fig. 5(a)) and (ii) anchor long-chain hydrocarbons on the nanoparticle surface (steric stabilization, Fig. 5(b)) [135]. The two methods are discussed herewith.

The stability of a nanoparticle system due to electrostatic stabilization can be evaluated by zeta potential measurements. Fig. 6 summarizes the relationship of the zeta potential with pH and its influence on surface plasmons in silver and gold nanoparticles [136]. The relatively unstable nature of borohydride reduced silver nanoparticles vis-à-vis citrate reduced silver nanoparticles (measured through shift in absorption maximum) can be explained by the higher value of zeta potential (Fig. 6(a,b)). Citrate-reduced silver nanoparticles are stable in a wider range of pH values, extending from 2 to 12 whereas borohydride reduced silver nanoparticles dissolve in acidic pH and precipitate in alkaline pH. Citrate-reduced gold nanoparticles (Fig. 6c) have strongly negative zeta potential values and thus they are highly stable under a wide pH range.

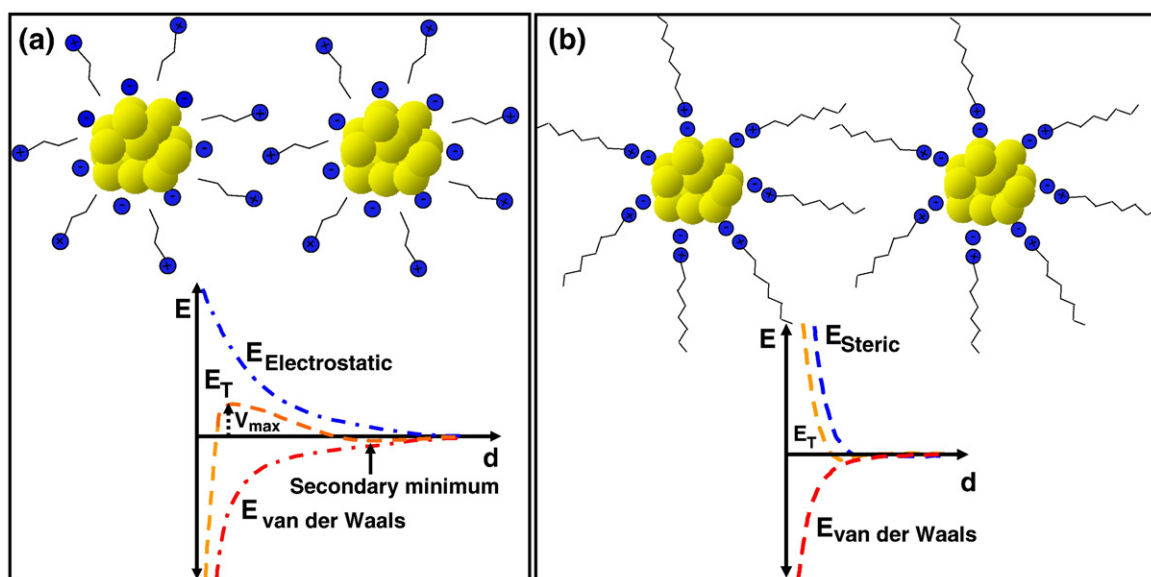


Fig. 5. (a) Electrostatic stabilization and (b) steric stabilization of metal nanoparticles.

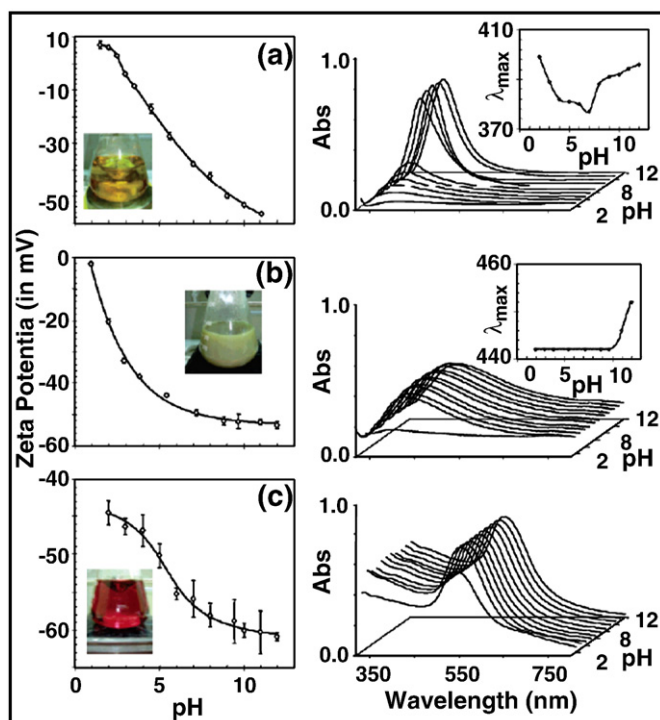


Fig. 6. Variation of  $\zeta$  potential (left) and surface plasmon (right) of (a) silver borohydride, (b) silver citrate, and (c) gold citrate colloids, as a function of the pH of the medium. Insets in the surface plasmon spectra present the behavior of the absorption maximum as a function of pH [136].

**Electrostatic stabilization:** The concept can be understood through the example of citrate reduced gold nanoparticles. The adsorption of citrate and chloride ions leads to the formation of a double layer around gold nanoparticles with a coulombic interaction between oppositely charged ions. Thus, the local concentration of cations increases near anions resulting in the formation of a charge bearing spherical environment around the nanoparticle. The interaction between oppositely charged ions decreases the Gibbs free energy of the nanoparticle. The corresponding change in the energy diagram of the system is illustrated below (Fig. 5(a)). There are a multitude of factors affecting the system stability: ambient temperature, dielectric constant of the surrounding medium, ionic strength of the medium and the nature of other ligands. The weak potential energy minimum that exists at a moderate interparticle distances leads to stability of the nanoparticle solution. An example of how an ionic cloud around the

nanoparticle can be interrupted causing aggregation of nanoparticles, is shown by the addition of uncharged species (e.g., pyridine) which bind to the gold surface [112,137,138].

**Addition of charged species to the nanoparticle system:** The adsorption of a multitude of anions and cations on the surface of silver nanoparticles and the accompanying effects on optical properties have been investigated [137,139–141].

A number of nucleophiles have been investigated for their interaction with silver nanoparticles. The nature of interaction has been studied using absorption spectroscopy, Surface-Enhanced Raman Spectroscopy (SERS), and transmission electron microscopy. In the case of UV–visible spectroscopy, it has been found that the shape of the absorption band, position of the absorption maximum as well as the absorption intensity are affected by the addition of the ionic species to the silver particles (Fig. 7). SERS investigation has confirmed the presence of such species on the silver surface. Microscopic images revealed the aggregation of silver nanoparticles upon the addition of different ionic species. It is to be noted that only the ions which complex directly with the silver particle can produce optical effects in the silver sol, such as SERS and the red shift of the absorption band.

The strong adsorption of nucleophiles on silver surface is attributed to the large surface area and the availability of a large number of coordinatively unsaturated adatoms which can be saturated by adsorbates. The halides show an adsorbability sequence of  $I^- > Br^- > Cl^-$ , which is the same as their nucleophilicity sequence. It has been found that adsorption process is spontaneous indicating the favorable nature of the reaction. The adsorbed ion can saturate the residual valence force of the silver adatom on the particle surface by coordinating with the unoccupied orbitals. As a result, the surface energy of the silver particle is decreased.

The explanation for the changes in the absorption behavior arises from the fact that only the electrons in the surface layer of the particle are sensitive to light excitation [141]. It is known that surface plasmon resonance is determined by the density of the free electrons. The frequency of the plasmon oscillation ( $\omega_p$ ) is proportional to the square root of the free electron density in the silver particle. The penetration depth of light into metal is given by  $\delta = \sqrt{\epsilon_0 c^2 / 2\sigma_0 \omega}$  where  $\epsilon_0$  is the permittivity in vacuum,  $c$  is the speed of light,  $\sigma_0$  is the direct current conductivity and  $\omega$  is the frequency of light. Using a frequency between UV and visible light of  $10^{15} \text{ s}^{-1}$  gives a penetration depth of around 1 nm, i.e. a few atomic monolayers. This means that the adsorption of nucleophiles on the silver surface will reduce the electron density due to electrostatic repulsion.

**Steric stabilization:** An important method for stabilizing a nanoparticle surface is the use of organic ligands to form a protective layer. This is primarily accomplished by the use of polymers (e.g., vinyl

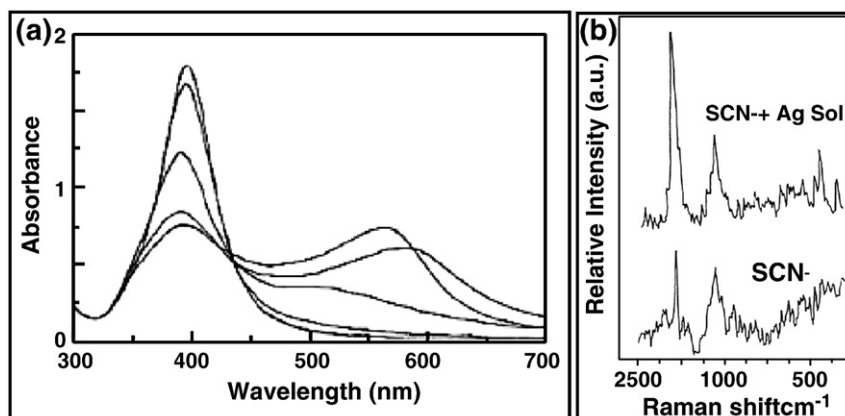


Fig. 7. (a) UV–vis absorption spectra of the silver sol containing different concentrations of  $Cd^{2+}$ : (1) 0, (2)  $1.5 \times 10^{-6}$ , (3)  $3 \times 10^{-6}$ , (4)  $5 \times 10^{-6}$ , and (5)  $2 \times 10^{-5}$  mol/l, respectively [140]. (b) Raman spectra of  $SCN^-$  in the presence and absence of silver sol.  $[SCN^-] = 0.05 \text{ mol l}^{-1}$ ;  $[Ag] = 1.0 \times 10^{-4} \text{ mol/l}$  [141].



polymers like polyvinyl alcohol), surfactants (e.g., ionic surfactants like cetyl trimethylammonium bromide) or ligands (e.g., mercapto-succinic acid). Use of polymers as stabilizers began quite early – the work published by Hans Helcher in 1718 described the use of boiled starch for imparting stability to gold solution [6]. Other polymers used as stabilizing agent are cellulose acetate, cellulose nitrate, and cyclodextrin [142,143]. Owing to the explosion of research in synthetic organic chemistry, a variety of synthetic polymers have been prepared. Synthetic polymers stabilize nanoparticle surfaces against aggregation through the presence of long-chain hydrocarbons in their structure. Polymer molecules also bind weakly to the nanoparticle surface through the heteroatom [144]. It is important to highlight that the polymer should also get solvated by the dispersing fluid (i.e. amphiphilic). Historically, the effectiveness of a polymer as a stabilizer was measured through the *gold number* and *protective value*. Gold number is defined as the mass of the stabilizing agent which is just insufficient to prevent 10 ml of a gold sol from changing to violet upon the addition of 1 ml of a 10% aqueous NaCl solution [145]. Similarly, the protective value is defined as the mass of the red sol that is just protected against (visual) flocculation by 1% NaCl by 1 g of the protective agent for 3 min [146]. The protective values of poly(N-vinyl-2-pyrrolidone) (PVP), poly(vinyl alcohol), poly(acrylamide), poly(acrylic acid) and poly(ethyleneimine) are 50.0, 5.0, 1.3, 0.07 and 0.04, respectively [147]. However, the difficulty in the use of these parameters to classify the polymer's capability to act as a stabilizing agent arises due to the inherent qualitative nature of the measurement; it applies only to gold colloids and doesn't account for the effect of other species in the solution. Recently efforts have been devoted to understand the stabilizing effect of polymers from the kinetic standpoint [144,148–154]. Briefly, the evaluation criteria for comparing the stabilizing effect of polymers, as developed for the formation and stabilization of iridium nanoclusters, are as follows: (i) the ratio of autocatalytic surface growth to nucleation, (ii) the degree to which near monodisperse nanoclusters are formed as verified by TEM, (iii) the degree to which the nanoclusters can be isolated from solution, bottled for future use, and fully re-dissolved on demand for subsequent use, (iv) the relative catalytic hydrogenation activity of the isolated nanoclusters once redissolved in solution with fresh cyclohexene substrate, and (v) the total catalytic lifetime of the nanoclusters generated in-situ for cyclohexene hydrogenation.

Recently, copolymers have received some attention [155–157] (a copolymer is a polymer derived from two or more monomeric species i.e., having two or more constitutional units). The self-assembly behavior of amphiphilic block copolymer/nanoparticle mixture has been studied. It is found that block copolymers self-assemble into micelles with controllable sizes and morphologies. The hydrophilic headgroup forms the corona, which provides the stabilization, while the hydrophobic blocks produce the core which isolates the nanoparticles from the solvent. The properties of copolymer/nanoparticle system can be varied by varying the co-monomer ratio. For example, the use of vinylpyrrolidone-vinyl alcohol copolymers is reported for the preparation of platinum and silver hydrosols [158].

One of the popular anionic surfactants used for nanoparticle stabilization is sodium bis(2-ethylhexyl) sulfosuccinate (commonly known as AOT). The organization of AOT is such that it consists of a hydrophilic core, compartmentalized by the hydrophilic headgroup, and a hydrophobic alkyl tail in contact with the non-polar solvent. The size of the micelle core formed is described by the molar ratio of water to surfactant molecules in solution ( $R = [H_2O]/[AOT]$ ). For AOT reverse micelles, the size of the core in nanometers is approximately 1.8R [159].

### 5.1.1. Turkevich's method for citrate-reduced gold nanoparticles

Monodisperse gold nanoparticles are prepared by the addition of tri-sodium citrate to a boiling solution of HAuCl<sub>4</sub> [87]. On addition of citrate ions, the color of the solution gradually changes to grayish-blue

and finally the color turns to wine-red. The effect of temperature, precursor concentration and reducing agent concentration is varied to investigate their effect on the shape and size of the nanoparticles.

While the precise role of the citrate ion as a reducing agent is not fully elucidated, it is reported that oxidation of citric acid leads to the formation of acetone dicarboxylic acid in the first step. The independent action of separately prepared sodium acetone dicarboxylate on boiling HAuCl<sub>4</sub> solution is very similar to that obtained with the addition of tri-sodium citrate. It has been reported that oxidation products of acetone dicarboxylic acid are formic acid, formaldehyde and CO<sub>2</sub> [160].

Taking inputs from Turkevich's work, efforts have been devoted to utilize the recipe for the synthesis of differently sized gold nanoparticles. This was attempted by varying the tri-sodium citrate to gold ratio [161]. Similarly, Turkevich's recipe for the synthesis of gold nanoparticles has been utilized for the preparation of silver nanoparticles. [162,163] It is found that it leads to the formation of large size particles (60–200 nm) with high polydispersity. The surface plasmon resonance band for citrate reduced silver nanoparticles appears at 420 nm with broad features pointing to high polydispersity. This being in contrast with the citrate reduced gold nanoparticles and other methods used for the synthesis of silver nanoparticles [164], suggests the difference in the mechanism of formation of silver nanoparticles through the citrate reduction route [165,166]. Experimental evidence suggests an additional role of citrate ion in the synthesis of silver nanoparticles (complexation agent), in addition to a reducing agent and stabilizing agent. In the beginning of the reaction, citrate reduces a few silver ions to form seeds of silver particles (Note: citrate ion is a mild reducing agent for silver). During this process, one of the intermediates formed in the reaction ( $Ag_2^+$ ) strongly complexes with citrate [165]. This complexation leads to decrease in the extent of reduction of silver ion to the zerovalent state. Therefore, due to the presence of residual charge on the seed, the growth of the seed is inhibited after an optimal size, thus preventing further aggregation. This point onwards, growth happens due to Ostwald ripening [166]. The Ag<sup>+</sup> ions, released in the solution, get reduced on larger crystallites and facilitate the further increase in the size of silver nanoparticles. This leads to greater reaction time as well as the large polydispersity observed in the synthesis of citrate reduced silver nanoparticles.

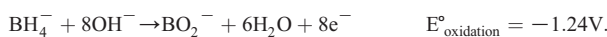
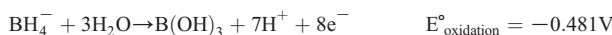
This generalistic approach of aqueous phase reduction of metal ion salts has been adapted for the synthesis of other noble metal nanoparticles [167]. Other reducing agents can be used in place of sodium citrate: ascorbic acid [168–170], sodium borohydride [171], sodium formate [172,173], hydrogen [174], EDTA [175], hydrazine hydrate [176], hydrazine dihydrochloride [177], poly(N-vinyl-2-pyrrolidone) [178,119], methanol [119,179], ethanol [180], polyethylene glycol [181], etc.

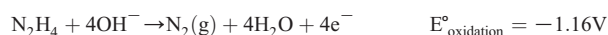
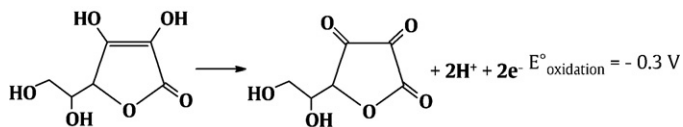
The corresponding electrochemical reactions for different reducing agents are tabulated here:

*Reduction reaction for a few noble metal ions:*



*Sodium borohydride as a reducing agent:*



*Hydrazine hydrate and hydrazinium ion as reducing agent:**Ascorbic acid as a reducing agent [182]:*

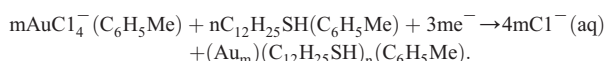
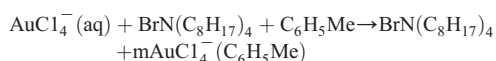
Based on the above information, it may be interpreted that the reduction of any noble metal with an  $E^\circ$  more positive than  $-0.481\text{V}$  should be possible at room temperature, given a sufficient excess of reducing agent and proper control of pH. However, there are other challenges, these include the formation of metal borides with borohydride [183] and complexation of metal cations with hydrazine [184]. Similarly, formation of thiol protected gold clusters begins with the polymerization of  $\text{Au}(1)\text{-SR}$  complex (discussed in the next section) [185].

*5.1.2. Brust-Schiffrin method for organic soluble gold nanoparticles*

The method developed by Brust et al. is usually followed for the preparation of thiol protected gold nanoparticles which can easily be re-dispersed in many organic solvents [125]. This method was developed based on two earlier works: (a) Faraday's approach of two-phase synthesis of gold nanoparticles using an aqueous solution of chloroauric acid and phosphorus dispersed in carbon disulfide [10], and (b) the role of alkanethiol in protecting the gold surface through monolayer coverage [186].

The important steps in the reaction are as follows:

- Transfer of  $\text{AuCl}_4^-$ , present in the aqueous medium, to the organic medium (e.g. toluene) using a phase-transfer reagent (e.g., tetraoctylammonium bromide)
- Reduction of metal cations to zerovalent form through a reducing agent in aqueous phase (e.g., sodium borohydride)



- Stabilization of growing metal nuclei by the use of a long-chain thiol (e.g., dodecanethiol)

The characterization of gold nanoparticles prepared by Brust-Schiffrin method leads to a few interesting revelations:

- The size of the particle is in the range of 1–3 nm.
- Gold is present in the zerovalent state and thus the gold–thiol bond doesn't have the characteristics of gold sulfide.
- Elemental analysis along with IR confirms the presence of thiol on the surface.

One of the difficulties faced with the synthesis of noble metal nanoparticles by Turkevich's method, is the difficulty to recover nanoparticles in the solid phase. The removal of the aqueous phase usually leads to the agglomeration of the particles. However, in the case of the Brust-Schiffrin method, the thiol-protected gold nanoparticles can easily be precipitated by concentrating the organic solution and adding ethanol to precipitate the gold nanoparticles. The availability of the gold nanoparticles in the solid phase has helped

in the thorough characterization of the material. It has been studied with techniques such as IR spectroscopy, TEM, XPS and elemental analysis.

A number of advantages from this method has led to many studies being conducted on thiol-protected gold nanoparticles. The particle size has been controlled by varying the thiol to gold ratio, interruption of the reaction at different steps and by the use of bulky ligands [185,187–192]. Many different varieties of thiol ligands were attempted for stabilizing the gold surface [187,188,193]. An important development in the monolayer protected clusters (MPC), as thiol-protected gold nanoparticles are called, was the functionalization of the cluster surface with multiple ligands, offering newer possibilities in the chemistry of MPCs [185,191,192]. The synthesis of organic soluble silver nanoparticles was similarly based on detailed studies of silver thiolates [194,195]. In a manner similar to that of gold nanoparticles, thiol-protected silver nanoparticles have been synthesized [196–198].

A few reactions have been attempted using monolayer-protected clusters: oxidation in air in presence of halide ions and TOAB [199], reactivity with amines [191], ozone [200], UV-irradiation in presence of  $\text{CCl}_4$  [201]. An important area of research opened by the discovery of MPCs was the formation of 2D and 3D superlattices [202–210]. It was enabled by the research on control of particle size by a method called digestive ripening (heating a colloidal suspension near the boiling point in the presence of alkanethiols) [211,212]. Similar studies were also conducted for silver superlattices [213–216].

The approach of organic phase synthesis of ligand-protected gold nanoparticles led to the development of many approaches for the preparation of monodisperse gold nanoparticles [217]. A few of these approaches also helped in the synthesis of other noble metal nanoparticles [218]. One of these approaches is the preparation of noble metal nanoparticle in aqueous phase and their consequent transfer to an organic phase for thiol stabilization [197]. The transfer of gold clusters from aqueous phase to organic phase was facilitated by the addition of HCl, which helps in the cleaning of the surface of Au particles and facilitates their transfer to the organic layer. This method has also been adapted for the preparation of other transition metal nanoparticles.

*5.1.3. Dendrimer-assisted nanoparticle synthesis*

Dendrimers represent a novel category of uniformly sized polymeric molecules, with a regular and highly branched three-dimensional architecture. Dendrimers have been interesting substrates for metal nanoparticle synthesis, primarily due to their uniform structure and their ability to protect the nanoparticle surface from agglomeration through the steric effect of the dendritic chain.

The synthesis, interesting properties and applications of dendrimers have been discussed in many review articles and books [219–221] and are not discussed here.

The two most commonly used dendrimers are polyamidoamine (PAMAM) dendrimers and poly(propylene imine) (PPI) dendrimers. Typical chemical structures are represented in Fig. 8 and physical characteristics are given in Table 7. PAMAM dendrimers consist of a core, branch cells and a terminal group. The synthesis usually initiates with ethylenediamine which undergoes Michael addition of methyl acrylate to the amine group. This step is followed by amidation reaction with excess ethylenediamine. The synthesis of PPI dendrimers initiates with 1,4-diaminobutane which undergoes Michael addition of acrylonitrile to the primary amino groups followed by hydrogenation reaction. The diameter of PAMAM dendrimers increases by roughly 1 nm per generation whereas the molecular weight and number of functional groups increase exponentially. PPI dendrimers are considerably smaller than the equivalent PAMAM dendrimers (e.g., G4 PPI: 2.8 nm, G4 PAMAM: 4.5 nm where Gn represents the generation, refer to Table 7). Some of the interesting properties of dendrimers reveal themselves through their structure. High

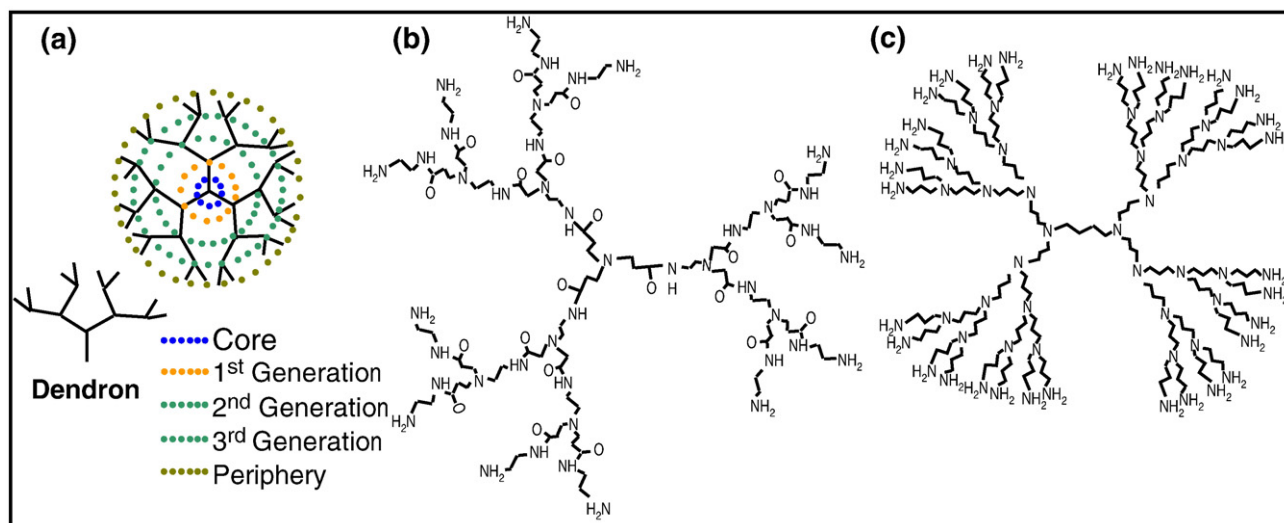


**Fig. 8.** (a) Cartoon representation of a three-dimensional dendrimer. A dendrimer and dendron are represented with solid lines. The colored, broken lines identify the various key regions of the dendrimer. (b) G-2 PAMAM dendrimer (c) G-3 PPI dendrimer [222].

generation PAMAM dendrimers have a three-dimensional structure with more closely spaced terminal groups (which accommodate metal ions) and interior void spaces (which accommodate nanosized matter). The PPI dendrimers similarly interact with incoming guest molecules, with an exception of the absence of amide groups. PPI dendrimers are stable at very high temperatures and thus can be utilized for high-temperature catalysis (the onset of weight loss for G4 PPI is 470 °C) [222]. The terminal functional group of dendrimers can easily be used to engineer the interaction with molecules of interest. That is, long aliphatic chains can be activated on dendrimer surfaces so as to render the dendrimers lipophilic, without affecting the binding properties of organic species with dendritic macromolecules. Similarly, the dielectric gradient between the core and the surface (owing to the presence of different reacting species) can be tuned for the encapsulation of the incoming guest molecule. In addition, the target molecules can be engulfed in the cavity of the dendrimer by providing appropriate molecular functionality within the cavity [222,223].

#### Overview of dendrimer-cation chemistry:

The presence of multiple functional groups and the large 3-D shapes make them useful for attracting ions and molecules. The chemistry and the nature of the interactions are largely dependent on the porosity of the dendrite, presence of functional groups and the nature of incoming species. An example is widely studied  $\text{Cu}^{2+}$ -PAMAM system [222].

To increase the metal adsorption capacity and form metal nanoparticles, it is imperative that metal ions be trapped in the interior structure of the dendrimer (protection against agglomeration). This is usually attempted by selective protonation or hydroxylation of surface amines (surface amine is more basic as it is primary in nature) [225,226]. The  $\text{Cu}^{2+}$ -PAMAM composite is formed by homogenizing the aqueous solution of  $\text{Cu}^{2+}$  salt and methanolic solution of hydroxyl-terminated PAMAM (G4-OH). In aqueous phase,  $\text{Cu}^{2+}$  exists primarily as a hydrated ion,  $[\text{Cu}(\text{H}_2\text{O})_6]^{2+}$ , which has a broad, weak absorption band centered at 810 nm (d-d transition, Fig. 9(a)). The interaction of  $\text{Cu}^{2+}$  with PAMAM leads to two changes in the absorption spectrum: a band due to d-d transition gains more prominence and shifts to 605 nm, a new band due to strong ligand-to-metal interaction appears at 300 nm [227]. Further investigations of the  $\text{Cu}^{2+}$ -(G4-OH) composite revealed interesting information:

- The interaction between  $\text{Cu}^{2+}$  and G4-OH is quite strong (no absorbance intensity change after dialysis with pure water)

- With increasing  $[\text{Cu}^{2+}]/[\text{G4-OH}]$  ratio, the absorbance intensity increases and then saturates. This indicates the saturation adsorption of  $\text{Cu}^{2+}$ . Titration results indicated that each G4-OH dendrimer sorbs up to 16  $\text{Cu}^{2+}$  ions at  $\text{pH} > 7.5$ .
- There exists a linear relationship between the number of complexed  $\text{Cu}^{2+}$  ions and generation of the dendrimer (Gn-OH) since the number of tertiary amine group varies linearly with the generation of the dendrimer.
- Innermost amine groups are likely to be utilized for binding of amide groups or water molecules. Each metal ion coordinates with two amine groups and the outermost 16 pairs of tertiary amine groups are utilized in the case of G4-OH (Fig. 9(b)).
- The nature of the interaction between the metal ion and dendrimer varies with the form in which the metal ion exists in the aqueous phase.  $\text{Cu}^{2+}$  interacts with tertiary amine groups by complexation;  $\text{PtCl}_4^{2-}$  undergoes a slow ligand-exchange reaction involving substitution of one chloride ion for one interior tertiary amine.

#### Overview of dendrimer-metal nanoparticle chemistry:

Dendrimer-metal nanoparticle composites can easily be prepared by the reduction of  $\text{Cu}^{2+}$ -(G4-OH) with excess sodium borohydride.

**Table 7**  
Physical characteristics of PAMAM and PPI dendrimers [224].

Generation	Surface groups	Tertiary amines	Molecular weight (amu) <sup>a</sup>		Diameter (nm) <sup>b</sup>	
			PAMAM	PPI <sup>c</sup>	PAMAM	PPI <sup>c</sup>
1	4	2	517	317	1.5	0.9
2	8	6	1430	773	2.2	1.4
3	16	14	3256	1687	2.9	1.9
4	32	30	6909	3514	3.6	2.4
5	64	62	14,215	7168	4.5	2.8
6	128	126	28,826	14,476	5.4	–
7	256	254	58,048	29,093	6.7	–
8	512	510	116,493	58,326	8.1	–
9	1024	1022	233,383	116,792	9.7	–
10	2048	2046	467,162	235,494	11.4	–
	4096	4094	934,720	469,359	13.5	–

<sup>a</sup>Molecular weight is based on defect-free, ideal structure of dendrimers. <sup>b</sup>For PAMAM dendrimers, the molecular dimensions were determined by size-exclusion chromatography and the dimensions of PPI dendrimers were determined by Small Angle Neutron Scattering (SANS); data for the high-generation PPI dendrimers are not available. <sup>c</sup>We have used the generation nomenclature typical for PAMAM dendrimers throughout this chapter. In the scientific literature, the PPI family of dendrimers is incremented by one.



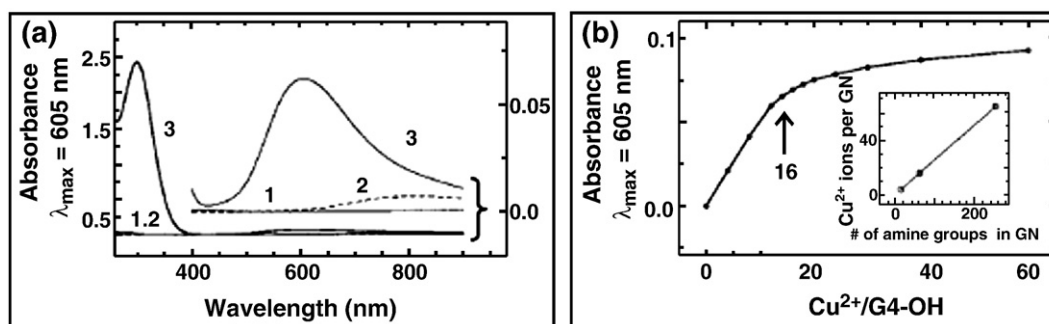


**Fig. 9.** (a) Absorption spectra of 0.6 mM  $\text{CuSO}_4$  in the presence (spectrum 3) and absence (spectrum 2) of 0.05 mM G4-OH. The absorption spectrum of 0.05 mM G4-OH vs. water is also shown (spectrum 1) [224]. (b) Spectrophotometric titration plot: absorbance at the peak maximum of 605 nm as a function of the number of  $\text{Cu}^{2+}$  ions per G4-OH. The inset shows the relationship between the number of  $\text{Cu}^{2+}$  ions complexed within Gn-OH and the number of tertiary amine groups within Gn-OH [224].

The reduction leads to changes in the spectroscopic signatures, i.e., the disappearance of the d-d transition band and the band due to ligand-to-metal interaction together with the appearance of a monotonically increasing intensity around 570 nm. The exponential shape in the UV region of the absorption spectrum is characteristic of a band-like electronic structure, suggesting the presence of zerovalent Cu as clusters. This is confirmed by TEM images revealing the particle size to be less than 1.8 nm. The intra-dendrimer Cu clusters (prepared with G4-OH) are extremely stable despite their small size. Curve 3 in Fig. 10(a) shows the appearance of a plasmon peak when  $\text{Cu}^{2+}$ -(G4-NH<sub>2</sub>) was reduced with  $\text{NaBH}_4$ . This indicated the formation of larger size Cu nanoparticles, which is likely to be on the exterior of the dendrimer.

The syntheses of dendrimer protected nanoparticles of other noble metals such as gold [228–230], palladium [226] and platinum [226,231] have been reported. Effort has been made to synthesize dendrimer protected silver nanodots exhibiting fluorescence [232]. It is quite clear that dendrimer plays a critical role in stabilizing the cluster/nanoparticle surface and thereby dramatically increasing the stability of such species.

#### 5.1.4. Biological synthesis of metal nanoparticles

The interaction of biological systems with metal ions is an old subject. Detailed studies have been conducted on the interaction of micro-organisms with toxic metal ions. The key interest is to explore the long-term toxicity effects of metal accumulation in micro-organisms, bioleaching processes of ores, biological metal recovery systems and bioremediation of metal contamination. During this process, it was understood that there are multiple mechanisms by which micro-organisms tackle metal ions: modification of the re-

dox state of metal ions, extra-cellular complexation or precipitation, outward flux of metal ions and the lack of specific metal transport systems [233].

The evolution of the understanding on how living systems can be a factory for nanomaterials production presents a compelling story. Research began with the discovery of magnetic materials inside living systems. This led many researchers to study the interaction of living system with external magnetic fields, which was thus utilized to effect an externally controlled alignment of the cellular system. This interaction was attributed to the presence of magnetite (iron as Fe(II) and Fe(III)) in intra-cellular spaces [234–236]. The presence of Fe(II) was quite surprising. The subsequent research to understand the presence of Fe(II) led to an important revelation: living systems are capable of reducing ferric oxide through a metabolic cycle [237]. This was indeed the first evidence of the living systems' capability to reduce metal to the zerovalent form. It also gave the first indication towards the presence of nano-sized magnetite in the cell structure. This led to a sudden spurt in interest to explore the bio-reduction capabilities of micro-organisms [238,239]. Studies were also conducted on the formation of gold colloid by a soil bacterium, *Bacillus subtilis* [239,240].

Interesting possibilities were opened by the study of a bacterial strain, *Pseudomonas stutzeri*, with silver ions [241]. It was found that bacterial cells synthesize silver nanoparticles with well-defined compositions and shapes (Fig. 11). A new line of research based on bio-synthesis of noble metal nanoparticles was established. This led to a rapid increase in scientific interest to explore micro-organisms as a bio-factory. Many microorganisms including living plants [242], plant extracts [243], bacteria [241,244], fungi [245–247] and human cells [248] have been studied for bio-synthesis of noble metal

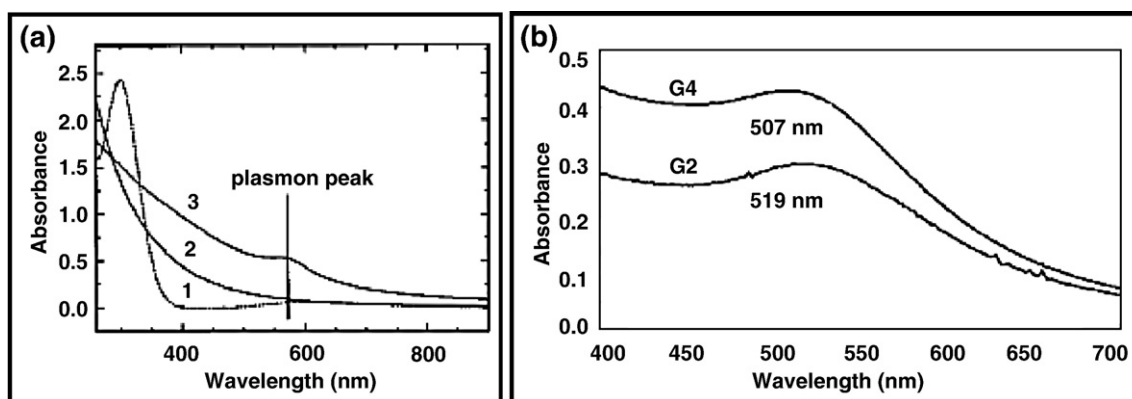


**Fig. 10.** (a) Absorption spectra of a solution containing 0.6 mM  $\text{CuSO}_4$  and 0.05 mM G4-OH before (dashed line, curve 1) and after (solid line, curve 2) reduction with a 5-fold molar excess of  $\text{NaBH}_4$ . Curve 3 was obtained under the same conditions as those for curve 2 except 0.05 mM G4-NH<sub>2</sub> was used in place of G4-OH [224]. (b) UV-vis spectra of ethanolic solutions of Au-colloids prepared using G4 and G2 dendrimers. The peaks arise from the surface-plasmon absorption for Au. Spectra are normalized to an absorbance of ~1 at 250 nm (not shown) to facilitate comparison [224].

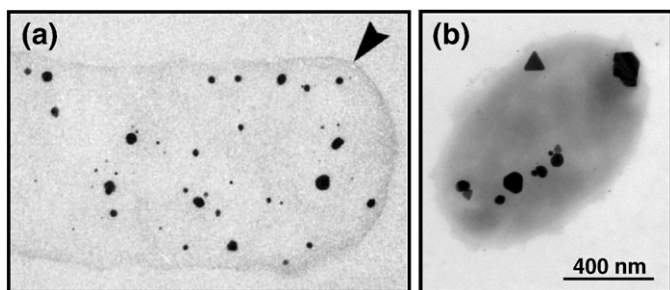
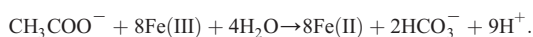


**Fig. 11.** (a) Unstained thin-section electron micrograph of part of a *Bacillus subtilis* cell (arrowhead) with intracellular gold colloids [239]. (b) Triangular, hexagonal, and spherical Ag-containing nanoparticles accumulated at different cellular binding sites (produced by *P. stutzeri* AG259) [241].

nanoparticles. A few review articles have been written on the subject [249–252] and readers are advised to refer to them for details.

A number of observations on the study of metal ions with different micro-organisms throw light on the synthesis mechanism. Extracellular as well as intracellular synthesis of metal nanoparticles has been reported for different living systems. While the fungus *Fusarium oxysporum* synthesizes noble metal nanoparticles extracellularly [253], the fungus *Verticillium sp.* does it intracellularly [245]. During the process of bio-synthesis of nanoparticles, cells continued to remain viable even in the absence of any growth medium, indicating the involvement of metal ions in the cellular metabolic process [248]. The presence of periplasmic silver binding protein has been studied. It is suggested that the action of this protein protects the cytoplasm from silver toxicity. The initially formed clusters aggregate to a larger size, so as to reduce their effective surface energy. The larger aggregates are neutralized by the silver binding proteins, inactivating the silver particles for any participation in cellular toxicity [244]. It is also likely that the aggregation may be induced by the presence of various salts in the cellular system. The reduction of metals in anaerobic environment is a result of direct enzymatic action by bacteria, for example, Fe(III) reducing microorganism, strain GS15, grows under the anaerobic conditions by enzymatically coupling the oxidation of acetate to carbon dioxide with the reduction of Fe(III) to Fe(II) as per the following reaction [238]:



The detailed understanding of the mechanism began with the isolation of various proteins involved in the transport and reduction of metal ions and their subsequent stabilization. It was found that a number of peptides specifically bind to inorganic surfaces [254,255]. A multiple repeat 14-amino acid sequence, [MHGKTQATSGTIQS]<sub>n</sub>, expressed on the outer surface of *Escherichia coli*, was found to interact with gold substrates. In a separate study, a variety of repeating poly-

peptides encoded in genes containing a specific amino acid sequence were found to influence the crystal growth of gold nanoparticles [256]. A subsequent study suggested that the 14-amino acid sequence, expressed on the outer surface of *E. coli* within the phage  $\lambda$ -receptor protein *lamB*, binds Au(III) ions in the form of a 1:1 complex [257]. The polypeptide maintains its unfolded confirmation upon addition of Au(III).

Similar studies were conducted with other noble metals to explain their uptake and reduction. It was reiterated that the overall charge of the peptide plays a key role in the nanoparticle synthesis [258]; peptides with isoelectric pH in acidic region are suited for nanoparticle synthesis. Pure amino acids such as proline, lysine, arginine or serine are incapable of forming silver nanoparticles. Enrichment of proline residue and conservation of polar, hydrophobic, and hydroxyl-containing small amino acids leads to increased formation of silver crystals. The second aspect is highlighted in the gold-binding [259] and platinum-binding polypeptide sequences [251]. The formation of flat-plate like morphology was explained by peptide-induced crystal growth on low-energy [111] surfaces.

### 5.1.5. Brief glimpse into the synthesis protocols for anisotropic structures of metal nanoparticles

Two cornerstones of nanomaterials research have been the size and shape dependence of chemical properties. As mentioned earlier, the origin of novel properties in metal nanoparticles with variation in size of the particle is attributed to an increase in surface to bulk atoms and appearance of surface plasmon resonance. The dependence of properties on the shape of the particles originates due to different reasons: The surface energy, electronic structure and the stability of different facets vary to a large extent. This is illustrated by optical properties of gold nanostructures, as observed for a variety of anisotropic structures (Fig. 12), for example, spherical particles absorb electromagnetic spectrum in the visible region whereas nanotriangles also absorb in the near-infrared region [260]. On the contrary, gold nanorods show two plasmonic structures: longitudinal plasmon (owing to electronic oscillations parallel to the longitudinal axis) and transverse plasmon (owing to electronic oscillations parallel to the transverse axis). There are changes in the SERS activity with shape, which is reviewed elsewhere (Section 5.4.4). Shape-dependent variation in the catalytic properties of noble metal nanoparticles has been observed (Section 5.2).

It is important to know that many of the noble metals crystallize in the face-centered-cubic structure when present in the bulk form. Therefore, the process of anisotropic structure formation is thermodynamically hindered [261]. In this section, we highlight a few important aspects of shape-specific synthesis of noble metal nanomaterials, using specific examples. Detailed review articles are available on the subject of synthesis of anisotropic nanostructures [89,262–266].

#### Metal nanorods

Gold nanorods have gained immense scientific popularity, owing to their multiple plasmon bands with synthesis-driven tenability [267], an absorption feature in the NIR region [268,269], a dramatic

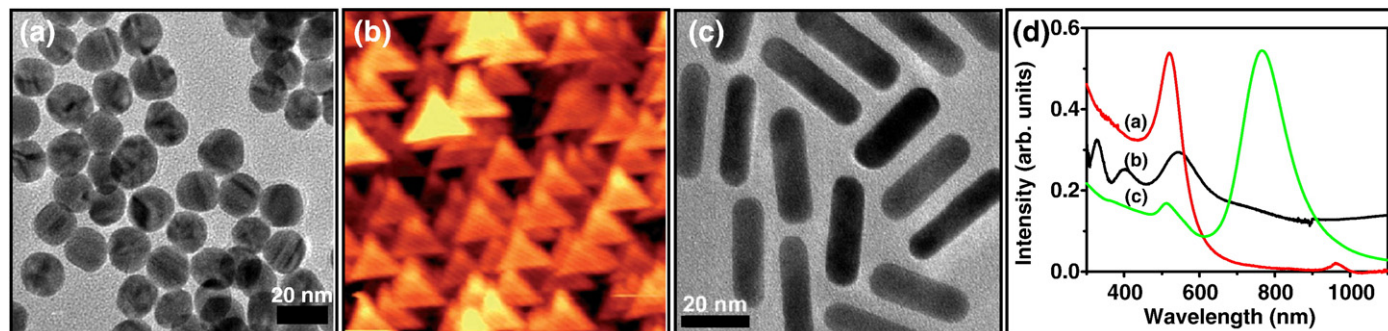


**Fig. 12.** (a) TEM image of citrate-capped gold nanoparticles, (b) contact mode AFM image (2  $\mu\text{m}$  X 2  $\mu\text{m}$ ) of gold nanotriangles, (c) TEM image of gold nanorods and (d) corresponding absorption spectra. Data from the author's laboratory.

increase in fluorescence quantum yield [270], large SERS activity and self-assembly in the presence of externally added reagents [271,272].

In a typical process based on seed-mediated chemical synthesis, 4 nm spherical gold particles (“seed”) are obtained by the reduction of  $\text{HAuCl}_4$  with  $\text{NaBH}_4$  in the presence of CTAB. Subsequently, CTAB,  $\text{HAuCl}_4$  and  $\text{AgNO}_3$  solutions were added in that order, followed by gentle mixing (color: bright brown-yellow). Thereafter, the addition of ascorbic acid leads to a colorless solution. A seed solution is added and the mixture is left undisturbed for 2 h. A weak reducing agent such as ascorbic acid, by itself, can't reduce metal salt completely at room temperature. However, the presence of seed particles helps in initiating nucleation process on their surface to yield gold nanorods.

**Role of seed particles:** Seeds invariably play a critical role in the synthesis of anisotropic structures. Due to the inherent instability of small metal nanoparticles, structural changes are natural even at room temperature. It is known that the surface potential energy goes through various minima with each minima corresponding to a stable configuration at those conditions. As the particles go to small sizes, the energy gap between minima reduces drastically, and a transition can even be induced at room temperature.

**Role of surfactant:** The role of surfactant in the nanorod synthesis is based on two aspects: nature of surface charge of the seed particles and nature of synthesized nanorod [262]. Negatively charged seeds (e.g., citrate) produced nanorods with a wider range of aspect ratios whereas positively charged seeds (e.g., CTAB) produced nanorods with relatively high monodispersity. Surfactant also plays a key role in determining the size of the seed particle which in turn affects the aspect ratio of the nanorod.

**Role of co-metal ion:** Formation of nanorods relies on the coordination chemistry between the surface of the seed particle and additives such as surfactants, passivants, chelating agents, or polymers which hinder the growth of certain crystal faces, promoting an overall lengthening of the seed particle as the metal ions of a growth solution are reduced at the exposed faces [273].

## 5.2. Origin of reactivity

In Section 1, we briefly touched upon the properties of noble metals in the bulk state. Primarily the nobility of noble metals in bulk

is explained using standard reduction potentials, molecular orbital theory, density of states and relativistic contraction.

To understand the origin of reactivity at the nanoscale, it is imperative to understand the following two aspects: (i) electronic states and (ii) shape and size dependence of chemical properties. Review articles have covered these aspects in greater detail [112,274].

**Electronic states:** The underlying building blocks of any material, be it nanoparticle or bulk material, are atoms and molecules, each of which have discrete energy levels or orbitals. The concept of atomic orbitals has been used to present a simplified view of energy states in an atom. Similarly, molecular orbital theory has been developed to explain the molecular energy states. As the number of atoms keeps increasing, the complex nature of interactions between multiple atoms leads to the formation of a variety of energy bands (Fig. 13(a)). Challenges in theoretical modeling due to the complex interactions in multi-atom systems have been addressed by certain assumptions: perfect translational symmetry of the crystal structure and neglect of contributions from the crystal surface due to the assumption of treating multi-atom system as an infinite solid [112]. The discrete energy levels as observed in the atom pave way for the formation of broad energy bands in the bulk material. Many of the properties at the bulk scale arise owing to movement of electrons in such broad energy bands; e.g., the electrons in metals are highly delocalized and thus the energy gap between valence and conduction bands disappears which leads to electrical conduction. Similarly, the electronic excitation from valence band to conduction band, induced by electromagnetic radiation, leads to the formation of electrons and holes which are utilized for photo-catalytic applications.

Some of the assumptions mentioned above to explain the organization of bulk material, point towards interesting possibilities: what if perfect translational symmetry doesn't hold true (variation of properties with asymmetrical organization i.e., shape-dependent properties) and what if the assumption of an infinite solid doesn't hold true (variation of properties with extent of lattice organization i.e., size-dependent properties).

The nanodimension can be thought of as a transition point from atomic scale properties to bulk properties. This is usually explained by quantum-size effects, as the free-electron gas is confined in a sphere [275–278]. The electron energy spectrum of small metal particles

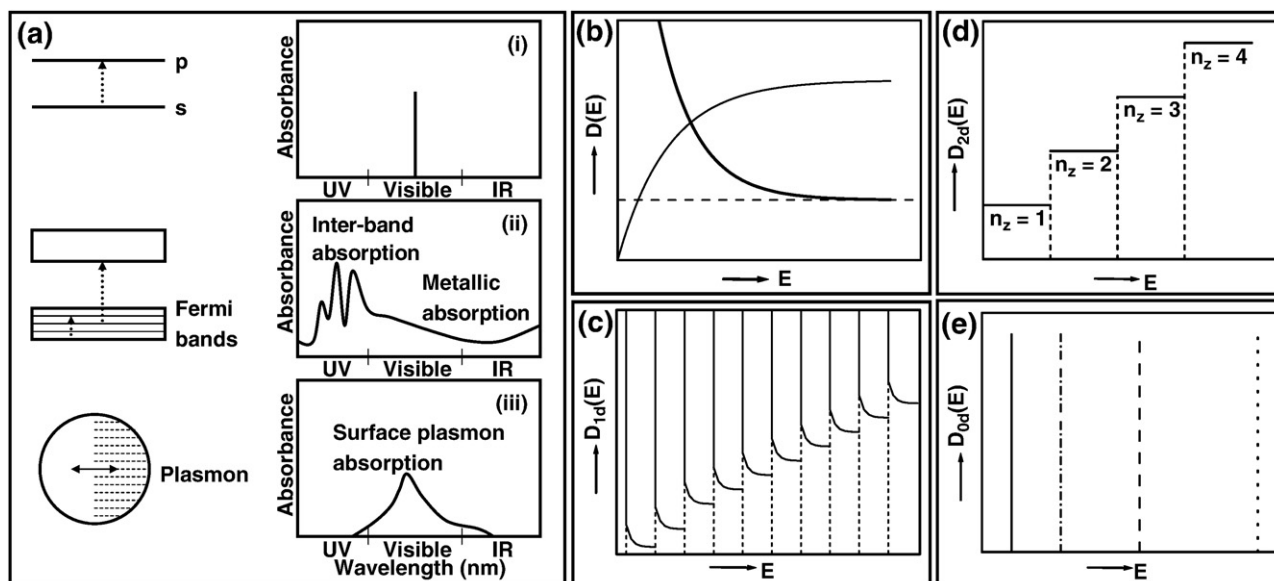


**Fig. 13.** (a) Schematic representation of band transitions and corresponding UV-visible-NIR spectra for (i) atoms, (ii) metals and (iii) clusters. (b) Schematic plot of density of states of an ideal electron gas in three, two and one dimensions (represented as  $D_{0d}(E)$ ,  $D_{1d}(E)$  and  $D_{2d}(E)$  respectively): light solid line – quantum dot, dashed line – quantum plane, dark solid line – quantum well. (c) Quantum well: Electrons can occupy quasi-continuous energy states in one dimension and discrete states in the other two. Each of the hyperbolas corresponds to discrete energy state of two dimensions. (d) Quantum plane: Electrons can occupy quasi-continuous energy states in two dimensions and a discrete state in the third. The density of states for a given discrete energy state ( $n_z = 1, 2, 3, 4, \dots$ ) does not depend on the energy. (e) Quantum dot: Electrons can occupy only states with these discrete energies.



exhibits discrete behavior (in contrast to a continuum energy spectrum at the bulk scale) owing to the presence of a limited number of conduction electrons. This manifests itself in the form of property changes at the nanoscale. Explanations based on Fermi energy developed in the free-electron gas model, offer a better understanding [276]:

For electrons in a sphere, the Fermi energy is calculated as  $E_F = (\hbar/2\pi)^2(3\pi^2n/2m)^{2/3}$  where  $n$  represent the density of electrons. Now, as one keeps reducing the size of the particle, the number of conduction electrons continuously shrinks. By definition,  $E_F$  is the energy of the highest occupied quantum state at absolute zero and is thus fixed. Since all the energy states up to  $E_F$  are occupied, at smaller particle size, the spacing between the degenerate energy level increases.

The energy spacing  $\delta$  is calculated as  $\delta \approx E_F/N$  where  $N$  is the number of conduction electrons. Here  $N$  is inversely proportional to the particle size,  $V$ .

The effect of particle size on the energy spacing becomes pronounced below a critical size when the energy band spacing becomes greater than the thermal energy,  $k_B T$ , and thus below the temperature  $T$ , metals start exhibiting *non-metallic* properties. This can be calculated for silver ( $n = 6 \times 10^{22} \text{ cm}^{-3}$ ) as follows:

$$\delta = \left(\frac{\hbar^2}{2Vm}\right) (3\pi^2n)^{-1/3}$$

i.e.  $\delta/k_B = 1.45 \times 10^{-18}/V$  (Note :  $\delta/k_B$  is a dimensionless quantity).

At  $T = 1 \text{ K}$ , for the energy band spacing to be greater than the thermal energy,  $\delta > k_B T$ , the particle diameter  $d \leq 14 \text{ nm}$ . This means that small *metal* particles will remain electrically neutral and exhibit an energy gap, lacking sufficient energy to enable delocalization of electrons (“*non-metallic state*”) [276]. This justifies the presence of size-dependent transitions from metallic properties (i.e. metal like behavior) to non-metallic properties (i.e. atom-like behavior).

The concept of quantum confinement of electrons in a solid has been studied in detail [279,280], resulting in explanations for electronic structure in the case of confinement shrinking to nanoscale [64]. To understand quantum confinement, it is important to note that for metals, the wavelength of the Fermi electron is typically around 10 nm. Calculations based on quantum confinement revealed interesting predictions [112]:

- Confinement in all three directions (*Zero-dimensional electron gas*): All the dimensions of the particle are comparable to an electron wavelength i.e. the delocalization of free electron in the particle is confined. In a solid, the allowed wavenumbers for a wave propagation are separated by  $\Delta k = 2\pi/d_{x,y,z}$  where  $d_{x,y,z}$  is the

thickness of the solid. In case of small particles, energy levels become discrete as  $\Delta k$  becomes finite. Thus, for the confined electron gas, electrons can occupy only states with discrete energies (Fig. 13).

- Confinement in two directions (*One-dimensional electron gas*): The delocalization of a free electron in the particle is restricted in two dimensions due to the solid boundary. Electrons occupy quantized states in two dimensions; whereas, there is a quasi-continuous energy state in the other dimension. The density of states (number of states per unit interval of wavevector  $k$ ) is calculated as  $D_{1d}(k) = dN(E)/dE = [dN(k)/dk]dk/dE \propto 1/\sqrt{E}$ .
- Confinement in one direction (*Two-dimensional electron gas*): The delocalization of free electrons in the particle is infinitely extended in two dimensions and is restricted along the third dimension. The quasi-continuous energy state in two directions is calculated based on periodic boundary conditions whereas movement in third direction is quantized.

The density of states is  $D_{2d}(k) = dN(E)/dE = [dN(k)/dk]dk/dE \propto \sqrt{E[1/\sqrt{E}]} \propto 1$ .

Thus, for a quantum plane, while the energy spectra in two dimensions are quasi-continuous, the density of states is a step function. The two-dimensional conductivity property of a quantum-plane has significant technological impact in, for example, the electrical conductivity of grapheme [281,282].

*Shape and size dependence of chemical properties:* While significant changes at the scale of clusters are defined through the origin of molecular behavior, considerable changes in chemical properties are observed even due to size and shape variations at the nanoscale.

(a) Shape dependence: The unusual enhancement in chemical reactivity due to the presence of high-energy index planes have been extensively studied with bulk scale materials; examples include catalytic decomposition of NO with Pt[4 1 0] [283], electro-reduction of  $\text{CO}_2$  with Pt[2 1 0] [284] and hydrogenolysis of isobutene with Pt[10 8 7] [285]. Similar results have been obtained with platinum nanocrystals containing high-energy facets [286].

Nanoparticles of different shapes have differences in the exposed surfaces. This leads to differences in atomic distribution across the nanoparticle surface, which in turn affects the electron transfer rate kinetics between metal nanoparticles and corresponding adsorbed species. Accordingly, nanoparticles have been reported to have higher catalytic activity when they are present in the tetrahedral structure vs. cubic vs. spherical structure [287]. This is attributed to enhancement in chemical reactivity at the sharp edges and corners and can easily be correlated with the number of atoms found at the respective places (Fig. 14a). A 4.5 nm sized tetrahedral nanoparticle is composed entirely of [1 1 1] facets, with sharp edges and corners, which contain ~28% of the total atoms and ~35% of the surface atoms in the nanoparticle. A 7.1 nm sized cubic nanoparticle is composed entirely

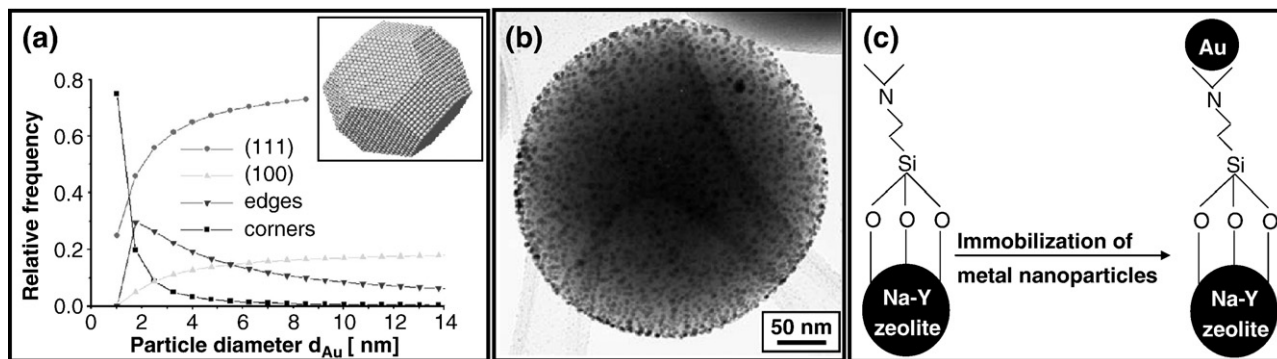


Fig. 14. (a) Graphical representation of percentage of atoms found on various facets of a nanoparticle, calculated using a theoretical modeling scheme for a cubo-octahedron model (shown in the inset) [292]. (b) TEM image of gold nanoparticles deposited on silica using an incipient wet impregnation method [298]. (c) Direct assembly of gold nanoparticles on an amine-functionalized zeolite particle [299].

of [1 0 0] facets, with a smaller fraction of atoms on their edges and corners, which contain ~0.5% of total atoms and ~4% of surface atoms in the nanoparticle. A recent study demonstrated the variations in the reaction selectivity of different platinum surfaces on the hydrogenation reaction of benzene [288]. Cubo-octahedrons bound by both [1 1 1] and [1 0 0] facets, produces both cyclohexane and cyclohexene, whereas cubic nanocrystals, bound by only [1 0 0] facets, produces cyclohexane only. Recently, it has been suggested that introduction of a second metal to an existing metal nanoparticle creates surface defects. This may help in introducing a new dimension to catalytic activity of bimetallic nanoparticles [289].

It is also to be understood that due to high surface energies of most high-index planes, crystals usually grow perpendicular to such planes. Novel nanoparticle synthesis mechanisms have however, solved this problem. This has contributed significantly to the improvement in high efficiency catalysis [286]. However, high-index planes may get destroyed during the course of catalysis reaction, affecting the catalyst performance and reusability [290]. This issue can be addressed by the use of an appropriate capping agent for surface protection, in which the capping agent leads to minimal loss in catalytic activity [291].

(b) Size dependence: Size dependence of chemical reactivity arises due to the presence of a large number of atoms at the surface of smaller particles. Surface atoms differ from atoms in the bulk of the crystal in that they have an incomplete set of nearest neighbors. The dominant effect of size variation is seen at the lower size domains where variations in the exposed facets composition of a nanoparticle are manifested up to a size range of 10 nm (Fig. 14a). This is clearly evident through changes in the physical properties of the material (2 nm gold particles melt at about 300 K whereas the bulk melting point is 1337 K [44]) as well as in its chemical reactivity (e.g., oxidation of CO on gold nanoparticle surface happens only for nanoparticle size below 4 nm) [90–92]. Thus, a small metal nanocrystal of 1 nm diameter will have ~100% of its atoms on the surface. A nanocrystal of 10 nm diameter on the other hand, would have only 15% of its atoms on the surface.

A useful example of size-dependent catalysis has been demonstrated through gold nanoparticle-catalyzed reduction of nitrophenol to aminophenol [293]. It has been found that the reduction reaction proceeds faster with smaller sized gold nanoparticles. This has been explained through a decrease in the activation energy of the reaction with the particle size, attributed to higher reactivity of the coordinatively unsaturated surface atoms in small particles compared to low-index surface atoms prevalent in larger particles. It has also been found that the catalytic activity of growing nanoparticles is larger than for fully-grown nanoparticle [294].

### 5.3. Heterogeneous catalysis – methods for nanoparticle deposition on supports

Contaminants such as pesticides are removed through homogeneous or heterogeneous chemistry. In the homogeneous process, the molecules of relevance are degraded by the nanoparticles dispersed in the solution phase. This methodology is attractive because it utilizes all the available surface area offered by nanoparticles. However, a major issue of concern is the possible presence of nanoparticles contaminating the purified water. This is important as the dispersed nanoparticles cannot be easily separated. Heterogeneous chemistry utilizes supported nanoparticles. Here, highly dispersed nanoparticles on supports such as oxides, polymers, fibers, etc. are used and water is passed through such media. The binding between the particle and the support must be strong enough to avoid leaching of the particles into water. Additionally, with decrease in size, metal particles gradually become unstable without protecting agents, due to increasing surface energy [68]. Consequently, immobilization of metal nanoparticles on a suitable high-surface-area solid helps in avoiding agglomeration, even though it leads to changes in the properties and behavior of the isolated particles [295].

It is also important to highlight that chemical reactivity of nanoparticles (especially in the lower size regime) can be significantly altered by the nature of the support. A remarkable example is the catalytic oxidation of CO with supported gold nanoparticles [296]. It has been shown that gold nanoparticles around 3 nm in diameter on supports such as TiO<sub>2</sub>, Fe<sub>2</sub>O<sub>3</sub> and Co<sub>2</sub>O<sub>3</sub> are very active for CO oxidation, while particles on more conventional supports like SiO<sub>2</sub> and Al<sub>2</sub>O<sub>3</sub> are practically inactive.

As mentioned, there are numerous methods to attach nanoparticles on supports. Some of these strategies are discussed below.

Impregnation: This is one of the earliest methods used for particle immobilization on supports. In a generalist representation of the method, an aqueous solution of the metal precursors (e.g., HAuCl<sub>4</sub>, AgNO<sub>3</sub>, H<sub>2</sub>PtCl<sub>4</sub>, etc.) is added to the cleaned supports (porous materials – (a) metal oxides such as Al<sub>2</sub>O<sub>3</sub>, SiO<sub>2</sub>, MgO, TiO<sub>2</sub>, MnO<sub>2</sub>, binary, ternary and quaternary oxides, etc. (b) organic supports: activated carbon [297], dendrimers, etc.). The choice of metal oxides is quite important because they also play a critical role in water purification e.g. ternary and quaternary metal oxides containing manganese act as a good choice for heavy metal removal. Therefore, synergistic effects could be driven by the use of noble metal nanoparticles loaded on suitable substrates. The choice of activated carbon as a support is quite important because it has large surface area on which nanoparticles can be loaded efficiently and it also plays important role in water purification. An example is the loading of silver nanoparticles on activated carbon, where both components work synergistically to remove a variety of pesticides from drinking water [297]. Surface cleaning helps in the removal of trapped air and surface impurities. Subsequently, the solution is subjected to a reducing medium (such as NaBH<sub>4</sub>, H<sub>2</sub>, sodium citrate or thermal decomposition). Later, the solution is subjected to high temperature heating for surface activation. This method suffers from an inherent disadvantage as it results in the formation of large, and thus catalytically inactive, particles. This is attributed to the presence of inorganic anions in the solid leading to sintering during thermal activation [298]. One of the major advantages of this method is that it leads to high surface loading of nanoparticles (Fig. 14(b) illustrates the high loading density of gold nanoparticles on silica surface).

In another procedure, nanoparticles can be supported on the support through direct impregnation. In a generalist representation of the method, noble metal nanoparticles prepared separately can be impregnated with metal oxide supports such as Al<sub>2</sub>O<sub>3</sub> or organic supports such as activated carbon [324–326,297].

Ion-exchange: In this method, the cations present on the surface or porous structure of the support are replaced by metal cations followed by calcination at high temperature and reduction. This procedure leads to the formation of extremely small metal particles. However, it suffers from the disadvantage of low cation exchange efficiency leading to a limited number of cationic sites for nanoparticle formation.

The method is illustrated through a representative example. In a typical procedure to synthesize Na-Y zeolite, aluminum powder and sodium chloride were dissolved in an appropriate amount of tetramethyl ammonium hydroxide (TMAOH) solution, followed by the addition of tetraethyl orthosilicate. The resulting solution was left for ageing which results in a gel that was heated at 100 °C for a few days. The solid obtained after heating is centrifuged and washed with distilled water (composition: SiO<sub>2</sub>-Al<sub>2</sub>O<sub>3</sub>-(TMA)<sub>2</sub>O-Na<sub>2</sub>O-H<sub>2</sub>O). To load the metal nanoparticles on the zeolite support, the functionalized zeolite was dispersed in the metal nanoparticle solution and it was centrifuged and washed (Fig. 14c) [299].

Co-precipitation: The salts of first-row metals of the transition series in Groups 4–12, and a few other metals such as aluminum and magnesium, form hydroxides or hydrated oxides in basic medium. Co-precipitation of two hydroxides has often been used to prepare supported base metal catalysts, usually with alumina acting as the support.

The method is illustrated through a representative example: An aqueous solution of metal salt is mixed with the nitrate form of the support and a mild solution of ammonium carbonate is added for pH control. The resultant co-precipitate is dried under vacuum, followed by calcination at high temperature.

**Deposition–Precipitation:** In this method, the precursor for the active species is brought out of solution in the presence of a suspension of the support (e.g., by raising the pH in order to precipitate the salt as a hydroxide). The surface of the support acts as a nucleating agent, and the method, if properly performed, leads to the greater part of the active precursor being attached to the support. The secret lies in preventing the precipitation away from the support surface by avoiding local high concentrations of hydroxide. The chemistry as it applies to the active component therefore closely resembles the one followed in co-precipitation. Deposition–precipitation has the advantage over co-precipitation in that the entire active component remains on the surface of the support and none is buried within it. In addition, a narrower particle size distribution is achieved.

The method is illustrated through a representative example. The nitrate salt of the metal concerned is mixed with oxide based supports. The pH of the solution is adjusted using mild basic reagents. The resulting product is centrifuged and washed to remove excess anions present in the solution, followed by calcination at high temperature. A mixture of metal precursor salts may be used for the preparation of multi-metallic nanoparticles.

**Vapor-Phase Deposition and Grafting:** In this method, a gaseous stream of volatile metal compound is flowed through a porous support, assisted by an inert gas. The chemical interaction between metal salt with the porous support leads to the formation of a precursor. The method is illustrated through a representative example [300]. Carbon spheres, which are used for deposition of metal nanoparticles, are produced through an iron salt catalyzed high temperature reaction between methane and hydrogen gas. The as-produced material was washed with acetone so as to remove heavy hydrocarbon contamination. The nitric acid based oxidative treatment is used for increasing the concentration of grafting sites on the surface, decreasing the surface area and increasing the micro-porous volume without affecting the structure. The resulting carbon support is then mixed with organometallic compounds of desired metal nanoparticle and passed through a fluidized bed CVD reactor using an inert carrier gas.

#### 5.4. Drinking water purification: novel reactions at the nanoscale

The major focus of this section is to review the use of noble metal nanoparticles for the removal and detection of severely toxic contaminants such as pesticides, halogenated organics, heavy metals, and micro-organisms, found in drinking water.

##### 5.4.1. Chemistry of organic compounds with noble metal nanoparticles

The chemistry of noble metals in the bulk form for catalytic synthesis of organic compounds was explored during the early 20th century. While in many cases, salts of noble metals were used as catalysts, the most promising highlight of the research from that period was that *finely divided* noble metals including gold and silver have the capacity to absorb reasonable quantities of hydrogen and oxygen on the surface [301]. This was reportedly playing a critical role in the hydrogenation or oxidation reactions of organic compounds [301]. Thereafter, noble metals have played a critical role in commercial scale organic compound synthesis [302–304]. Recently, the chemistry of noble metal nanoparticles has been utilized to effect several organic reactions. Several review articles are available on the subject [133,264,305–308].

Here, we discuss noble metal nanoparticle-based chemistry for the detection and removal of two sets of organic compounds – pesticides and halogenated organics – from drinking water.

##### *Removal of pesticides with noble metal nanoparticles*

The earliest study of interaction between halogenated organics and transition metals began with the discovery of zero-valent iron catalyzed degradation of halogenated aliphatics [309–311]. It was reported that carbon tetrachloride induces corrosion in the metals, in a way similar to air and water [309–311]. The concepts of corrosion held true: metal surface is oxidized to metal chloride, the degree of corrosion differs with metals as protective layers are formed on some metal surfaces and reactivity is dependent on the reduction potential [309–311]. The reaction product was found to be metal chloride and partially dehalogenated organic compound. This was subsequently followed by the study of other organics with iron metal [113] and then iron nanoparticles for enhanced degradation of pesticides became popular. Several review articles are available on the subject [312–316]. From the elucidation of the reaction mechanism, it became increasingly clear that zerovalent iron (ZVI) acts as a good reducing agent.

The use of ZVI for commercial scale pesticide removal is detrimentally impacted by the following challenges: Reaction by-products and corrosion of catalyst.

In a similar approach, the use of other reactive metals such as magnesium, tin and zinc was attempted to study the degradation of halocarbons [317]. It is to be remembered that in the case of extremely reactive metals, two competing processes happen: metals will catalyze the dehalogenation of organic compounds and metal being thermodynamically unstable in water, will react to form the corresponding metal hydroxide. It was found that in case of magnesium – second process dominates; in case of tin, CO<sub>2</sub> is the dominant product; in case of zinc, CH<sub>4</sub> is the dominant product. Additionally in all the cases, the mineralization of CCl<sub>4</sub> was not complete.

Interestingly, in all the previously studied metal-halocarbon systems over the past 20 years and in early 20th century, noble metals were never thought to be attacked by halocarbons. One of the prime reasons was the extremely low reactivity of noble metals. In early 1998, based on the absorption studies of silver colloid with oxygen and carbon tetrachloride, it was postulated that carbon tetrachloride induces oxidation of silver colloid in a manner similar to oxygen [318]. Another study pointed towards degradation of noble metal clusters through chlorine radicals, produced by UV-irradiation of halogenated organics [200]. It was also suggested that many of the organosulfur compounds adsorb on noble metal nanoparticle surfaces [319]. An interesting result from the latter study is the irreversible adsorption of carbon disulfide. It was suggested that carbon disulfide undergoes dissociation on the silver surface.

In early 2003, the first detailed report appeared on the interaction of noble metal nanoparticles with halocarbons [320]. It was found that noble metals at nanodimensions, react with halocarbons in a manner similar to other metals (i.e. reductive dehalogenation) leading to the formation of metal halide. However, an interesting result was the formation of amorphous carbon in this process [320], i.e. no reaction by-products are formed post-reaction. The reaction was later extended to several halocarbons and was found to be completely efficient at room temperature [320]. As the noble metals in bulk form are not attacked by halocarbons, the reaction of noble metal nanoparticles with halocarbons became a classic example of particle size-based reactivity of metals [320].

The reaction was studied with a number of spectroscopic techniques to understand the reaction mechanism [320]. A gradual decrease in the plasmon intensity of the absorption spectrum was observed, without any shift in the plasmon peak (Fig. 15a). The XRD features of the precipitate obtained after the end of the reaction matched exactly with AgCl confirming the oxidation of metal to metal halide. There were no features for carbon in XRD, indicating that it is amorphous in nature (Fig. 15b). Broad G and D-band signatures of the amorphous carbon centered at 1550 and 1288 cm<sup>-1</sup> appeared in the Raman spectra which confirmed the presence of amorphous carbon (Fig. 15c). Gas chromatography and IR spectroscopy measurements also confirmed the complete mineralization of halocarbon, as no



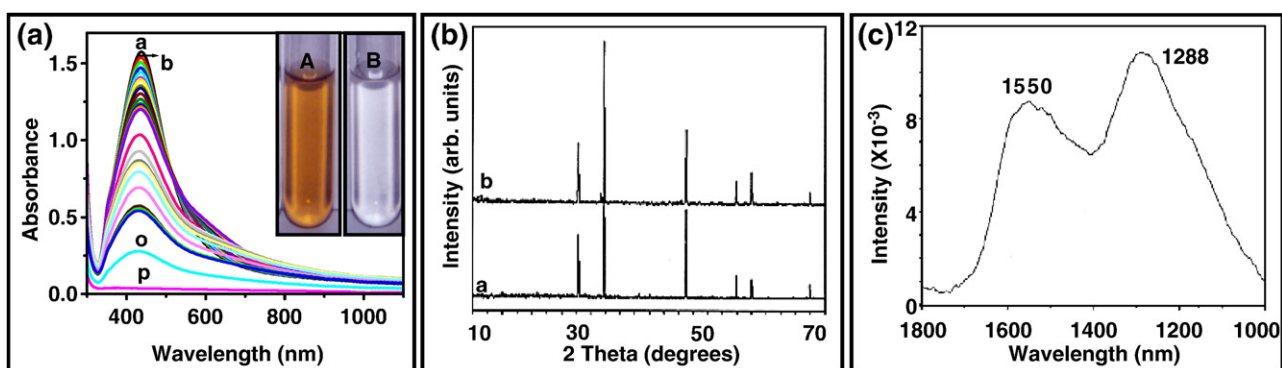


**Fig. 15.** (a) Variation of the UV–visible absorption spectrum of silver nanoparticles upon the addition of  $\text{CCl}_4$ : the feature labeled a represents the plasmonic feature of pure silver nanoparticle whereas b–p are at collected at various time intervals after the addition of  $\text{CCl}_4$ . The inset shows the nanoparticle solution and the reaction product 12 h after adding  $\text{CCl}_4$  [320]. (b) A comparison of the powder diffractograms of a: reaction product of silver nanoparticles with  $\text{CCl}_4$  and b:  $\text{AgCl}$  prepared by adding  $\text{Ag}^+$  to a dilute solution of  $\text{Cl}^-$  [320]. (c) Raman spectrum of amorphous carbon obtained in the reaction between  $\text{Ag}$  clusters and  $\text{CCl}_4$  (G band:  $1550\text{ cm}^{-1}$ , D band:  $1288\text{ cm}^{-1}$ ) [320].

reaction products were detected. The mineralization is also suggested by the increase in the solution conductivity (before reaction:  $3.3 \times 10^3\ \mu\text{S/cm}$ , after reaction:  $3.5 \times 10^4\ \mu\text{S/cm}$ ) and decrease in pH of the solution (before reaction: 9.7, after reaction: 1.2) [321]. The change in conductivity is due to release of  $\text{Cl}^-$  ions from halogenated organics, while the change in pH is due to release of  $\text{H}^+$  during the conversion of 2-propanol, used in the medium, to acetone.

Based on the spectroscopic observations, a reaction mechanism was suggested [320]. The reductive dehalogenation of carbon tetrachloride can be represented as:



The reaction is nearly thermoneutral with bulk noble metal at room temperature. The reaction can also be considered from an electrochemical standpoint:



The reason the reaction proceeds at nanodimensions, can be attributed to the excess surface energy as reviewed in an earlier section. This helps in overcoming the thermochemical barrier and makes the reductive dehalogenation reaction exothermic [320].

The research was extended to another important family of halogenated organics. The reaction of noble metal nanoparticles was studied with widely used pesticides such as endosulfan [322], malathion [323–325] and chlorpyrifos [323–325]. The interaction of pesticides with gold and silver nanoparticles showed different spectroscopic behavior [322]. With endosulfan on gold, a decrease in plasmonic absorption intensity was observed with the emergence of an additional peak at higher wavelength (Fig. 16a) [322]. This is attributed to adsorbate binding on the nanoparticle surface which leads to particle aggregation. This was also observed in the IR signature of the residue obtained after the reaction, where all the features had broadened substantially (Fig. 16c(a,b)). Significant changes in the feature at  $1192\text{ cm}^{-1}$  ( $\text{S}=\text{O}$  bond) and negligible changes in the feature at  $750\text{ cm}^{-1}$  indicate that the interaction largely occurs through the sulfur. In contrast, the plasmon absorption didn't change significantly in the case of endosulfan on silver surfaces. The adsorption of endosulfan on silver surface was confirmed by the IR spectrum of the residue obtained after the reaction (Fig. 16c(a,c)).

An important aspect of the reaction chemistry was highlighted by heterogeneous adsorption of pesticides on nanoparticle surfaces [323,325,326]. The noble metal nanoparticles supported on alumina were very effective for the removal of pesticides from solution (Figs. 16b, 17(a,b)). The gas chromatographic signature confirmed the complete removal of pesticide in the aqueous phase, using alumina supported noble metal nanoparticles, when the input concentration is 50 ppb [323].

Realizing the fact that a number of pesticides found in drinking water are organochlorine (e.g. simazine, lindane, atrazine, etc.) or

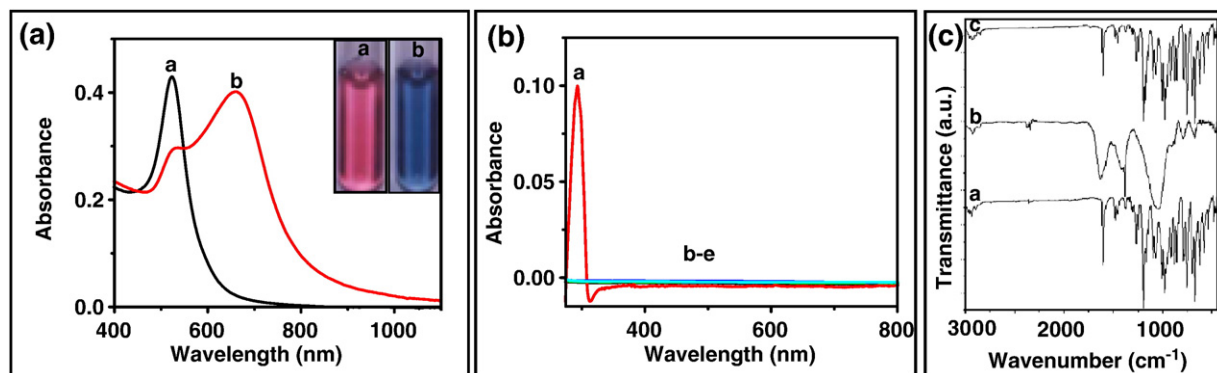


**Fig. 16.** (a) UV–visible absorption spectrum of: a- citrate stabilized gold nanoparticles and b- the effect of exposure of endosulfan at 2 ppm. Corresponding image of the solution are shown in the inset [322]. (b) Absorption spectra showing the complete removal of chlorpyrifos when contaminated water was passed through a column of the supported nanomaterial. Trace a is the spectrum of the parent pesticide solution, b–e after passing through the nanoparticle-loaded column, in repeated experiments [323]. (c) Comparison of the infrared spectra of (a) pure endosulfan, residue after reaction with (b) gold and (c) silver [322].

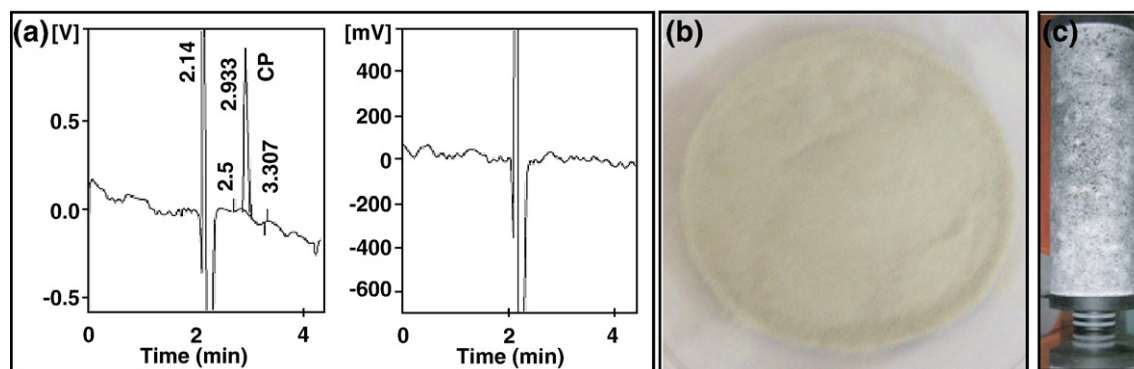


**Fig. 17.** (a) (Left) Gas chromatogram of 1 l of a 50 ppb chlorpyrifos solution extracted with 150 ml of hexane thrice, evaporated to nearly 2 ml in a rotavapor and made up to 10 ml using hexane. The peak at 2.933 is that of chlorpyrifos (labeled CP) and at 2.14 is that of the solvent. (Right) Chromatogram of the chlorpyrifos solution (same concentration as above) after passing through the activated alumina column loaded with silver nanoparticles, extracted with hexane and made up to 10 ml as above, showing the complete disappearance of chlorpyrifos [323]. (b) Silver nanoparticles coated on activated alumina and (c) photograph of a pesticide filter device using supported nanoparticles [321].

organosulfur pesticides (e.g., triazophos, quinalphos, etc.) or contain nitrogen based functional groups (e.g. carbaryl, carbofuran, monochrotofos, etc.), the chemistry of supported noble metal nanoparticles can comfortably be utilized for the complete removal of such pesticides from drinking water. This aspect of complete removal of a wide-variety of pesticides makes the chemistry of supported noble metal nanoparticles unique for drinking water purification.

A separate off-shoot of this work resulted in the formation of a novel class of nanomaterials: halocarbon-induced corrosion of metal cores in core-shell nanoparticles (oxide shell of  $ZrO_2$  and  $SiO_2$ ) which led to the formation of nanobubbles and nanoshells [327,328], having implications in the development of methods for probing the porosity of nanoshells and for studying drug-delivery mechanisms [329–331].

#### 5.4.2. Detection of pesticides in drinking water with noble metal nanoparticles

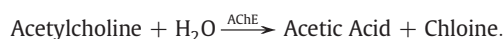
As important as it is to develop novel materials for removal of toxic pesticides from drinking water, it is also imperative to realize that such compounds have become extremely important analytes for ultralow concentration sensing. The large-scale use of different pesticides across the world has contaminated a number of water sources, and thus it is a necessity that rapid, sensitive and selective detection protocols be developed for such molecules [332,333]. Over the past 25 years, many methods have been developed for ultra-low concentration detection of pesticides [334,335]. A number of widely-practiced methods such as chromatography, mass spectrometry, and biosensors, offer high sensitivity and selectivity. However, the aspect of rapid measurement is now being improved by use of nanomaterial chemistry [336]. An important work on the utilization of nanomaterials for biomolecular detection was the use of oligonucleotide-modified gold nanoparticles for colorimetric low-concentration detection of polynucleotide [337]. It is important to realize that while in the case of contaminant removal, a higher surface area of the adsorbent is a pre-requisite whereas in the case of contaminant detection, change in the surface with adsorbate interaction and a consequent manifestation in reliable spectroscopic signatures is a necessity. The selectivity of molecular detection is an important dimension to contaminant detection which can be ensured through the use of appropriate nanomaterials and the choice of an appropriate ligand immobilization on the surface of nanoparticles; e.g., selective detection of cysteine and glutathione at micromolar concentrations using gold nanorods [337].

Overall, there are two approaches followed for ultralow concentration detection of pesticides using gold nanoparticles.

(a) *Changes in the signature properties of a functional group attached to noble metal nanoparticle surface in the presence of organic molecules:* Mostly this approach has not so far been utilized for the detection of pesticides in drinking water. However, the nature of molecules

detected by this technique is similar and thus it can be developed for the detection of pesticides as well. The fluorescence intensity of  $Eu^{3+}$  ions is significantly enhanced when bound to gold nanoparticles [338,339]. The fluorescence can be quenched by the addition of organophosphorus molecules which bind to the gold nanoparticles and consequently lead to the release of  $Eu^{3+}$  ions. In another study, gold nanoparticles supported on silica gel are modified with zirconium ( $Zr^{4+}$ ) and  $POCl_3$  so as to have a zirconium-phosphate terminated surface [340,341]. This surface exhibits strong interaction with organophosphorus compounds and the interaction is manifested through changes in the optical properties of gold nanoparticles. In another approach, gold nanoparticle surfaces have been modified with antibody specific to paraoxon [342] and subsequent exposure to paraoxon is reflected through changes in electrochemical properties. The method has been found to be sensitive at low ppb level. In yet another approach, the ability of a metalloenzyme, organophosphorus hydrolase (OPH), to hydrolyze a large variety of organophosphate pesticides and neurotoxins can be utilized for ultralow concentration detection [343]. Gold nanoparticle surfaces can be modified with the OPH enzyme and fluorophore molecules are positioned at the OPH active sites. The addition of organophosphorus compounds, leading to the release of fluorophore molecule, is measured through the changes in the fluorescence intensity.

Gold nanoparticles are grown through the reducing properties of the product obtained by enzyme-mediated hydrolysis of acetylthiocholine [344]. The enzyme, acetylcholine esterase (AChE), is extremely sensitive to the presence of toxic organic molecules and its catalytic activity gets strongly inhibited. The inhibition of enzyme leads to the blocking of growth of gold nanoparticles as the production of reducing agent is inhibited. The loss of growth is manifested even with nanomolar concentration of toxic organic molecules and is reflected in the optical properties of gold nanoparticles. The AChE (bound on gold nanoparticle surfaces) mediated hydrolysis reaction of acetylthiocholine has also been utilized as pesticide sensor through measurement of electrochemical current, which depends on the extent of formation of thiocholine in the presence of pesticides [345]. A recent review article summarizes the role of gold nanoparticles in immobilization of biomolecules and its use in electrochemical sensing of biomolecules [346]. Thus, it can possibly be utilized for pesticide detection. The enzyme is also known to catalyze the conversion of acetylcholine chloride in the following way [347]:



In presence of organophosphorus pesticide molecule, the activity of AChE to hydrolyze ACh is inhibited. This inhibition is manifested in the form of the attenuation of light when AChE is covalently bound on

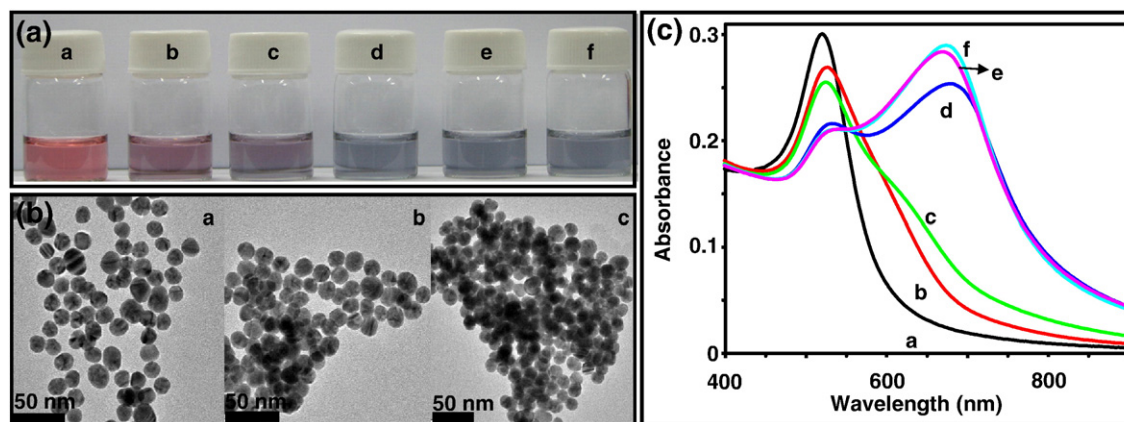


**Fig. 18.** (a) Colorimetric detection of chlorpyrifos using the gold nanoparticle- $\text{Na}_2\text{SO}_4$  system. a: as-prepared gold nanoparticles, b: gold nanoparticles- $\text{Na}_2\text{SO}_4$  mixture and c to f: are 50 ppb, 100 ppb, 500 ppb and 1 ppm chlorpyrifos in gold nanoparticle- $\text{Na}_2\text{SO}_4$  mixture, respectively [351]. (b) TEM images of a: as prepared gold nanoparticles, b: gold nanoparticles after the addition of  $\text{Na}_2\text{SO}_4$  and c: gold nanoparticles after the addition of  $\text{Na}_2\text{SO}_4$  and chlorpyrifos [351]. (c) UV-vis spectra of gold nanoparticles before and after the addition of  $\text{Na}_2\text{SO}_4$  and chlorpyrifos. Trace 'a' is the UV-vis spectrum of as-prepared gold nanoparticles. Trace 'b' is the UV-vis spectrum of a gold nanoparticle- $\text{Na}_2\text{SO}_4$  mixture. Traces 'c-f' are UV-vis spectra of 50 ppb, 100 ppb, 500 ppb and 1000 ppb chlorpyrifos in gold nanoparticles- $\text{Na}_2\text{SO}_4$  mixture, respectively [351].

gold nanoparticle surfaces, and can be correlated with the pesticide concentration [348]. The deactivated AChE can be reactivated with dephosphorylation by 2-pyridine-aldoxime methiodide (2-PAM), and thus the sensor can be reutilized. This method has shown the capability to detect pesticides at low ppb concentrations. A similar method has also been reported with silver nanoparticles where a correlation exists between the shift in plasmon wavelength and pesticide concentration [349]. In another approach, the fluorescence properties of indoxyl, the product of reaction between certain organophosphorus compounds and indole attached to gold nanoparticle surfaces, is utilized for the detection of pesticides [350]. This method is reported to reach a detection limit in ppt level.

(b) *Changes in the optical properties of noble metal nanoparticles upon interaction with pesticides:* From the interaction studies of pesticides with nanoparticles, it is well-understood that chemistry at the nano regime is extremely sensitive even at ultra-low concentrations of the adsorbate. While spectroscopic studies of endo-sulfan-noble metal nanoparticle system offer many methods to detect the changes in signatures of nanoparticles as an indicator to the presence of pesticide on nanoparticle surfaces (e.g., absorption spectrum, FTIR spectrum, etc.), a more defining change was in the color of the solution [322]. Intensity of color change is nearly quantitative and therefore offers a colorimetric method for detection (inset of Fig. 16(a)). It was reported that pesticides can be detected through the colorimetric method, at a concentration level of 1 ppm.

To extend the nanoparticle chemistry at concentrations of relevance in drinking water, salt-induced aggregation of noble metal nanoparticles in the presence of pesticide was studied [351]. The salt-induced aggregation of noble metal nanoparticles is well-studied [352], however, the colorimetric changes due to the presence of pesticides at low concentrations is indeed surprising. The changes in the optical properties are also reflected in absorption measurements. It is suggested that the addition of chlorpyrifos to gold nanoparticle- $\text{Na}_2\text{SO}_4$  solution induces severe aggregation, which is manifested in the form of change in solution color and thus absorption characteristics (Fig. 18) [351]. The simplicity and the quick response time of the measurement offers possibilities for on-field detection [351]. Humic acid protected silver nanoparticles have also been utilized for detection of herbicides through changes in the surface plasmon (position and intensity). The method is reported to show changes only at high concentrations of herbicides [353].

In addition to the two general approaches reviewed earlier, the enhancement of Raman signals in the presence of noble metal nanoparticles has been extensively utilized for the detection of organic molecules. The most highlighting example of SERS-based detection is

the detection of a single Rhodamine 6G molecule [354–357]. With the recent investigations revealing significant Raman signal enhancements in the presence of anisotropic silver nanostructures, the detection of ultra low concentrations of organic molecules is indeed feasible [260,358]. The detection limit can be further improved by the use of Langmuir-Blodgett assembly of anisotropic nanostructures [359]. This approach has recently been utilized for studying the molecular details of protein-DNA interactions [360]. A recent study suggested the use of humic acid protected gold nanoparticles for the detection of organic contaminants [361]. This method is based on the fact that humic acid has high affinity towards a number of organic molecules and the background SERS spectrum of HA is relatively weak in absolute intensity; thus SERS-based detection of organic molecules can be attempted.

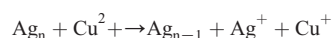
#### 5.4.3. Chemistry of heavy metal ions with noble metal nanoparticles

One of the interesting application areas of noble metal nanoparticles in drinking water purification is the sequestration of heavy metals. The first studies of the interaction of metal ions with noble metal nanoparticles were in the early 1990s [318]. It became clear that many of the previously known properties of metals do not hold true as the size of the crystal reaches the nanometer regime. The redox potential of the microelectrode becomes more positive as the particles grow.

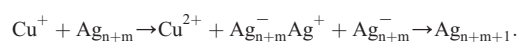


For  $n = 1$  (free silver atom), the potential is  $-1.8$  V and, finally, for  $n \rightarrow \infty$  a potential of  $0.799$  V of the conventional silver electrode is reached [45]. The impact of such size-dependent changes in the electrochemical properties was visible in the interaction studies with pesticides, which has relevance in the sequestration of heavy metals from drinking water.

The reaction of stabilized silver clusters with  $\text{Cu}^{2+}$  was suggested to catalyze the transformation of the clusters into colloidal metal particles, by the following scheme [164]:



followed by similar reaction of  $\text{Ag}_{n-1}$ ,



(Here,  $\text{Ag}_n$  represents cluster composed of  $n$  atoms and  $\text{Ag}_{n+m}$  represents colloidal particle composed of  $n + m$  atoms. The unstable clusters undergo agglomeration to form colloidal particles).



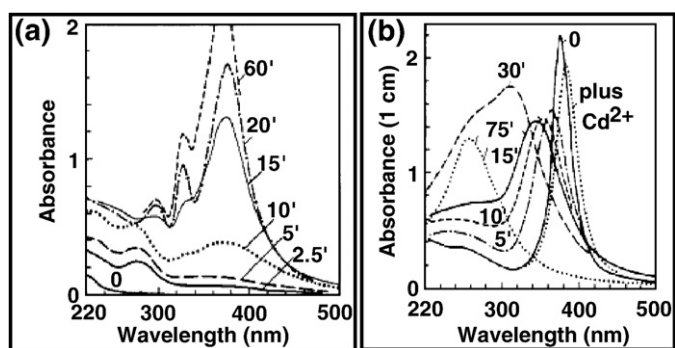


**Fig. 19.** (a) Absorption spectra of a silver salt solution containing polyphosphate during radiolytic reduction after various times of  $\gamma$ -irradiation (time, in minutes, is indicated next to spectrum) [164]. (b) Absorption spectrum of the 0.1 mM silver sol before and after the addition of 0.19 mM  $\text{Cd}^{2+}$ , and after various times of  $\gamma$ -irradiation [362].

The electrochemical feasibility for the first reaction was explained by the rather negative potential of silver clusters. The mechanism was based on the disappearance of the absorption feature of clusters and an increase in the intensity of the 380-nm band of metallic silver, indicating the strong reactivity of clusters with  $\text{Cu}^{2+}$  (Fig. 19a).

The studies were extended to the interaction of  $\text{Cd}^{2+}$  with 4 nm colloidal silver particles [362]. It was suggested that radiolytically generated 1-hydroxyethylmethyl radicals (solvent: acetone + 2-propanol) causes electron transfer leading to the formation of colloidal cadmium. The appearance of an absorption band for colloidal cadmium ( $\lambda = 250\text{--}280$  nm) confirms the reduction. One of the interesting results was the red shift experienced by the silver plasmon band ( $375\text{ nm} \rightarrow 383\text{ nm}$ ). A separate study reported the appearance of a separate absorption feature in the  $550\text{--}600$  nm region, during the interaction of 0.25 mM aqueous solution of silver nanoparticles with 0.02 mM  $\text{Cd}^{2+}$  solution (Fig. 7a) [140]. It is important to mention that the size of the silver nanoparticles was essentially the same in the two experiments. However, while one system shows no change after the addition of metal ions, the other shows an instantaneous appearance of a new feature. This difference in the observation seems to hold true for other metal ions as well.

Many adsorbents have been developed for the removal of mercury from drinking water such as activated carbon [363], polyethyleneimine modified cellulose [364], functionalized membranes [365], functionalized clay [366] and silica [367]. Similarly there have been

research reports on nanomaterial-based removal of mercury from drinking water (Section 7). The pre-requisites of an ideal adsorbent are: extremely high metal adsorption capacity, minimum contamination of the water (e.g., minimum ion-exchange), zero desorption under environmental conditions and economics of operation.

Metal chemistry (as an adsorbent) plays a critical role in the sequestration of heavy metals from drinking water. A number of metal-metal systems exist in the form of alloys, with varying composition depending on phase stability. Gold and mercury exist in several phases such as  $\text{Au}_3\text{Hg}$ ,  $\text{AuHg}$ ,  $\text{AuHg}_3$ . That is, 3.05 g of mercury can be removed using 1 g gold. Thus, a dramatic improvement in the adsorbent capacity can be reached through the use of metal-alloying.

The first sign of metal alloying for sequestration of heavy metals was seen from the data of zerovalent iron (Section 7) [369]. The surface corrosion reduces the capacity of iron to alloy with heavy metals. The importance of the concept for drinking water was first elaborated through the use of noble metal nanoparticles [368]. It was found that reduction of mercury to the zerovalent state followed by alloying with gold nanoparticles translates to an adsorption capacity of 4.065 g/g of gold. The mechanism of the reaction was studied using a number of techniques; e.g., microscopic images revealed a significant growth of the parent gold nanoparticles after addition of mercury (Fig. 20a). An amorphous layer of mercury was also observed around the nanoparticles. A shift in the plasmon position was also observed along with a significant modification in the peak shape (Fig. 20b). The formation of an alloy was confirmed by the existence of the  $\text{Au}_3\text{Hg}$  phase in the X-ray diffractogram (Fig. 20c). It means that only 738 mg of gold is required to treat 3500 l of 1 ppm mercury, a concentration which is 100 times the detected level in many places of India [368].

To explore further, we recently studied the interaction of silver nanoparticles with  $\text{Hg}(\text{II})$  ions [370]. As mentioned earlier, the zerovalent form of heavy metals can be adsorbed by noble metal nanoparticles, with high adsorption capacity. The interest in silver nanoparticles is driven by two aspects: the enhanced ability of silver to participate in a reaction as a reducing agent for mercury and its ability to exist with mercury in different phases.

It was found that the surface plasmon of silver nanoparticles experience a blue shift along with a decrease in the intensity, immediately after the addition of  $\text{Hg}^{2+}$  ions (Fig. 21(a)). The decrease in intensity is attributed to partial oxidation of silver nanoparticles to silver ions. The shift is attributed to the incorporation of mercury into the silver nanoparticles. A separate study of mercury metal with silver

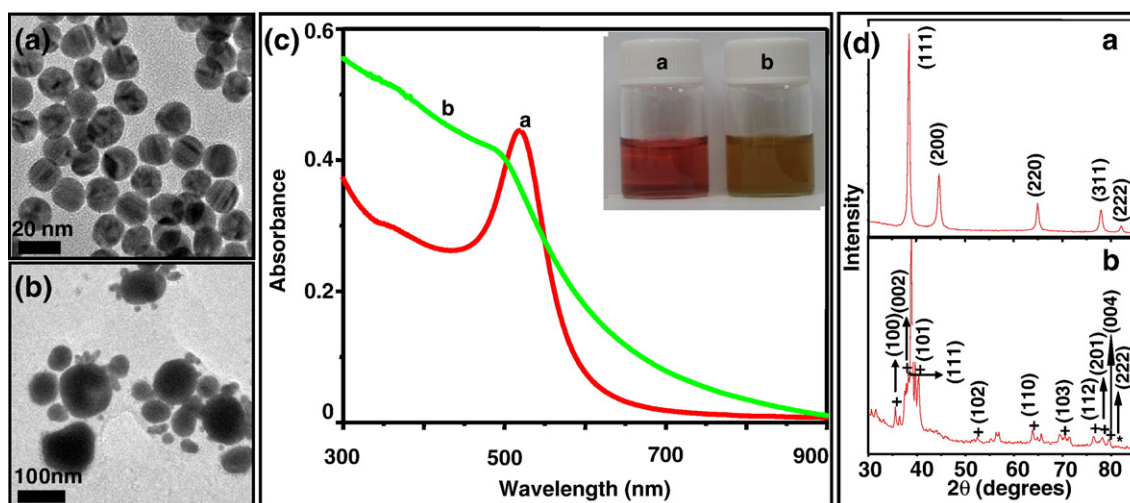


**Fig. 20.** (a) Large area TEM image of gold nanoparticles before  $\text{Hg}(0)$  treatment, (b) Large area TEM image of gold nanoparticles after the  $\text{Hg}(0)$  treatment and (c) UV-vis absorption spectra of gold nanoparticles before and after mercury treatment. Inset of (c): photographs of gold nanoparticles and mercury treated gold nanoparticles (d) XRD patterns of gold nanoparticles before and after mercury treatment. (a) XRD pattern of gold nanoparticles before reaction. (b) XRD pattern of mercury-treated gold nanoparticles (symbols: +  $\text{Au}_3\text{Hg}$ , \* Au) [368].

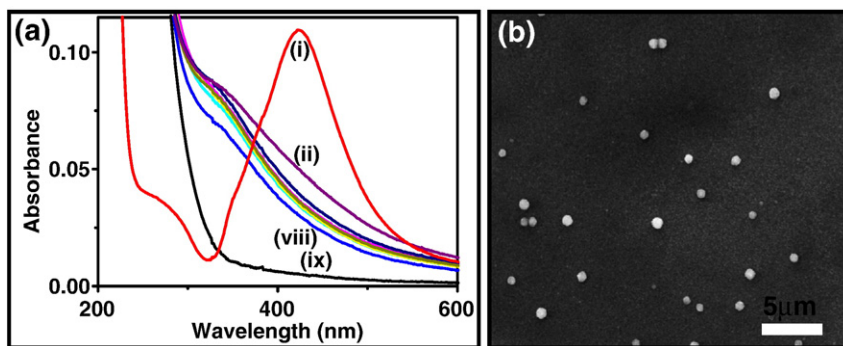


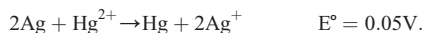
**Fig. 21.** (a) UV-vis absorption spectra of silver nanoparticles (prepared by the Turkevich method, 1 mM, 5 ml) with 50 ppm  $\text{Hg}^{2+}$  solution (0.25 mM, 50 ml). (i) represents the spectrum for silver nanoparticles. (ii–viii) represent the spectra after addition of  $\text{Hg}^{2+}$  solution at intervals of 5 min and (ix) is the spectrum after 6 h. (b) Large area SEM image of the Ag–Hg bimetallic nanoparticles [370].

nanoparticles also exhibited a blue shift, albeit to a much smaller degree [371,372]. It was earlier reported that aqueous mercury nanoparticle solutions exhibit plasmon absorption band below 300 nm [373]. The Hg–Ag alloy nanoparticles, prepared by simultaneous reduction with sodium borohydride, exhibits a plasmon in the region of 300–400 nm (the precise location is controlled by the molar ratio) [374].

Fig. 21(b) reveals the microscopic changes in the silver nanoparticle. Silver nanoparticles are prepared by the Turkevich method, yielding a size range of 60–80 nm. The size of the particles has grown to over 600 nm upon mercury incorporation. This indicates the nucleation of reduced mercury on the silver surface.

The homogeneous distribution of mercury in silver nanoparticles is confirmed by EDAX imaging (Fig. 22). It was found that the concentration of mercury at the edges of the particle is slightly higher than at the center. It is likely that mercury atoms adsorbed on the silver surface rapidly diffuse into the silver core. An important point to note here is the pace at which the plasmon band of silver nanoparticles starts to disappear (Fig. 21a). This has to be understood from a thermodynamic standpoint.

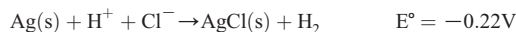
*Reduction reaction:*



At the bulk scale, the reaction is thermodynamically favorable. However, an interesting property of nanochemistry plays a role here. As highlighted earlier, the reduction potential for  $\text{Ag}^+|\text{Ag}$  (atom) is  $-1.80$  V. Thus, the reduction potential of the silver nanoparticle is likely to be much less than 0.8 V, which creates a strong driving force for the galvanic reaction to happen.

The change in the reduction potential of silver nanoparticles can also be understood from the Ag–HCl system [375]. In bulk form, silver is not attacked by HCl. However, silver nanoparticles prepared by reduction of silver ions with sodium borohydride, exhibit an unusually high reactivity with HCl. The disappearance of the plasmon band of silver nanoparticles, after the addition of HCl, confirms the dissolution (Fig. 23a). This is further confirmed by the analysis of the white residue obtained after the reaction of silver nanoparticles with HCl. It shows the characteristic diffraction pattern of AgCl (Fig. 23b).

This result can also be understood from the reaction:



Thus, there is no driving force for the reaction with bulk silver, however, at the nanoscale, the feasibility of the reaction (i.e.  $E > 0$ ) confirms the increasing reducing nature of the silver nanoparticle surface.

The potential of silver nanoparticles to reduce a number of heavy metals can also be looked at as a method to prepare alloy nanoparticles; e.g., Ag–Hg bimetallic nanoparticles. A demonstration of the galvanic etching for the preparation of alloy nanoparticles is illustrated through the preparation of Pd–Ag and Pt–Ag nanoparticles [376].

#### 5.4.4. Detection of heavy metals in drinking water with noble metal nanoparticles

Recently, there has been an in-depth review of the maximum contamination limit (MCL) for various contaminants in drinking water, for example, MCL for lead has been changed from 15 ppb to 10 ppb and MCL for arsenic has been revised from 50 ppb to 10 ppb. Multiple protocols have been developed for the detection at ultralow concentrations of, for example, mercury [377], arsenic [378], lead [379] and anions [380].

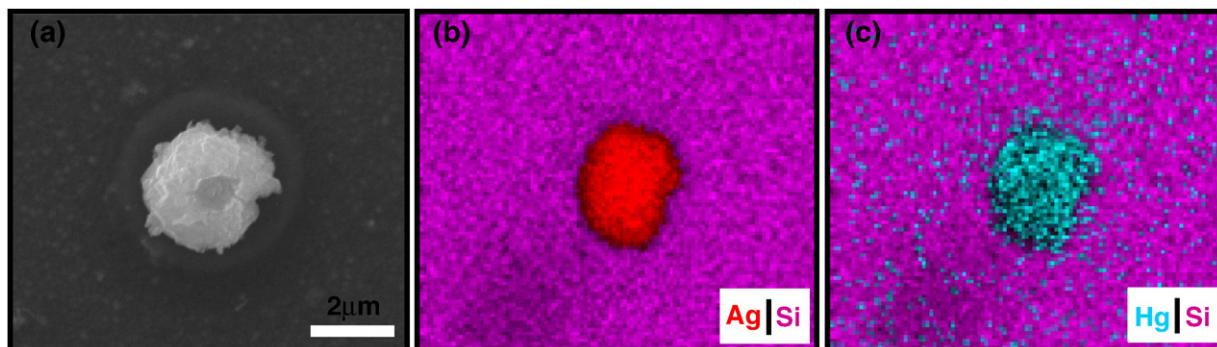


**Fig. 22.** (a) SEM image of an Ag–Hg alloy nanoparticle, (b) elemental image of Ag and (c) elemental image of Hg overlaid on Si (Si is from ITO substrate) [370].

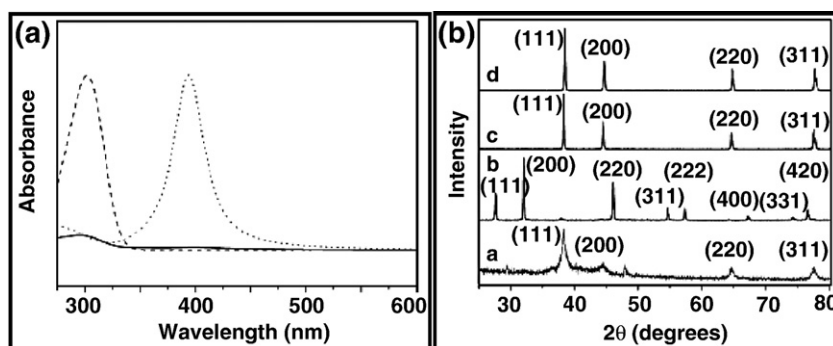


**Fig. 23.** (a) UV-vis absorption spectra. Dotted curve: the as-prepared Ag colloidal solution. Dashed curve: AgNO<sub>3</sub> aqueous solution. Solid curve: the upper transparent solution after the reaction of the Ag colloid with hydrochloric acid. (b) XRD patterns of the samples. (a) Ag nanoparticles prepared by using AgNO<sub>3</sub> as the silver source and after drying the Ag colloidal solution on a single crystal silicon substrate, (b) the product of AgCl obtained from the reaction of Ag nanoparticles with hydrochloric acid, (c) commercial Ag powder, and (d) after commercial Ag powder was added into hydrochloric acid under magnetic stirring for 3 days [375].

In a manner similar to that explained for the detection of pesticides, noble metal nanoparticles offer two possibilities.

- *Colorimetric detection:* An important property of noble metal nanoparticles is to host a variety of ligands on its surface, and assist in ligand-mediated reactions. An interesting aspect of this functionalization is the resulting changes in optical properties [381]. This has been widely utilized for biological applications [382], catalysis [190] and devices [205].

One of the important properties exhibited by functionalized noble metal nanoparticle surfaces is the detection of heavy metals [384]. In one such method, heavy metal specific biomolecule functionalized gold nanoparticles can be utilized. An example of this approach is the interaction of metal ions with nucleotides: Hg<sup>2+</sup> promoted formation of thymine-thymine base pairs [385,386]. This approach has also been extended to low concentration detection through a scanometric device involving use of the oligonucleotide chip array [387]. In another illustration of this approach, the gold nanoparticle, typically functionalized with a DNA strand, undergoes aggregation due to the hybridization action of enzymes in the presence of a substrate [388–391]. In the presence of specific metal ions, the hybridization can be arrested by catalytic cleavage of the substrate. That is, the aggregates of gold nanoparticles can be disengaged by the addition of metal ions. Such methods can be utilized for the selective detection of the heavy metal ions present in concentrations higher than 100 ppb. In a similar approach, the peptide-functionalized gold nanoparticles are utilized for colorimetric detection of Hg<sup>2+</sup> and Pb<sup>2+</sup> at the ppb level, with distinct color response for two ions [392]. The peptide sequence utilized for the detection is the Flg-A3 peptide (–Asp–Tyr–Lys–Asp–Asp–Asp–Lys–Pro–Ala–Tyr–Ser–Ser–Gly–Pro–Ala–Pro–Pro–Met–Pro–Pro–Phe–) which stabilizes gold surfaces due to its negative charge (pI = 3.9). It is suggested that aromatic, charged and hydroxyl groups in the peptide sequence recognize heavy metal ions. Using this approach, nanomolar concentrations can be detected through plasmon shifts in the absorption spectrum. In another approach, metal ion induced assembly of gold nanoparticles in the presence of carboxylated peptide (tryrosine-containing peptide NH<sub>2</sub>–Leu–Aib–Tyr–OMe) can be utilized for detection of ions at the ppm level [393].

Recent developments have found DNA enzymes specific to various other metal ions (e.g., Cu<sup>2+</sup> and Zn<sup>2+</sup>) which can be utilized for developing simple colorimetric approaches for heavy metal detection [394,395]. In a similar approach, ligands functionalized on noble metal nanoparticle surfaces complex with specific metal ions. This ligand-metal ion complexation leads to observable optical changes at concentrations in the ppm level. Examples of such ligands are gallic acid (Pb<sup>2+</sup>) [396], cysteine (Hg<sup>2+</sup>, Cu<sup>2+</sup>) [397], and mercaptoundecanoic acid (Pb<sup>2+</sup>, Cd<sup>2+</sup>, Hg<sup>2+</sup>) [398]. The chemistry of heavy metal removal with noble metal nanoparticles can be utilized. The aspect of metal-metal alloying induces changes in the optical properties of the noble metal nanoparticles (refer to previous section) [368,370,399].

Carboxylate group modified surface of gold nanoparticles can be induced to aggregate in the presence of Hg<sup>2+</sup> and pyridinedicarboxylic acid, which is manifested in the form of colorimetric response [400,401], fluorescence quenching [402] and enhancement of hyper-Rayleigh scattering intensity [403]. The choice of carboxylate group determines the selectivity for Hg<sup>2+</sup>. Examples are 3-mercaptopropionic acid [400,401,403], adenosine monophosphate [400] and mercaptoundecanoic acid [402].

- *SERS based detection:* The SERS activity of noble metal nanoparticles can be utilized for the detection of trace quantities of contaminants in drinking water. The activity is largely attributed to the electric field amplification near the metal surface owing to collective oscillations of conduction electrons with the incident light. It is also suggested that charge transfer between the chemisorbed species and the metal surface leads to HOMO–LUMO transitions. A number of review articles have been authored on the subject [404,354,355]. Various discoveries in the area of Raman enhancement are likely to be applied for the detection of contaminant molecules in drinking water: enhancement based on size of the SERS substrate [355], single molecule detection [356] and assembled nanostructures [405].

In a protocol developed for the ultra-low concentration detection of arsenic in drinking water, shape dependency of SERS based detection is demonstrated [97]. Closely-packed monolayers of polyhedral silver nanostructures, fabricated using the Langmuir-Blodgett technique, have been utilized for the study. The role of surface-passivating agents has also been demonstrated. The important conclusions are as follows.

- Octahedron shaped nanocrystals exhibit higher SERS activity than other shapes (Fig. 24(a)).
- Polyvinyl Pyrrolidone (PVP)-protected particles give orders of magnitude stronger response from arsenate, when compared with other capping agents (Fig. 24b).
- The LB assemblies of polyhedral Ag nanocrystals are highly active SERS substrates. The two oxidation states of arsenic (As<sup>III</sup> and As<sup>V</sup>) can be distinguished even at low concentrations (Fig. 24c). The co-ion effect is found to be minimal, even at low concentration detection.

Hg<sup>2+</sup> is utilized for inducing conformational change in thymine rich single stranded DNA, tagged with a fluorescent dye [406]. Conformational change in the DNA significantly alters its ability to bind to the gold nanoparticle surface and thus it can't prevent salt-induced aggregation [407]. Hg<sup>2+</sup> is utilized for catalyzing the formation of stable DNA duplex, from single-stranded DNA functionalized gold nanoparticles, through thymine-Hg<sup>2+</sup>-thymine linkage [408]. This process is also temperature dependent which can be controlled by the extent of thymine-thymine mismatch.



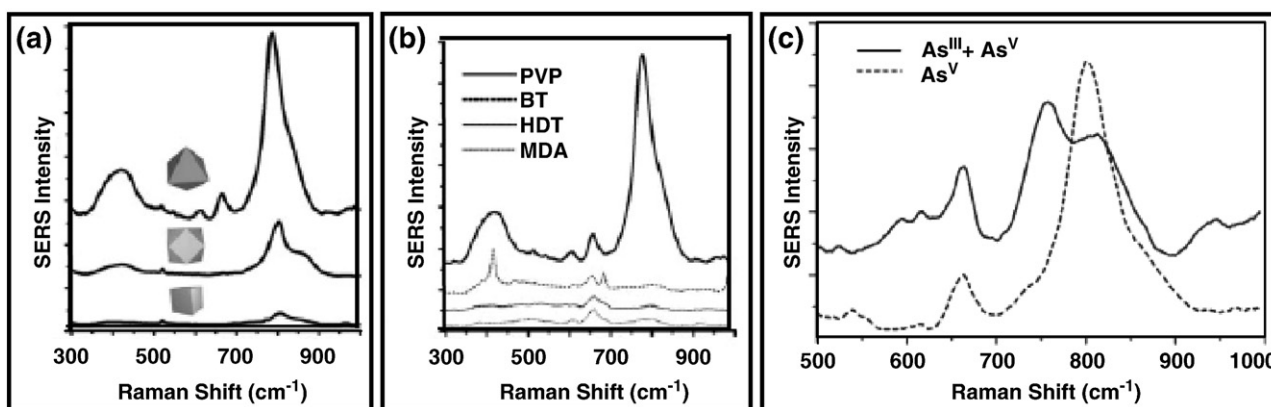


**Fig. 24.** (a) SERS spectra collected on Langmuir-Blodgett films of PVP protected silver nanocrystals exposed to  $1 \times 10^{-6}$  M arsenate solution. Peaks at 800 and  $425 \text{ cm}^{-1}$  can be assigned to  $\text{Na}_2\text{HAsO}_4$ . (b) SERS response of LB arrays of silver octahedra coated with various organic species. BT: benzenethiol, HDT: hexadecanethiol, MDA: mercaptodecanoic acid. (c) Chemical sensitivity of PVP-coated nanocrystal arrays for speciation of arsenate and arsenite ions (18 ppb) [97].

Gold nanoparticle surfaces have been modified with suitable molecules which bind with metal ions as well [409]. The vibrational modes in the molecule are very sensitive to heavy metal co-ordination and thus yield improved SERS response when coupled with noble metal nanoparticles. SERS based detection has also been utilized for detection of ultra low concentrations of anions. Positively charged silver nanoparticle protected amino and amide group and immobilized on silica surfaces has been utilized for the detection of perchlorate, thiocyanate and cyanide ions [410].

#### 5.4.5. Chemistry of micro-organisms with noble metal nanoparticles

The anti-microbial effects of silver, in zerovalent and ionic form, have been widely studied in great detail [411–415]. It has also been used widely as a common disinfectant for surgical masks [416], textile fibers [417], wound dressing [418], etc. Due to the numerous scientific investigations published on this topic and its consequences in different applications, review articles may be consulted for a detailed understanding [419–424]. Here, we summarize the important aspects of nanoparticle chemistry and its relevance to drinking water purification.

Significant efforts have been devoted to study the toxic effects of silver nanoparticles on a broad spectrum of micro-organisms including *E. coli* [411–413,425–427], *Pseudomonas aeruginosa* [425], *Vibrio cholera* [425], *Bacillus subtilis* and *HIV-1* [428].

Prior to discussing the chemistry behind the biocidal activity of silver nanoparticles, it is useful to understand how silver ions act against micro-organisms. While the precise details are not yet elucidated, protein inactivation and loss of replication ability of DNA are suggested. A few important observations are highlighted.

- It was pointed out that cells protect the DNA by forming a defense around the nucleus, when the cells are subjected to external stimuli such as heat [429]. Under severe external stimulus, the defense mechanism fails leading to the denaturation of the DNA (loss of replication ability). A similar observation was found in the case of silver ions with *E. coli* and *Staphylococcus aureus* [430]. The formation of protective layers around DNA and DNA's condensation was clearly evident in the study [430]. The large-scale movement in the cellular components in the presence of silver ions is indeed surprising and reflects the ability of the cell to protect itself against external stimuli.
- It was also found that the interaction of silver ions with sulfur present in many proteins, leads to protein inactivation [431,432]. While the external addition of sulfur-containing compounds led to the neutralization of anti-bacterial activity of silver ions, the presence of sulfur in silver-rich regions confirmed the interaction between sulfur and silver.

- The nature of the charge on the cell surface (due to presence of different functional groups) and the anti-bacterial composition plays a key role in determining the effectiveness. It was found that the same nature of charge on the antimicrobial composition and cell surface (negative charge) leads to repulsion and decreased contact [433].
- The ability of silver to absorb oxygen in atomic form has been widely utilized immensely for many organic reactions such as conversion of methanol to formaldehyde [434]. It is revealed that bulk silver in an oxygen charged aqueous medium catalyzes the complete destructive oxidation of microorganisms [435].
- It is largely understood that cellular membranes play a critical role in maintaining the viability of cells [436]. The cellular permeability in the case of gram-negative bacteria such as *E. coli* is largely controlled by the presence of a lipopolysaccharide (LPS) layer on the outer surface of the cellular membrane. The heavily saturated fatty acids on LPS links it to the membrane backbone, which itself contains many negative ions. Thus, LPS binds cations, which is also confirmed by the presence of  $\text{Mg}^{2+}/\text{Ca}^{2+}$  as an electrostatic linker to bind adjacent LPS chains [437]. The affinity of LPS towards cations has been utilized for permeation of polycationic antibiotics in the cytoplasm. It is also suggested that the binding of even simple cations to LPS weakens the membrane backbone [437], which may lead to the disintegration of the membrane. On the contrary, negatively charged ions have been reported to bind with  $\text{Mg}^{2+}/\text{Ca}^{2+}$ , which also leads to loss of cellular viability [437].

In the context of observations for silver ions, it is appropriate to understand the observations for silver nanoparticles.

- Silver nanoparticles cause irreparable damage to the cellular membrane [413,426,438] which enables the accumulation of nanoparticles in the cytoplasm (Fig. 25(a,b)) [413]. It is suggested that action of silver nanoparticle arises due to this damage and not its toxicity [426]. The pits in the cell wall, post-treatment, are quite significant. An important aspect of the biocidal action of silver nanoparticles is the requirement of supported nanoparticles for anti-bacterial effects. As explained in an earlier section on biosynthesis of metal nanoparticles, cells protect themselves from metal toxicity through the action of cellular proteins which bind to the nanoparticle surface leading to nanoparticle aggregation and thus rendering nanoparticles immobile. This was suggested by the studies of nanoparticle solutions with bacteria [413].
- It is therefore expected that small size nanoparticles are able to easily penetrate across membranes [425,426]. Similarly, anti-bacterial activity of nanocrystals is found to have a dependence

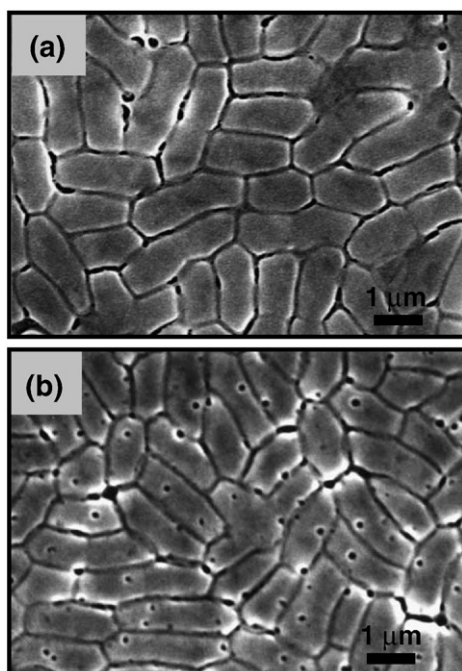


Fig. 25. Scanning electron micrographs of (a) native *E. coli* cells and (b) cells treated with  $50 \mu\text{g cm}^{-3}$  of silver nanoparticles in a liquid Luria Bertani (LB) medium for 4 h [413].

on crystal shape. The activity is found to be higher for truncated triangular nanoplates when compared with nanorods and spherical particles (Fig. 26(a,b)). The interaction of bacteria with high-atom density (111) crystal plane has been proposed [425] and thus, a crystal exhibiting higher concentration of (111) facet exhibits higher anti-bacterial activity [426].

- Recently, it has been proposed that the activity of silver nanoparticle arises due to the formation of superoxide, which has been detected by the dismutation activity of superoxide dismutase. The addition of dismutase leads to reduction in anti-bacterial activity [439].
- It is also suggested that the chemistry of silver ions is important in the anti-bacterial effect of silver nanoparticles. That chemisorbed  $\text{Ag}^+$  ions is important in determining the silver nanoparticle toxicity was confirmed by the non-toxicity of oxidized nanoparticles to silver-resistant *E. coli* strains [427].
- Silver nanoparticles interact with the glycoproteins of HIV-1 (particles greater than 10 nm attach to the viral envelope) (Fig. 26(c)).

The glycoprotein bind with the receptor sites on the host cells enabling the host cell infection. The interaction of silver nanoparticles with glycoprotein may be due to the presence of sulfur bearing residues on the protein surface which renders glycoprotein incapable of binding with host cells [428].

An important aspect of silver nanoparticle chemistry for anti-bacterial action is to stabilize the nanoparticles in organic medium such as plastics, oils, etc. Two major ways adapted in this direction are as follows:

- Synthesis of organic soluble silver nanoparticles by various means, for example, polymerization of benzylthiocyanate on silver nanoparticles [440].
- Synthesis of silver nanoparticle in vegetable oil medium through the reduction of metal salt by the naturally occurring oxidative drying process in oils [441].

The anti-bacterial properties of silver nanoparticles have also been utilized in imparting biocidal properties to the separation membranes [442–445]. This is an important contribution of silver nanoparticles to membrane processes: a number of membrane-based technologies suffer from frequent biofouling and inability to remove viruses. The addition of silver nanoparticles to the membrane solves both problems. The loading of silver nanoparticles on the membrane matrix can be achieved by two processes involving the addition of silver, in zerovalent form or reduction of silver ions, to the membrane casting solution. In addition to improvement in the bio-resistance of the membrane, silver nanoparticle-membrane composites have been observed to exhibit higher permeability [444]. It is suggested that biocidal properties of silver nanoparticle loaded membranes arise due to the release of  $\text{Ag}^+$  ions [446].

## 6. Case study: nanoparticles based chemistry for pesticides removal

### 6.1. Noble metal nanoparticle-based mineralization of pesticides

One of the areas of interest of our research group is the interaction of noble metal nanoparticles with organochlorine and organophosphorus pesticides. Specifically, the nanoparticles used for the study are gold and silver whereas the pesticides are endosulfan, malathion and chlorpyrifos. This study is a consequence of our finding on the possibility of degrading different halocarbons using noble metal nanoparticles [320].

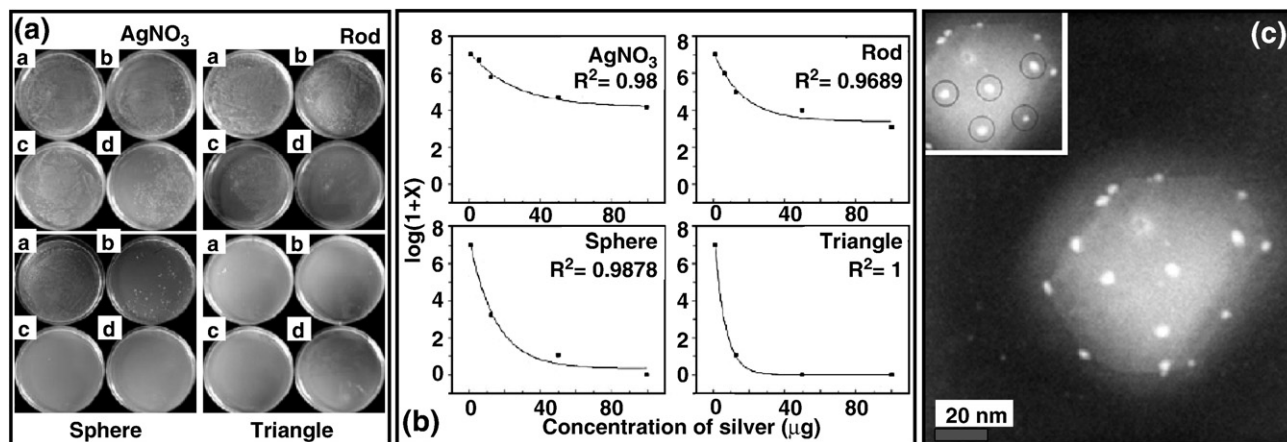
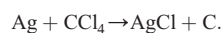
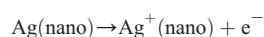


Fig. 26. (a) Petri dishes initially supplemented with  $10^7$  CFU/ml of *E. coli* and incubated with different forms of silver nanoparticles at (a) 1, (b) 12.5, (c) 50, and (d) 100  $\mu\text{g}$ . (b) Number of *E. coli* colonies, expressed as  $\log(1 + \text{number of colonies grown on plates under the conditions used for panel a})$  as a function of the amount of silver nanoparticles in agar plates. (c) HAADF image of an HIV-1 virus exposed to Bovine Serum Albumin (BSA)-conjugated silver nanoparticles. The inset shows the regular spatial arrangement between groups of three nanoparticles [428].

It was discovered that mineralization of halocarbons happens in two steps: adsorption of halocarbons on the nanoparticle surface and its consequent mineralization to metal halides and amorphous carbon [320]. A few of the important results from this study are as follows [68].

- *Environmentally benign nature of the reaction products and zero production of by-products:* One of the key issues to resolve in tackling the pesticide contamination problem in its entirety is the elimination of reaction products. The products from such a catalytic decomposition are metal halides and amorphous carbon, both of which are environmentally benign. Using advanced mass spectroscopic techniques, it was established that there are no reaction by-products left in the solution and mineralization of pesticides (chlorpyrifos and malathion) is complete for the molecules investigated. At this juncture, the fate of phosphorus, present in a number of commonly used pesticides, is not understood.
- *Demonstration of size selective reactivity of nanoparticles:* The experiments were conducted with bulk form of noble metals and it was concluded that this property is demonstrated only in the case of nanoparticles. The absence of such a property being exhibited by the bulk form of noble metals is explained from thermo-chemical calculations (explained later).
- *Capability to target a broad range of organochlorine and organophosphorus pesticides:* The reactivity was studied with a broad range of halocarbons (e.g., benzyl chloride, chloroform, and bromoform), organochlorine pesticides (e.g., endosulfan) and organophosphorus pesticides (e.g., chlorpyrifos, malathion). Using sensitive instrumentation, it was established that all such organics undergo complete mineralization at low concentrations.

Based on a study conducted at various reaction conditions, it is postulated that the catalytic decomposition of halocarbons is initiated through the transfer of electrons from metal nanoparticles to the solvent, which in-turn causes the mineralization of the halocarbons. The scheme of reactions is suggested to be the following (not balanced by stoichiometry as it is difficult to predict the number of metal atoms in a nanoparticle) [320]:



In the specific case presented above,  $(\text{CH}_3)_2\text{CHOH}$  was used as a solvent for the bulk mineralization of  $\text{CCl}_4$  in a  $(\text{CH}_3)_2\text{CHOH}/\text{H}_2\text{O}$  solvent mixture. The protons produced are responsible for the low pH. Mineralization can happen even without such a solvent. From a thermodynamic standpoint, the reaction of halocarbons with silver is not favored due to a small positive reaction enthalpy (standard enthalpy values for  $\text{CCl}_4$  and  $\text{AgCl}$  are  $-128.2$  and  $-127.0$   $\text{kJ mol}^{-1}$ , respectively). It is suggested that the nano form of the noble metal particles along with the presence of energetic surface atoms help in overcoming the thermochemical and entropic barriers.

It is easy to comprehend that the decrease in particle size leads to dramatic changes in the rate kinetics of the reaction owing to an increase in the availability of reaction sites on the metal nanoparticle surface. The other variable of the reaction kinetics is the activation energy which is known to be affected by many parameters such as the nature of the reactants, crystallinity of the reactive surfaces, ease of charge transfer, surface impurities such as dopants etc. The reaction outlined above can result in the removal of the metal nanoparticles as ions.

*Mode of decomposition for organic species:* For a large variety of organic molecules, the principal mode of decomposition is electron transfer from the metal particles. As the oxidation of metals is

generally favored and as these processes are facilitated in aqueous medium, there is availability of electrons at the metal particle surfaces. Oxidation of nanoparticles is even more facile compared to bulk. Recall that oxidation is the removal of an electron from the whole nanoparticle and not from an atom. Oxidation can also be tuned by varying the particle dimension, by providing appropriate functionalization and by attaching the particle on suitable substrates. The oxidized species can be one of the many different oxides or hydroxides, which may have reduced solubility in water.

The electron removed from the particle surface can be made available for appropriate reduction chemistry. For molecules such as halocarbons, the electron is transferred to the halogen making the C–X bond weak, resulting in the formation of the halide ion. The organic species can participate in various other reactions, depending on the medium or other reagents present. The halide ion formed can also produce the metal halide and it again is dissolved in the medium or precipitated depending on the solubility product. The mineralization is also suggested by the increase in the solution conductivity (due to the release of chloride ions in the solution) and a decrease in the pH of the solution.

*Discharge of metal ions in water:* The presence of metal ions in aqueous solution in water is an important concern, especially in the case of toxic chemicals. However, for Fe, Ag,  $\text{TiO}_2$ , ZnO and  $\text{CeO}_2$  derived materials, the solubility of the species concerned is low, and therefore the ionic concentration is not beyond the permissible limits. This is very important in designing water quality applications. As water in general is contaminated with several ionic species, the nature of the metal ion can be different from case-to-case. The solubility and stability of ions is strongly dependent on pH. Therefore, the latter is an important parameter in deciding the type of the ion. The important issue of concern is the self-oxidation of metal nanoparticle surface in presence of air/water. This leads to the formation of an oxide/hydroxide cover on the nanoparticle surface inhibiting the electron transfer, thereby reducing the surface activity. Highly dispersed particles of smaller dimensions make it possible to use all the available metals for the chemistry concerned.

## 6.2. Technology to product – a snapshot view

The ultimate objective of a scientific discovery is to create value for society – the utilizable form of the technology in the form of a product. A scientific discovery is a fusion of novel materials, their characterization, understanding the process of interaction and postulation. Product development is a blend of technology optimization, engineering the prototype, cost-effectiveness, customer satisfaction and strict adherence to quality control norms. The authors' work in the area of product development for pesticide removal from drinking water is utilized here for providing an overview of the development phase and associated challenges. The underlying technology utilized for this example is the application of noble metal nanoparticles for the mineralization of pesticides. This product is hailed as the first nanomaterial based drinking water purifier [447] and thus it gave us a number of important experiences required for successful product commercialization. An overview is summarized here.

The first phase of the product development programme was to extend the applicability of metal nanoparticles for other pesticides of relevance to Indian drinking water. This step demonstrated the capability of metal nanoparticles for complete mineralization of organochlorine, organophosphorus and organosulfur pesticides. In general, the removal of nanoparticles from solution is difficult due to their small size. Thus, the second phase of this programme was to adapt the technology to the needs of domestic customers, i.e. online, point-of-use drinking water purifier. An important aspect of the adaptation is to remove pesticides through heterogeneous catalysis using supported nanoparticles. Heterogeneous catalysis ensures that removal of pesticide-bearing nanoparticle from drinking water is



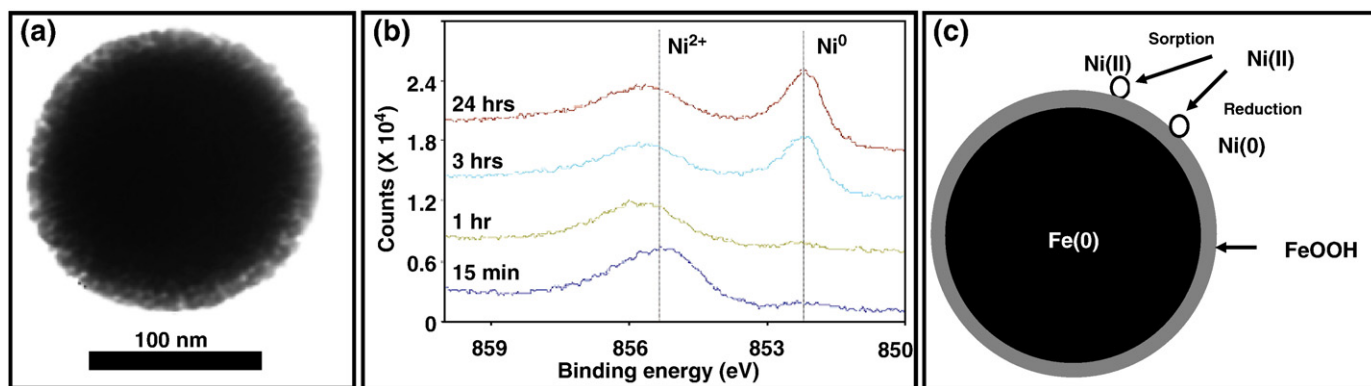


Fig. 27. (a) TEM images of iron nanoparticles (b) HR-XPS survey on the Ni  $2p^{3/2}$  of iron nanoparticles, and (c) a conceptual model for nickel deposition on iron nanoparticles [369].

not a difficulty and contamination of drinking water with nanoparticles is prevented [448]. This necessitated the study of nanoparticles incorporated on suitable supports such as activated alumina, magnesia and carbon (Fig. 17(a,b)). It is important to understand the need for a suitable support, i.e. non-reactivity between support and nanomaterials, availability of large nanomaterial surface area for pesticide adsorption, extremely low solubility of support in drinking water and non-toxicity. This phase also involved the development of a pre-treatment mechanism for contaminated water using activated carbon since the excess free chloride ions (and chlorine) adsorb on nanoparticle surfaces, rendering them inactive for the pesticide mineralization reaction.

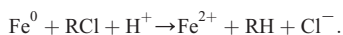
The third phase of this programme was to develop a commercial-scale production plant for producing large quantities of noble metal nanoparticles coated on activated alumina (Fig. 17(b,c)). The large-scale production of nanoparticles is usually challenged by issues such as precise control over the processes, commercial viability of the process, availability of sophisticated instrumentation for production, quality tests and workforce development for continuous production. This programme utilized wet chemistry-based synthesis for the production of noble metal nanoparticles, as it offers a larger degree of control over production processes. One innovation involved cost-effective and controlled immobilization of metal nanoparticles on alumina supports [324–326].

The fourth phase of this programme was to develop a suitable mechanism for environmentally responsible disposal of residuals as well as materials recovered from the spent filters and recovery of precious metals. This entailed study of cost-effective separation of support, metal chlorides and other organic species binding on the nanomaterial surface. The product development involved various levels of field trials, extending over a year and incorporation of the inputs from the field into the manufacturing process. Product commercialization involved the development of suitable audio-visual aids to inform the public of various aspects of the technology.

## 7. Other nanomaterial based approaches for water purification

**Iron-based nanoparticles:** One of the most important nanomaterials studied for water purification is zero-valent iron (ZVI). Amongst the nano-adsorbents popular today, ZVI is the most utilized, primarily because it covers the broadest range of environmental contaminants [312,313]: halogenated organics, pesticides, arsenic, nitrate and heavy metals.

The mechanism of reactivity for ZVI is similar to the mechanism of corrosion (i.e. oxidation of iron) [68] and involves the generation of electrons which in turn reduces the organic species through dechlorination (Fig. 27a):



Similarly, ZVI acts as a reducing agent for sequestration of metal ions having reduction potential higher than Fe. The chemistry can be understood by an example of interaction of  $\text{Ni}^{2+}$  with ZVI (Fig. 27(b, c)). In the beginning of the reaction,  $\text{Ni}^{2+}$  is physically adsorbed (outer sphere interaction) and then is chemisorbed (inner sphere interaction) and finally reduced to metallic nickel. This happens through the following step: At  $\text{pH} > \text{pH}_{\text{zpc}}$ , the ZVI surface will be negatively charged and thus, will attract the metal ion. The metal ion is adsorbed on the surface and gradually becomes reduced to zerovalent metal. This chemistry has been applied for sequestration of many metal ions: Pb, Cd, Cr, Co, Cu, Hg, Ni, and Se. The chemistry is clearly evident from Fig. 27(c).

However, there are a few challenges associated with the use of ZVI at the commercial scale:

- Corrosion of metal surface: The constant interaction of iron with water leads to the formation of iron hydroxide on the ZVI surface. A few attempts have been made to increase the lifetime of metal surfaces e.g., the use of palladium coating. The surface protection of ZVI with palladium also leads to enhancement in catalytic properties due to the action of palladium.
- Reaction by-products originating during the decomposition of chlorinated hydrocarbons: Nano-sized metallic iron has been reported to show low reactivity toward lightly chlorinated hydrocarbons. It may also be possible that some of the reaction by-products are highly toxic in nature or have high solubility in water (e.g., 1,1-dichloro-2,2-bis (p-chlorophenyl) ethane, a de-chlorinated derivative of DDT, has 50 times more solubility in water compared than DDT).

Another important class of adsorbent based on iron is the use of  $\text{Fe}_3\text{O}_4$  nanoparticles for drinking water purification. The most highlighted work to date has been the removal of arsenic from drinking water using low-magnetic field induced separation [449]. The study suggested that decrease in size dramatically enhances the capacity of the adsorbent. Functionalization of  $\text{Fe}_3\text{O}_4$  surfaces has also led to the preparation of promising adsorbents for other heavy metals such as copper [450], lead [451] and mercury [451].

**Carbon nanotubes:** Carbon nanotubes have been one of the most studied materials in nano research. A recently published review article captures the work in detail [452]. The application of carbon nanotubes to drinking water purification started with the study of its capillary action [453]. It was found that incoming fluid having surface tension less than 200 mN/m are drawn inside the nanotubes by the action of capillary forces. A subsequent study reported the superhydrophobicity of a nanotube array prepared by functionalized, vertically aligned carbon nanotubes with a nonwetting poly(tetrafluoroethylene) (PTFE) coating [454]. Experiments showed that the hydrophobicity of nanotube arrays induce fast water flow [455] due to ordering of

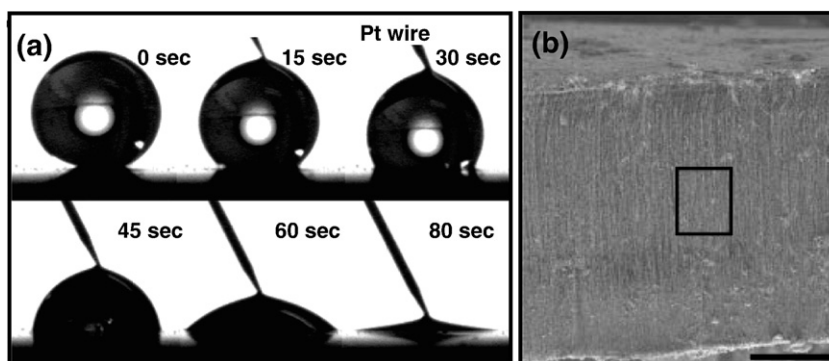


**Fig. 28.** (a) Images of water droplet shape change with a +2.6 V potential applied with a multiwalled nanotube film as anode and Pt wire as cathode. The droplet sinks into the nanotube membrane in about 90 s. A deionized water droplet (~2  $\mu\text{l}$  volume) rests on the surface of a superhydrophobic nanotube membrane. A Pt wire probe is inserted into the droplet to establish electrical contact [457]. (b) SEM image of a cylindrical macrostructure assembly showing the wall of the bulk tube consisting of aligned MWNTs with lengths equal to the wall thickness (scale 100  $\mu\text{m}$ ) [458].

hydrogen bonds between the water molecules [456]. The hydrophobicity of nanotube arrays was manipulated by applying a low voltage to overcome the energy barrier to effect the transition from a superhydrophobic to hydrophilic state. This leads to transport of water through the carbon nanotube array (with water transport taking place between the MWNTs) (Fig. 28a) [457]. Recently, macroscale hollow carbon cylinders have been fabricated with walls consisting of aligned multi-walled nanotubes (Fig. 28b) [458]. Such uniform nanoporous, cylindrical membrane walls present a new line of research to synthesize CNT based membrane filtration. The CNT based membrane has been studied for filtration of *E. coli*.

**Nanoclays:** Clay is one of the naturally occurring materials which has been utilized by nature for maintaining flow of groundwater (due to relatively high impermeability to water), removing toxic species present in the water (due to the presence of surface charge on the clay structure) and imparting rigidity to natural structures (due to natural plasticity). Clays are aluminosilicates with a planar silicate structure. There are three main categories of clay: kaolinite, montmorillonite-smectite and illite, amongst which the first two are the most widely studied [68].

Usually the structure contains silicate sheets ( $\text{Si}_2\text{O}_5$ ) bonded to aluminum oxide/hydroxide layers ( $\text{Al}_2(\text{OH})_4$ ) called gibbsite layers. The primary structural unit of this group is a layer composed of one octahedral sheet with one tetrahedral sheet (kaolinite is 1:1 clay mineral). The condensation of two sheets happens by coordination of an oxygen atom with one silicon atom in the tetrahedral sheet and two aluminum atoms in the octahedral sheet. In the case of kaolinite, additional empty sites are created in the octahedral sheet as the charge balance of oxygen atoms by aluminum requires the occupation of only 2 out of 3 vacancies in the packing of oxygen atoms. Thus, instead of two trivalent aluminum atoms, three divalent atoms can also occupy octahedral sites: dioctahedral minerals (octahedral sites occupied by  $\text{Al}^{3+}$  such as in kaolinite, dickite, etc.) and trioctahedral minerals (octahedral sites occupied by  $\text{Mg}^{2+}$  and  $\text{Fe}^{2+}$  such as in antigorite, chamosite, etc.).

The smectite group refers to a family of non-metallic clays primarily composed of hydrated sodium calcium aluminum silicate. Montmorillonite belongs to the family of 2:1 smectite minerals having two tetrahedral sheets with the unshared vertex of each sheet pointing toward each other and forming each side of the octahedral sheet. Depending on the composition of the tetrahedral and octahedral sheets, the layer will have no charge, or will have a net negative charge (balanced by interlayer cations). A permanent negative charge is located on the clay layers because of isomorphous substitution of  $\text{Al}^{3+}$  atoms in the octahedral layer by  $\text{Mg}^{2+}$  and  $\text{Fe}^{2+}$  and of  $\text{Si}^{4+}$  atoms in the tetrahedral layer by  $\text{Al}^{3+}$ . Montmorillonite, being dioctahedral clay, contains one vacant site for every three octahedral positions. The exchangeable cations can easily be replaced by positively charged

species. Additionally, the outer silicate surface of a montmorillonite cell contains Si atoms bound to hydroxyls (Si–OH), which help in the adsorption of the organic species.

There are many approaches for increasing the adsorption of a specific molecule on clay. For example, to increase the adsorption of organic species, the inorganic cations are replaced by quaternary ammonium cationic surfactants containing long chain alkyl group to make it more organophilic. Similarly, depending on the nature of charge on the clay layer, metal cations (e.g., lead, arsenic and cadmium etc.) can be captured from water through intercalation [459].

**Alumina nanoparticles:** Alumina belongs to a larger category of oxides which have played a pivotal role in drinking water purification. Examples include silica as a disinfectant, titania as a photocatalyst [460], alumina as a metal adsorbent [461] and support for heterogeneous catalysis [323,325,326]. The major reasons behind the use of oxides for water purification are: high surface area for adsorption, and mesoporous structure, presence of surface charge, stability and low solubility in water.

Alumina nanoparticles have been utilized for the removal of heavy metals from drinking water [461]. The suggested mechanism involves the metal ion induced flocculation of negatively charged alumina nanoparticles (alkaline pH conditions). This happens because of the reduction in the particle-particle repulsive forces (due to surface charge neutralization) leading to increased particle-particle contact.

In another approach, electropositive alumina nanofibers possessing high surface area are synthesized by the sol-gel method [462]. The nanofibers are dispersed over microglass for supported nanoparticle based filtration. It is found that the nanofibers are effective against a variety of micro-organisms having negative surface charge.

Alumina nanofibers have also been utilized for the synthesis of ceramic membranes by casting titanate and boehmite nanofibers on porous substrates (Fig. 29a) [463,464]. The study of pore size reveals that such ceramic membranes exhibit pore sizes of around 60 nm (Fig. 29b). Thus, it can be utilized for effective filtration of many varieties of micro-organisms.

## 8. Commercial interests in drinking water purification

While the emerging applications of nanotechnology in drinking water purification have been outlined so far, it is vital that transformation of such technologies to commercial applications is emphasized. The need for quality and economic drinking water has always necessitated the utilization of newer technology breakthroughs for novel water purification products. Examples of nanotechnology based products in drinking water purification are described in Table 8. A number of technologies commercialized so far are based on already known properties of the bulk material and the improvement in performance achieved through “nanozation” of those

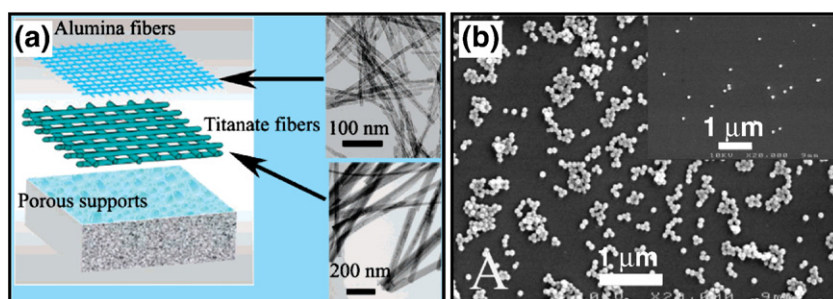


**Fig. 29.** (a) Schematic illustration of the layers in ceramic membranes and TEM images of the boehmite (top) and titanate (bottom) nanofibers [464], (b) SEM image of specimens taken from the feeding and the permeated (inset) fluid in filtrations of solutions of 60 nm latex spheres. Scale bars in the images indicate a length of 1  $\mu\text{m}$ . The membrane after three coatings of alumina fibers on top of the coatings of titanate fibers can filter out 96.8% of latex spheres of 60 nm [463].

materials. A few technologies have also emerged based on the novel properties exhibited by the materials at the nanoscale, an example of which is the chemistry of noble metals. The use of noble metal nanoparticles in domestic water purifiers (Tables 2 and 8) for pesticide removal probably marks the beginning of the use of nanoscale phenomena in this product range.

Commercial interests in the application of noble metals for drinking water purification can be judged from the intellectual property filed in the last few years. The most commercialized application of noble metal nanoparticles is utilization of the anti-bacterial property of silver for use in variety of products [465–468]. The discovery of noble metal nanoparticle-based removal of halogenated organics and pesticides has also been patented for its use in drinking water purification [324,325]. Gold nanoparticles also exhibit potential to remove inorganic mercury from drinking water. Quantum clusters of noble metals have been utilized for developing fluorescence-based detection devices, mainly to detect biomolecules [469]. As mentioned earlier, such methods have also been utilized for the detection of contaminant molecules in drinking water [377]. The shift in the optical plasmon of gold nanorod upon interaction with zerovalent mercury has been utilized for its detection at low concentrations in drinking water [470]. In another interesting study, a method has been developed to discharge ultra-fine particles of gold in water, aimed at utilizing the medicinal properties of gold [471].

## 9. Environmental implications of the use of noble metal nanoparticles

As discussed earlier, noble metal nanoparticle-based chemistry has immense advantages in the area of drinking water purification. The noble metal nanoparticles have multi-pronged use in drinking water purification (removal of organic compounds, heavy metals and microorganisms). While the chemistry of noble metal nanoparticles is

unique in the removal of many contaminants, their high energy surface results in system attempting to minimize the surface energy through protection or chemical transformation or agglomeration. Therefore, the nanoparticles are likely to adsorb a number of other species on the surface. The same properties of nanomaterials (increased surface area, chemical reactivity, etc.) which confer a unique ability to degrade toxic species present in the environment may also render them toxic to humans [472]. In addition, the sudden increase in the variety of novel nanomaterials have led to commercialization of many recent discoveries based on nanomaterials research. Another aspect to consider is that we have already learnt that many of the metal ions never remain in ionic form; they undergo reduction by participating in cellular processes and transform to nanoparticles. This capability has been expressed by human cells as well [248] and transformation leads to the formation and accumulation of metal nanoparticles in human body. Thus, metal toxicity for the human body (currently expressed as metals in ionic form) will soon be required to be studied as an issue of nanomaterial toxicity, implying toxicity as a function of nanoparticle size.

While limited studies on nanomaterial toxicity are available, a few conclusions can be drawn. Silver being a broad-spectrum anti-bacterial agent, is likely to have equally harmful effects on environment-friendly bacteria. Likewise, modified gold surfaces have also exhibited severe toxicity [473]. In the case of ionic silver, it is suggested that it can't cross the blood-brain barrier, and the regulatory activity of blood metallothioneins binds it as thiolate-cluster structures for detoxification [435]. In addition, silver nanoparticles (average size: 25 nm, standard deviation: 7.1 nm) are able to penetrate through stratum corneum and are found in outermost surface of the epidermis after a exposure of 24 h, even though the concentration is negligibly small (applied concentration: 70  $\mu\text{g}/\text{cm}^2$ , cell concentration: <2.32  $\text{ng}/\text{cm}^2$ ) [474]. In addition, long multi-walled carbon nanotubes produce asbestos-like pathogenic behavior (inflammation, formation of nodular lesions and

**Table 8**

Examples of a few nanotechnology-based products in drinking water purification market (compiled from multiple sources on the World Wide Web).

Product Name	Nanomaterial utilized	Contaminants removal	Adsorption capacity	Product life (in l)	Product price
Aquaguard Gold Nova, Eureka Forbes Limited (Launch: 2007, India)	Silver nanoparticle s supported on alumina	Pesticides and halogenated organics	100 mg Chlorpyrifos per g silver nanoparticles	6000	\$30
Adsorbisia, Dow Water Solutions (Launch: 2005, USA)	Titania nanoparticles	Arsenic and disinfection	12–15 g As(V) and 3–4 g As(III) per kg of adsorbent	–	–
AD33, Adedge Technologies, Inc. (Launch: 2002, USA)	Iron oxide nanoparticles	Heavy metals including arsenic, lead, chromium, zinc, copper	–	3800–11,400	\$50
Nanoceram, Argonide (Launch: 2006, USA)	Electropositive alumina nanofibers on a glass filter substrate	Disinfection, natural organic matter, turbidity, salt, radioactivity, heavy metals	–	–	\$3–10 per $\text{m}^2$ , \$75 per filter
ArsenX, SolmeteX, Inc. (Launch: 2004, USA)	Hydrous iron oxide nanoparticles on polymer substrate	Arsenic, vanadium, chromium, uranium	38 mg of Arsenic per g of adsorbent	–	\$0.07–0.20 per 1000 l (amortized)
Nanopore, Nanovation AG (Launch: 2003, Germany)	Membrane filters based on ceramic nanopowder supported on alumina	Disinfection	–	–	–



early fibrosis) when injected into the abdominal cavity of mice [475,476]. It is expected that carbon nanotubes being made of carbon, shouldn't cause toxicity due to their chemical nature. However, other properties of material play a critical role in determining the toxicity: electronic structure, particle dimensions, surface functionalities, chemical stability and accumulation. A number of such aspects have to be explored before a conclusion can be drawn on *nanotoxicity*.

Thus, it is important that for longevity of nanomaterials use in commercial applications, preventive care is taken [477] to minimize the *side-effects*, till those are known. During the intermittent time, several important aspects should be considered for the judicious use of nanomaterials in commercial applications.

- As far as possible, the use of nanoparticle supported on suitable substrates should be preferred. There are many advantages of supported nanoparticle chemistry: minimum leaching of nanoparticles into the environment, easy nanoparticle separation and lower loss in the efficiency of nanoparticle chemistry.
- Quantitative studies on the release of nanoparticles from supports under varying environmental conditions [448].
- Appropriate mechanisms for the recovery of nanomaterials have to be designed.
- Use nanosystems made of materials with minimum toxicity.

It is also important to realize that decision to choose the support should also be influenced by its environment-friendliness. This is important because we have to realize that all water purifiers, while delivering pure drinking water, also end up concentrating the contaminants present in a certain quantity of water (6000 l in during the life of a typical replacement cartridge). This is an environmental hazard leading to accumulation of non-degradable cartridges in the environment. Thus, it is important that eco-friendly support media are utilized. Activated carbon, derived from coconut shell, is an example to mention.

Having reviewed the anti-microbial properties of silver nanoparticles and realizing that silver is by-far the most researched material for anti-bacterial actions, it is important to reiterate the key factors required for optimal biocidal action of silver:

- With the stricter norms on allowed concentration for silver in drinking water, it is important to find novel mechanisms for preventing the release of silver during the process of drinking water purification.
- The anti-bacterial activity of silver needs to be comprehensively evaluated for all classes of bacteria, including environmentally-friendly bacteria. This is important for understanding the precautions required to be followed during the commercial use of silver nanoparticles.
- The influence of environmental conditions on silver nanoparticles needs to be thoroughly studied; e.g., anti-bacterial activity in presence of pesticides, effect of excess chloride in water, etc. Although effects of several of these ions have been examined, since water contains numerous species, no study can be said to be complete.

As mentioned earlier, noble metals have been historically associated with humankind due to their medicinal value. Largely they have been utilized as anti-microbial agents, with gold specifically used for arthritis treatment. Noble metals have been one of the most-utilized inorganic materials for therapeutic value. Similarly, an earlier highlighted work on reduction of gold ions by human cells suggests that gold exists in the nanoform if there is an exposure to it [248]. This offers a certain degree of comfort in the utilization of noble metals for drinking water purification. However, a thorough investigation of the interaction of noble metals with human cells is necessitated and in the interim period, the cautionary approach of avoiding nanoparticle

discharge in water is recommended. Thus, it is best to use supported nanoparticles in which the nanoparticle-support interaction is strong.

## 10. Summary and conclusions

Water has always been associated with the existence of life on earth. From early civilizations, water has been a central theme linked to economic development. The evolution of civilization has always revolved around water. Water is one of the purest signs of prosperity, health, serenity, beauty, and artistry. Similar to human civilization's association with water, a relationship has existed with noble metals. A number of examples from the historical civilizations have suggested the use of noble metals for medicinal purposes. During the long history with noble metals such as gold and silver, no hazards have been reported with such metals in the bulk form.

Moving to modern civilizations, as we progress through rapid phases of industrialization and economic upliftment, it is only natural to expect increasing ecological contamination, even though equilibrium with Nature is desired. The unavailability of quality drinking water is a critical problem across the world. A number of toxic species are present in large concentrations in drinking water. Examples include pesticides, heavy metals, micro-organisms, etc. especially around industrial locations. The severity of the situation can be understood from the fact that 1.8 million people die from diarrheal diseases every year, with children under the age of five most severely impacted. Similarly, 1 billion people lack access to safe drinking water. The discovery of pesticides and other synthetic organic compounds is a representative example. Hence, it becomes clear that without disturbing the path of scientific discovery for novel materials and their commercialization, we need to focus our attention on developing preventive technologies for inhibiting their detrimental impact on the environment.

A number of solutions have earlier been utilized for drinking water purification such as sand filtration, activated carbon based adsorption, distillation and reverse osmosis. While all of them have delivered enormous benefits to mankind, we are still far from ensuring availability of quality drinking water at an affordable price. It is an important goal for state-of-the-art science to deliver. This goal can only be achieved by discovering novel materials with unusual properties.

While traditional synthetic protocols have helped in controlling the spread of toxic species, the finest method has been practiced by Nature for ages. Although we have just started to understand and implement the chemistry of biological degradation of organic compounds, it is certain that Nature's path will remain by-far the most desired method for detoxification of the environment. The underlying theme of nanotechnology has been immensely influenced by Nature's methodology: complete mineralization of halogenated organics to non-toxic forms, environmentally benign nature of reaction end-products and large conversion efficiency with minimum quantity of catalyst. Thus one thing becomes clear to us. To do things in the most efficient fashion - whether chemical synthesis, energy transfer or water filtration - novel materials are likely to play a critical role. The unique properties of novel materials are likely to help in finding newer applications as well as solving the old problems, partially solved by conventional technologies.

Noble metals are historically known to be extremely non-reactive. This is understood from a number of facts: unusually high reduction potential, high ionization energy, high melting point, relativistic contraction, etc. A number of such properties have a dependence on the size of the particle, for example, the melting point of 4 nm gold crystals is 700 K whereas the bulk value is 1337 K. Research conducted over the past 20 years has established numerous methods for size-controlled synthesis of nanoparticles, especially noble metals. A number of new properties have been found which originate at the nanoscale. This points toward the size-dependent reactivity of noble metals, for example, oxidation of carbon monoxide on gold nanoparticle surface. The new found role of noble metals as an efficient catalyst is increasingly being utilized for drinking water purification.

A multitude of factors have been attributed to the chemical reactivity enhancement of nanoparticles: small particle size leading to an increase in specific surface area, increase in the surface energies for easier delocalization of electrons and perfection in atomic organization in the lattice. Besides increased reactivity, the availability of different forms of nanomaterials (e.g., nano-oxides, nanometals, dendrimers, nanoclays, etc) and enhanced knowledge about nanoparticle incorporation on support structures has opened new avenues for science to thoroughly investigate the potential of nanotechnology for large scale environmental detoxification.

Amongst all the recently developed nano-adsorbents for drinking water purification, the chemistry of noble metal nanoparticles is truly unique. As reviewed above, the chemistry of silver nanoparticles has been utilized to remove a number of toxic contaminants found in drinking water including pesticides, heavy metals and micro-organisms. There are several advantages of silver nanoparticle-based chemistry vis-à-vis other nano-based adsorbents: stability of silver nanoparticle against surface oxidation, complete degradation of pesticides, removal of heavy metals in high proportions and broad-range anti-microbial action. These capabilities associated with silver nanoparticles make them an effective nano-adsorbent for removal of toxic species found in drinking water.

The important aspect of how noble metal chemistry becomes unique at nanoscale can be understood from a simple explanation: in the bulk scale, many of the transition metals are chemical reactants whereas noble metals exhibit low reactivity. As mentioned earlier, the chemical reactivity is usually enhanced significantly at the nanoscale and thus most of the transition metals become extremely unstable. However, the reactivity of noble metals is enhanced to such an extent that they catalyze many important reactions without undergoing any self-oxidation.

Where do we go from here? Considering the fact that about a sixth of our global population still lacks access to a reliable water supply [49], the dream of safe water for all is still far away. Largely, it is the search of economical solutions for a number of *old* contaminants coupled with studies on the *emerging* contaminants [53] which will decide the type of technology to be used. Nanotechnology-based approaches, some of which have been described in the article, indeed offer a fresh way to meet such challenges – in which an important role is likely to be played by the chemistry of noble metal nanoparticles.

The fulfillment of the dream will indeed serve the cause of society. *An idea worth one's life.*

## Acknowledgements

We thank the Department of Science and Technology, Government of India for constantly supporting our research program on nanomaterials. We also thank World Gold Council for supporting a part of our program on noble metal nanoparticle-based drinking water purification. We thank Mr. K. R. Antony for the assistance in compiling the summary of different contaminants found in drinking water and the associated health effects.

## References

- [1] As quoted in. S.L. Sass, *The Substance of Civilization: Materials and Human History from the Stone*, Arcade Publishing, New York, 1999.
- [2] As quoted in. C.L. Brown, G. Bushell, M.W. Whitehouse, D.S. Agrawal, S.G. Tupe, K.M. Paknikar, E.R.T. Tiekink, *Gold Bull.* 40 (3) (2007) 245.
- [3] References exist in a book titled *Handbook of Prescription of Emergencies* authored by Ko Hung (Tsin dynasty, 265–419 AD).
- [4] F. Antonii, *Panacea Aurea-Auro Potabile*, Bibliopolio Frobeniano, Hamburg, 1618.
- [5] J. Kunckels, *Nuetliche Observaciones oder Anmerkungen von Auro und Argento Potabili*, Schutzens, Hamburg, 1676.
- [6] G. Savage, *Glass and Glassware*, Octopus Book, London, 1975.
- [7] H.H. Helcher, *Aurum Potabile oder Gold Tinstur*, J. Herbord Klossen, Breslau and Leipzig, 1718.
- [8] *Dictionnaire de Chymie*, Lacombe, Paris, 1769.
- [9] Mrs. Fulhame, *An Essay on Combustion with a View to a New Art of Dying and Painting*, J. Cooper, London, 1794.
- [10] W. Ostwald, *Kolloid Z.* 4 (1909) 5.
- [11] M. Faraday, *Philos. Trans.* 147 (1857) 145.
- [12] Note: Such a phenomenon can't be described by the Mie equation because it doesn't describe the optical properties of material with high particle volume fractions. Recently, an effort was made to study the thin films of gold and explanations were offered using the Maxwell-Garnett model [13].
- [13] M. Kumar, M. Grzelakowski, J. Zilles, M. Clark, W. Meier, *PNAS* 104 (2007) 20719.
- [14] The Royal Institution of Great Britain, cited 18 Dec. 2008; available from: <http://www.rigb.org/rimain/heritage/faradaypage.jsp>.
- [15] P.P. Edwards, J.M. Thomas, *Angew. Chem. Int. Ed.* 46 (2007) 5480.
- [16] S.P. Fricker, *Gold Bull.* 29 (1996) 53.
- [17] J.H. Liebarth, R.H. Persellin, *Agents. Actions.* 11 (1981) 458.
- [18] A.D. Hyatt, B.T. Eaton, *Immuno-Gold Electron Microscopy in Virus Diagnosis and Research*, CRC Press, Boca Raton FL, 1993.
- [19] As quoted in. Rev. William Beloe, *Herodotus, with notes and life of the author*, Jones & Co, London, 1830.
- [20] As quoted in. A.B.G. Lansdown, in: U.-C. Hipler, P. Elsner (Eds.), *Biofunctional textiles and the Skin*, vol. 33, Karger Publishers, 2006.
- [21] As quoted in. A.D. Russell, in: G.P. Ellis, D.K. Luscombe (Eds.), *Progress in Medicinal Chemistry*, Elsevier Science Pub Co, Amsterdam, 1994.
- [22] I.M. Rutkow, *The History of Surgery in the United States, 1775–1900*, Jeremy Norman Co, 1988.
- [23] Ophthalmia neonatorum is a form of bacterial conjunctivitis contracted by newborn babies. A number of bacteria found in the mother's birth canal contaminate the baby's eye during the time of birth; e.g., *Neisseria gonorrhoea*, *Chlamydia trachomatis*. Later, the use of silver nitrate was abolished as it was found that silver nitrate acts as a chemical irritant leading to conjunctivitis.
- [24] M.C. Lea, *Amer. J. Sci.* 37 (1889) 476.
- [25] G. Frens, J.Th.G. Overbeek, *Colloid Poly. Sci.* 233 (1969) 922.
- [26] G.A. Krause, US Patent No. 2046467, 7 Jul. 1936.
- [27] C.E. Renn, US Patent No. 3268444, 23 Aug. 1966.
- [28] O. Blank, German Patent No. DRP 228697, 1910.
- [29] T.E. Lefort, French Patent No. 729952, 27 Mar. 1931.
- [30] N. Krause, N. Morita, in: R.H. Crabtree, D.M.P. Mingos (Eds.), *Comprehensive Organometallic Chemistry III*, Elsevier, Oxford, 2006.
- [31] Health and Safety Executive, *Metallic Silver—HSE review 1996 (Report no. D97)*, HSE, London, 1998.
- [32] World silver survey 2004—a summary, Gold Fields Mineral Services, Washington DC and The Silver Institute, London, 2004.
- [33] S.F. Etris, C.R. Cappel, Kirk-Othmer encyclopedia of chemical technology, John Wiley & Sons, Inc, New York, 2003.
- [34] D.H. Brown, W.E. Smith, *Chem. Soc. Rev.* 9 (1980) 217.
- [35] W.M.H. Sachtler, C. Backx, R.A.V. Santen, *Catal. Rev. Sci. Eng.* 23 (1981) 127.
- [36] G.C. Bond, *Gold Bull.* 5 (1972) 11.
- [37] P. Pyykko, J.-P. Desclaux, *Acc. Chem. Res.* 12 (1979) 276.
- [38] I.P. Grant, *Proc. R. Soc. Lond., Ser. A* 262 (1961) 555.
- [39] J.P. Desclaux, *At. Data Nucl. Data Tables* 12 (1973) 311.
- [40] B. Hammer, J.K. Norskov, *Nature* 376 (1995) 238.
- [41] T. Pradeep, *Nano: The Essentials*, McGraw Hill Publications, New York, NY, 2008.
- [42] G. Mie, *Ann. Phys.* 25 (1908) 377.
- [43] There's Plenty of Room at the Bottom, cited 18 Dec 2008; available from: <http://www.zyvex.com/nanotech/feynman.html>.
- [44] P.A. Buffat, J.-P. Borel, *Phys. Rev. A* 13 (1976) 2287.
- [45] A. Henglein, *J. Phys. Chem.* 97 (1993) 5457.
- [46] G. Schmid, *Chem. Rev.* 92 (1992) 1709.
- [47] M.N. Baker, J.M. Taras, *The Quest for Pure Water: A History of the Twentieth Century*, vol. 1 & 2, American Water Works Association, Denver, 1981.
- [48] C.A. Lucy, *J. Chromatogr. A* 1000 (2003) 711.
- [49] The Millennium Development Goal Report 2007, United Nations, cited 18 Dec 2008; available from: <http://www.un.org/millenniumgoals/pdf/mdg2007.pdf>.
- [50] Global water supply and sanitation assessment 2000 report, cited 18 Dec 2008; available from: [http://www.who.int/water\\_sanitation\\_health/monitoring/globalassess/en/](http://www.who.int/water_sanitation_health/monitoring/globalassess/en/).
- [51] Economic and technical assessment of desalination technologies, Fawzi Banat, Geneva, June 07.
- [52] US Geological Survey, cited 18 Dec 2008; available from: <http://ct.water.usgs.gov/education/morewater.htm>.
- [53] US Environmental Protection Agency, National Primary Drinking Water Regulations and Contaminant Candidate List, cited 18 Dec 2008; available from: <http://www.epa.gov/ogwdw/contaminants/index.html> <http://www.epa.gov/ogwdw/ccl/ccl2.html>.
- [54] The WHO recommended classification of pesticides by hazard and guidelines to classification, cited 18 Dec 2008; available from: [http://www.who.int/ipcs/publications/pesticides\\_hazard\\_rev\\_3.pdf](http://www.who.int/ipcs/publications/pesticides_hazard_rev_3.pdf).
- [55] US Environmental Protection Agency, Environmental Fate and Effects Division, Pesticide Environmental Fate One Line Summary: DDT (p, p'), USEPA, Washington, DC, 1989.
- [56] R.D. Wauchope, T.M. Buttler, A.G. Hornsby, P.W.M.A. Beckers, J.P. Burt, *Rev. Environ. Contam. Toxicol.* 123 (1992) 1.
- [57] P.H. Howard, *Handbook of Environmental Fate and Exposure Data for Organic Chemicals*, Lewis Publishers, Chelsea, MI, 1991.
- [58] W.H. Ahrens (Ed.), *Herbicide Handbook: Weed Science Society of America*, Allen Press, Lawrence, USA, 1994.
- [59] C.O. Karunakaran, *J. Indian Med. Assoc.* 31 (1958) 204.

- [60] G.P. Larrick, J. Agric. Food Chem. 1 (1953) 877.
- [61] Legislations and Regulations, J. Agric. Food Chem. 2 (1954) 1005.
- [62] R. Carson, Silent Spring, Mariner Books, USA, 1962.
- [63] President's Science Advisory Committee, Use of Pesticides, The White House, Washington DC, 1963.
- [64] D.F. Ollis, Environ. Sci. Tech. 19 (1985) 480.
- [65] D.L. Becker, S.C. Wilson, in: P.N. Cheremisinoff, F. Ellebush (Eds.), Carbon Adsorption Handbook, Ann Harbor Science Publishers, Michigan, 1980, p. 167.
- [66] J.A. Bumpus, M. Tien, D. Wright, S.D. Aust, Science 228 (1985) 1434.
- [67] Pesticides industry sales and usage: 2000 and 2001 market estimates, cited 18 Dec 2008; available from: [http://www.epa.gov/oppbead1/pestsales/01pestsales/market\\_estimates2001.pdf](http://www.epa.gov/oppbead1/pestsales/01pestsales/market_estimates2001.pdf).
- [68] T. Pradeep, Anshup, in: N. Savage, M. Diallo, J. Duncan, A. Street, R. Sustich (Eds.), Nanotechnology Applications for Clean Water, William Andrew Publication, USA, 2009.
- [69] G. Shukla, A. Kumar, M. Bhandi, P.E. Joseph, A. Taneja, Environ. Int. 32 (2006) 244.
- [70] H.B. Mathur, H.C. Agarwal, S. Johnson, N. Saikia, Down Earth 14 (2005) 27.
- [71] H.B. Mathur, S. Johnson, A. Kumar, Down Earth 15 (2006) 28.
- [72] Centre for Science and Environment report on pesticide contamination in Kasargod, cited 18 Dec 2008; available from: [http://www.cseindia.org/html/endsulfan/endsulfan\\_index.htm](http://www.cseindia.org/html/endsulfan/endsulfan_index.htm).
- [73] D.C.G. Muir, P.H. Howard, Environ. Sci. Technol. 40 (2006) 7157.
- [74] S.D. Richardson, Anal. Chem. 79 (2007) 4295.
- [75] Y. Ku, H.-M. Chiou, Wat. Air Soil Poll. 133 (2002) 349.
- [76] P. Agre, L.S. King, M. Yasui, W.B. Guggino, O.P. Ottersen, Y. Fujiyoshi, A. Engel, S. Nielsen, J. Physiol. 542 (2002) 3.
- [77] B.L. de Groot, H. Grubmuller, Science 294 (2001) 2353.
- [78] U. Krämer, J.D.C. Howells, J.M. Charnock, A.J.M. Baker, J.A.C. Smith, Nature 379 (1996) 635.
- [79] J.A. Bumpus, M. Tien, D. Wright, S.D. Aust, Science 228 (1985) 1434.
- [80] J.C. Hall, R.E. Hoagland, R.M. Zablotowicz, Pesticide Biotransformation in Plants and Micro-organism: Similarities and Divergences, Oxford University Press, Canada, 2001.
- [81] D. Voet, J.G. Voet, Biochemistry – Biomolecules, Mechanisms of Enzyme action, and Metabolism, John Wiley and Sons, Inc, New Jersey, 2004.
- [82] Y. Zhou, R.S.J. Tol, Water Resour. Res. 41 (2005) 1.
- [83] S.A. Alonitis, K. Kouroumbas, N. Vlachakis, Desalination 157 (2003) 151.
- [84] M.A. Shannon, P.W. Bohn, M. Elimelech, J.G. Georgiadis, B.J. Marinas, A.M. Mayes, Nature 452 (2008) 301.
- [85] A. Asatekin, S. Kang, M. Elimelech, A.M. Mayes, J. Membr. Sci. 298 (2007) 136.
- [86] S. Veerapaneni, B. Long, S. Freeman, R.J. Bond, J. Am. Water Works Assoc. 99 (2007) 95.
- [87] J. Turkevich, P.C. Stevenson, J. Hillier, Discuss. Faraday Soc. 11 (1951) 55.
- [88] E.A. Hauser, J.E. Lynn, Experiments in Colloid Chemistry, McGraw Hill, New York NY, 1940.
- [89] C. Burda, X. Chen, R. Narayanan, M.A. El-Sayed, Chem. Rev. 105 (2005) 1025.
- [90] G.C. Bond, P.A. Sermon, G. Webb, D.A. Buchanan, P.B. Wells, J. Chem. Soc., Chem. Commun. 13 (1973) 444b.
- [91] D. McIntosh, G.A. Ozin, Inorg. Chem. 15 (1976) 2869.
- [92] M. Haruta, N. Yamada, T. Kobayashi, S. Iijima, J. Catal. 115 (2) (February 1989) 301.
- [93] A. Henglein, Chem. Rev. 89 (1989) 1861.
- [94] X. Gu, M. Ji, S.H. Wei, X.G. Gong, Phys. Rev. B 70 (2004) 205401.
- [95] G. Mie, Ann. Phys. (Leipzig) 25 (1908) 377.
- [96] G.C. Schatz, Proc. Nat. Acad. Sci. 104 (2007) 6885.
- [97] M. Mulvihill, A. Tao, K. Benjauthrit, J. Arnold, P. Yang, Angew. Chem. Int. Ed. 47 (2008) 6456.
- [98] K.L. Kelly, E. Coronado, L.L. Zhao, G.C. Schatz, J. Phys. Chem. B 107 (2003) 668.
- [99] F.F. Bohren, D.R. Huffman, Absorption and Scattering of Light by Small Particles, Wiley Interscience, New York, 1983.
- [100] U. Kreibitz, M. Vollmer, Optical Properties of Metal Clusters, Springer Series in Materials Science, Springer, Berlin, 1995.
- [101] U. Kreibitz, in: R.E. Hummel, P. Wissmann (Eds.), Handbook of Optical Properties, Vol. II: Optics of Small Particles, Interfaces and Surfaces, CRC Press, Boca Raton, 1997, p. 145.
- [102] C. Noguez, J. Phys. Chem. C 111 (2007) 3806.
- [103] C. Noguez, Opt. Mater. 27 (2005) 1204.
- [104] F.F. Bohren, D.R. Human, Absorption and Scattering of Light by Small Particles, John Wiley & Sons, New York, 1983.
- [105] G. Schmid, Clusters and Colloids, From Theory to Applications, VCH, Weinheim, 1994.
- [106] C.N.R. Rao, A. Muller, A.K. Cheetham, The Chemistry of Nanomaterials, vol. 1 & 2, Wiley-VCH Verlag, Weinheim, 2004.
- [107] C.N.R. Rao, A. Muller, A.K. Cheetham, Nanomaterials Chemistry: Recent Developments, Wiley-VCH Verlag, Weinheim, 2007.
- [108] C.N.R. Rao, A. Govindaraj, Nanotubes and Nanowires, RSC series on Nanoscience, , 2005, London.
- [109] C.N.R. Rao, A. Govindaraj, S.R.C. Vivekchand, Annu. Rep. Prog. Chem., Sect. A Inorg. Chem. 102 (2006) 20.
- [110] C.N.R. Rao, P.J. Thomas, G.U. Kulkarni, Nanocrystals: Synthesis, Properties and Applications, Springer series on material science, Berlin, 2007.
- [111] C.N.R. Rao, S.R.C. Vivekchand, K. Biswasa, A. Govindaraj, Dalton Trans. (2007) 3728.
- [112] G. Schmid, Nanoparticles: From Theory to Application, Wiley VCH, Weinheim, 2004.
- [113] R.W. Gillham, F.S.O. Hannesin, Ground Water 32 (1994) 958.
- [114] S.K. Das, S.U. Choi, W. Yu, T. Pradeep, Nanofluids: Science and Technology, Wiley-Interscience, USA, 2007.
- [115] Z.L. Wang, Y. Liu, Z. Zhang, Handbook of Nanophase and Nanostructured Materials Vol. 1: Synthesis, Kluwer Academic/Plenum Publishers, USA, 2002.
- [116] G. Cao, Nanostructures & Nanomaterials: Synthesis, Properties & Applications, Imperial College Press, London, 2004.
- [117] D.L. Feldheim, C.A. Foss Jr., Metal Nanoparticles: Synthesis Characterization & Applications, Marcel Dekker Inc, New York, 2002.
- [118] R. Ferrando, J. Jellinek, R.L. Johnston, Chem. Rev. 108 (2008) 845.
- [119] N. Toshima, T. Yonezawa, New J. Chem. 22 (1998) 1179.
- [120] D.V. Goia, E. Matijevic, New J. Chem. 22 (1998) 1203.
- [121] O. Masala, R. Seshadri, Annu. Rev. Mater. Res. 34 (2004) 41.
- [122] A. Roucoux, J. Schulz, H. Patin, Chem. Rev. 102 (2002) 3757.
- [123] The Hamaker constant is utilized for describing the van der Waals interaction between a pair of bodies. The magnitude of the Hamaker constant reflects the strength of the van der Waals interaction. The originally developed Hamaker's method ignores the influence of an intervening medium between the two particles of interaction. In a simplistic model of two interacting spheres (radius:  $a_1, a_2$ ) separated by a distance  $d$ , the van der Waals potential =  $-(A_H/6d)(a_1a_2/(a_1 + a_2))$ . Further research has incorporated the dependence of Hamaker constant to the dielectric constant of the medium. Further details: H.C. Hamaker, Physica, 4(1937) 1058.
- [124] P.C. Hiemenz, R. Rajagopalan, Principles of Colloid and Surface Chemistry, CRC Press, Boca Raton FL, 1997.
- [125] M. Brust, M. Walker, D. Bethell, D.J. Schiffrin, R. Whyman, J. Chem. Soc., Chem. Commun. (1994) 801.
- [126] T. Teranishi, I. Kiyokawa, M. Miyake, Adv. Mater. 10 (1998) 596.
- [127] T. Teranishi, M. Hosoe, T. Tanaka, M. Miyake, J. Phys. Chem. B. 103 (1999) 3818.
- [128] M.K. Corbierre, N.S. Cameron, M. Sutton, S.G.J. Mochrie, L.B. Lurio, A. Ruhm, R.B. Lennox, J. Am. Chem. Soc. 123 (2001) 10411.
- [129] T.K. Mandal, M.S. Fleming, D.R. Walt, Nano. Lett. 2 (2002) 3.
- [130] J. Shan, M. Nuopponen, H. Jiang, E. Kauppinen, H. Tenhu, Macromolecules 36 (2003) 4526.
- [131] P.E. Laibinis, G.M. Whitesides, J. Am. Chem. Soc. 114 (1992) 9022.
- [132] K.L. Prime, G.M. Whitesides, Science 252 (1991) 1164.
- [133] M.-C. Daniel, D. Astruc, Chem. Rev. 104 (2004) 293.
- [134] S. Flink, F.C.J.M. van Veggel, D.N. Reinhoudt, Adv. Mater. 12 (2000) 1315.
- [135] J.T.G. Overbeek, in: J.W. Goodwin (Ed.), Colloidal Dispersions, Royal Society of Chemistry, London, 1981, p. 1.
- [136] R.A. Alvarez-Puebla, E. Arceo, P.J.G. Goulet, J.J. Garrido, R.F. Aroca, J. Phys. Chem. B 109 (2005) 3787.
- [137] C.G. Blatchford, J.R. Campbell, J.A. Creighton, Surf. Sci. Lett. 120 (1982) A339.
- [138] J.A. Creighton, C.G. Blatchford, M.G. Albrecht, J. Chem. Soc., Faraday Trans. 2 (75) (1979) 790.
- [139] L. Zang, C.-Y. Liu, X.-M. Rent, J. Photochem. Photobiol. A: Chem. 74 (1993) 267.
- [140] Y. Liu, C.-Y. Liu, L.-B. Chen, Z.-Y. Zhang, J. Colloid Interf. Sci. 257 (2003) 188.
- [141] C.-Y. Wang, C.-Y. Liu, M. Wang, T. Shen, Spectrochim. Acta Part A 55 (1999) 991.
- [142] A. Duteil, R. Queau, B.M. Chaudret, C. Roucau, J.S. Bradley, Chem. Mater. 5 (1993) 341.
- [143] M. Komiyama, H. Hirai, Bull. Chem. Soc. Jpn. 56 (1983) 2833.
- [144] L.S. Ott, B.J. Hornstein, R.G. Finke, Langmuir 22 (2006) 9357.
- [145] R.Z. Zsigmondy, Anal. Chem. 40 (1968) 697.
- [146] H. Thiele, H.S. Von Lavern, J. Colloid Sci. 20 (1965) 679.
- [147] L.D. Pachon, G. Rothenberg, Appl. Organometal. Chem. 22 (2008) 288.
- [148] S. Özkar, R.G. Finke, J. Am. Chem. Soc. 124 (2002) 5796.
- [149] S. Özkar, R.G. Finke, Langmuir 18 (2002) 7653.
- [150] L.S. Ott, M.L. Cline, R.G. Finke, J. Nanosci. Nanotechnol. 7 (2007) 2400.
- [151] S. Özkar, R.G. Finke, Langmuir 19 (2003) 6247.
- [152] L.S. Ott, S. Campell, K.R. Seddon, R.G. Finke, J. Am. Chem. Soc. 127 (2005) 5758.
- [153] L.S. Ott, S. Campell, K.R. Seddon, R.G. Finke, Inorg. Chem. 46 (2007) 10335.
- [154] L.S. Ott, R.G. Finke, Inorg. Chem. 45 (2006) 8382.
- [155] Y. Kang, T.A. Taton, Angew. Chem. Int. Ed. 44 (2005) 409.
- [156] B.-S. Kim, J.-M. Qiu, J.-P. Wang, T.A. Taton, Nano Lett. 5 (2005) 1987.
- [157] L.E. Euliss, S.G. Grancharov, S. O'Brien, T.J. Deming, G.D. Stucky, C.B. Murray, G.A. Held, Nano Lett. 3 (2003) 1489.
- [158] K. Meguro, Y. Nakamura, Y. Hayashi, M. Torizuka, K. Esumi, Bull. Chem. Soc. Jpn. 61 (1988) 347.
- [159] J. Eastoe, B. Warne, Curr. Opin. Colloid Interf. Sci. 1 (1996) 800.
- [160] J. Kuyper, J. Am. Chem. Soc. 55 (1933) 1722.
- [161] G. Frens, Nature Phys. Sci. 241 (1973) 20.
- [162] P.C. Lee, D. Meisel, J. Phys. Chem. 86 (1982) 3391.
- [163] P.V. Kamat, M. Flumiani, G.V. Hartland, J. Phys. Chem. B 102 (1998) 3123.
- [164] A. Henglein, Chem. Phys. Lett. 154 (1989) 473.
- [165] Z.S. Pillai, P.V. Kamat, J. Phys. Chem. B 108 (2004) 945.
- [166] A.L. Smith, Particle Growth in Suspensions, Academic Press, London, 1983.
- [167] B.L. Cushing, V.L. Kolesnichenko, C.J. O'Connor, Chem. Rev. 104 (2004) 3893.
- [168] N.R. Jana, L. Gearheart, C.J. Murphy, Chem. Mater. 13 (2001) 2313.
- [169] E.C. Stathis, H.C. Gatos, Ind. Eng. Chem., Anal. Ed. 18 (1946) 801.
- [170] E.C. Stathis, A. Fabrikanos, Chem. Ind. 47 (1958) 860.
- [171] G.N. Glavee, K.J. Klubunde, C.M. Sorensen, G.C. Hadjapanayis, Langmuir 8 (1992) 771.
- [172] J. Turkevich, G. Kim, Science 169 (1970) 873.
- [173] H. Wieland, Ber. Dtsch. Chem. Ges. 45 (1912) 484 (in German).
- [174] D.D. Evanoff Jr., G. Chumanov, J. Phys. Chem. B 108 (2004) 13948.
- [175] A.J. Barnard Jr., W.C. Broad, H. Flaschka, Microchem. J. 3 (1959) 43.
- [176] A. Gutbier, Z. Anorg. Chem. 32 (1902) 347 (in German).
- [177] U. Nickel, A. zu Castell, K. Pöppel, S. Schneider, Langmuir 16 (2000) 9087.
- [178] H. Hirai, Y. Nakao, N. Toshima, Chem. Lett. (1978) 545.



- [179] H. Hirai, Y. Nakao, N. Toshima, K. Adachi, *Chem. Lett.* 5 (1976) 905.
- [180] N. Toshima, T. Yonezawa, K. Kushihashi, *J. Chem. Soc., Faraday Trans.* 89 (1993) 2537.
- [181] D.-H. Chen, Y.-W. Huang, *J. Colloid Interf. Sci.* 255 (2002) 299.
- [182] S. Steenken, P. Neta, *J. Phys. Chem.* 86 (1982) 3661.
- [183] G.N. Glavee, K.J. Klabunde, C.M. Sorensen, G.C. Hadjipanayis, *Langmuir* 10 (1994) 4726.
- [184] M. Boutonnet, J. Kizling, P. Stenius, G. Maire, *Colloids Surf.* 5 (1982) 209.
- [185] A.C. Templeton, W.P. Wuelfing, R.W. Murray, *Acc. Chem. Res.* 33 (2000) 27.
- [186] M.D. Porter, T.B. Bright, D.L. Allara, C.E.D. Chidsey, *J. Am. Chem. Soc.* 109 (1987) 3559.
- [187] S. Chen, *Langmuir* 15 (1999) 7551.
- [188] S. Chen, R.W. Murray, *Langmuir* 15 (1999) 682.
- [189] M.J. Hostetler, S.J. Green, J.J. Stokes, R.W. Murray, *J. Am. Chem. Soc.* 118 (1996) 4212.
- [190] R.S. Ingram, M.J. Hostetler, R.W. Murray, *J. Am. Chem. Soc.* 119 (1997) 9175.
- [191] A.C. Templeton, M.J. Hostetler, C.T. Kraft, R.W. Murray, *J. Am. Chem. Soc.* 120 (1998) 1906.
- [192] M.J. Hostetler, A.C. Templeton, R.W. Murray, *Langmuir* 15 (1999) 3782.
- [193] M. Brust, J. Fink, D. Bethell, D.J. Schiffrin, C.J. Kiely, *J. Chem. Soc., Chem. Commun.* (1995) 1655.
- [194] I.G. Dance, K.J. Fisher, R.M.H. Banda, M.L. Scudder, *Inorg. Chem.* 30 (1991) 183.
- [195] M.J. Baena, P. Espinet, M.C. Lequerica, A.M. Levelut, *J. Am. Chem. Soc.* 114 (1992) 4182.
- [196] S. Murthy, T.P. Bigioni, Z.L. Wang, J.T. Khoury, R.L. Whetten, *Mater. Lett.* 30 (1997) 321.
- [197] K.V. Sarathy, G.U. Kulkarni, C.N.R. Rao, *Chem. Commun.* (1997) 537.
- [198] N. Sandhyarani, T. Pradeep, *J. Mater. Chem.* 10 (2000) 981.
- [199] M. Dasog, R.W.J. Scott, *Langmuir* 23 (2007) 3381.
- [200] N. Sandhyarani, T. Pradeep, *Chem. Phys. Lett.* 338 (2001) 33.
- [201] N. Sandhyarani, T. Pradeep, J.S. Francisco, *Chem. Phys. Lett.* 342 (2001) 272.
- [202] R.P. Andres, J.D. Bielefeld, J.I. Henderson, D.B. Janes, V.R. Kolagunta, C.P. Kubiak, W.J. Mahoney, R.G. Osifchin, *Science* 273 (1996) 1690.
- [203] X.M. Lin, C.M. Sorensen, *Chem. Mater.* 11 (1999) 198.
- [204] L.O. Brown, J.E. Hutchison, *J. Phys. Chem. B* 105 (2001) 8911.
- [205] S.I. Stoeva, K.J. Klabunde, C.M. Sorensen, I. Dragieva, *J. Am. Chem. Soc.* 124 (2002) 2305.
- [206] R.L. Whetten, J.T. Khoury, M.M. Alvarez, S. Murthy, I. Vezmar, Z.L. Wang, P.W. Stephens, C.L. Cleveland, W.D. Luedtke, U. Landman, *Adv. Mater.* 8 (1996) 428.
- [207] M. Brust, D. Bethell, D.J. Schiffrin, C.J. Kiely, *Adv. Mater.* 7 (1995) 795.
- [208] S.W. Chen, R.S. Ingram, M.J. Hostetler, J.J. Pietron, R.W. Murray, T.G. Schaff, J.T. Khoury, M.M. Alvarez, R.L. Whetten, *Science* 280 (1998) 2098.
- [209] D.I. Gittins, D. Bethell, R.J. Nichols, D.J. Schiffrin, *Adv. Mater.* 11 (1999) 737.
- [210] C.J. Kiely, J. Fink, M. Brust, D. Bethell, D.J. Schiffrin, *Nature* 396 (1998) 444.
- [211] B.L.V. Prasad, S.I. Stoeva, C.M. Sorensen, K.J. Klabunde, *Langmuir* 18 (2002) 7515.
- [212] B.L.V. Prasad, S.I. Stoeva, C.M. Sorensen, K.J. Klabunde, *Chem. Mater.* 15 (2003) 935.
- [213] N. Sandhyarani, T. Pradeep, J. Chakrabarti, M. Yousuf, H.K. Sahu, *Phys. Rev. B* 62 (2000) 739.
- [214] S.A. Harfenist, Z.L. Wang, M.M. Alvarez, I. Vezmar, R.L. Whetten, *J. Phys. Chem.* 100 (1996) 13904.
- [215] K.V. Sarathy, G. Raina, R.T. Yadav, G.U. Kulkarni, C.N.R. Rao, *J. Phys. Chem. B* 101 (1997) 9876.
- [216] S. He, J. Yao, P. Jiang, D. Shi, H. Zhang, S. Xie, S. Pang, H. Gao, *Langmuir* 17 (2001) 1571.
- [217] M. Green, P. O'Brien, *Chem. Commun.* (2000) 183.
- [218] N.R. Jana, X. Peng, *J. Am. Chem. Soc.* 125 (2003) 14280.
- [219] G.R. Newkome, C.N. Moorefield, F. Vogtle, *Dendritic Molecules: Concepts, Syntheses and Perspectives*, Wiley VCH Weinheim, Germany, 1996.
- [220] A.W. Bosman, H.M. Janssen, E.W. Meijer, *Chem. Rev.* 99 (1999) 1665.
- [221] F. Zeng, S.C. Zimmerman, *Chem. Rev.* 97 (1997) 1681.
- [222] C.C. Lee, J.A. MacKay, J.M.J. Fréchet, F.C. Szoka, *Nat. Biotechnol.* 23 (2005) 1517.
- [223] J.F.G.A. Jansen, E.M.M. de Brabander-van den Berg, E.W. Meijer, *Science* 266 (1994) 1226.
- [224] R.M. Crooks, B.I. Lemon III, L. Sun, L.K. Yeung, M. Zhao, *Top. Curr. Chem.* 212 (2001) 81.
- [225] M. Zhao, L. Sun, R.M. Crooks, *J. Am. Chem. Soc.* 120 (1998) 4877.
- [226] M. Zhao, R.M. Crooks, *Angew. Chem. Int. Ed.* 38 (1999) 364.
- [227] M. Gerloch, E.C. Constable, *Transition Metal Chemistry: The Valence Shell in d-Block Chemistry*, Wiley-VCH, Weinheim, 1994.
- [228] M.E. Garcia, L.A. Baker, R.M. Crooks, *Anal. Chem.* 71 (1999) 256.
- [229] K. Esumi, A. Suzuki, N. Aihara, K. Usui, K. Torigoe, *Langmuir* 14 (1998) 3157.
- [230] F. Grohn, B.J. Bauer, Y.A. Akpalu, C.L. Jackson, E.J. Amis, *Macromolecules* 33 (2000) 6042.
- [231] M. Zhao, R.M. Crooks, *Adv. Mater.* 11 (1999) 217.
- [232] J. Zheng, R.M. Dickson, *J. Am. Chem. Soc.* 124 (2002) 13982.
- [233] S. Silver, *Gene* 179 (1996) 9.
- [234] R.P. Blakemore, *Science* 190 (1975) 377.
- [235] R.B. Frankel, R.P. Blakemore, R.S. Wolfe, *Science* 203 (1979) 1355.
- [236] S. Mann, R.B. Frankel, R.P. Blakemore, *Nature* 310 (1984) 405.
- [237] D.R. Lovley, J.F. Stolz, G.L. Nord, E.J.P. Phillips, *Nature* 330 (1987) 252.
- [238] D.R. Lovley, E.J.P. Phillips, Y.A. Gorby, E.R. Landa, *Nature* 350 (1991) 413.
- [239] G. Southam, T.J. Beveridge, *Geochim. Cosmochim. Acta* 58 (1994) 4527.
- [240] T.J. Beveridge, R.G.E. Murray, *J. Bacteriol.* 141 (1980) 876.
- [241] T. Klaus, R. Joergel, E. Olsson, C.-G. Granqvist, *Proc. Natl. Acad. Sci. U.S.A.* 96 (1999) 13611.
- [242] J.L.G. Torresdey, J.G. Parsons, E. Gomez, J.P. Vide, H.E. Troiani, P. Santiago, M.J. Yacaman, *Nano Lett.* 2 (2002) 397.
- [243] S.S. Shankar, A. Rai, B. Ankamwar, A. Singh, A. Ahmad, M. Sastry, *Nat. Mater.* 3 (2004) 482.
- [244] B. Nair, T. Pradeep, *Cryst. Growth Des.* 2 (2002) 293.
- [245] P. Mukherjee, A. Ahmad, D. Mandal, S. Senapati, S.R. Sainkar, M.I. Khan, R. Parishcha, P.V. Ajaykumar, M. Alam, R. Kumar, M. Sastry, *Nano Lett.* 1 (2001) 515.
- [246] P. Mukherjee, A. Ahmad, D. Mandal, S. Senapati, S.R. Sainkar, M.I. Khan, R. Ramani, R. Parishcha, P.V. Ajaykumar, M. Alam, M. Sastry, R. Kumar, *Angew. Chem., Int. Ed.* 40 (2001) 3585.
- [247] Z. Li, S.W. Chung, J.M. Nam, D.S. Ginger, C.A. Mirkin, *Angew. Chem. Int. Ed.* 42 (2003) 2306.
- [248] Anshup, J.S. Venkataraman, C. Subramaniam, R.R. Kumar, S. Priya, T.R.S. Kumar, R.V. Omkumar, A. John, T. Pradeep, *Langmuir* 21 (2005) 11562.
- [249] M. Sastry, A. Ahmad, M.I. Khan, R. Kumar, in: C.M. Niemeyer, C.A. Mirkin (Eds.), *Nanobiotechnology*, Wiley-VCH, Weinheim, Germany, 2004, p. 126.
- [250] M. Sastry, A. Ahmad, M.I. Khan, R. Kumar, *Curr. Sci.* 85 (2003) 162.
- [251] M. Sarikaya, C. Tamerler, D.T. Schwartz, F. Baneyx, *Annu. Rev. Mater. Res.* 34 (2004) 373.
- [252] M. Sarikaya, *Proc. Natl. Acad. Sci. USA* 96 (1999) 14183.
- [253] A. Ahmad, S. Senapati, M.I. Khan, R. Kumar, R. Ramani, V. Srinivas, M. Sastry, *Nanotechnology* 14 (2003) 824.
- [254] S. Brown, *Nat. Biotechnol.* 15 (1997) 269.
- [255] S. Brown, *Proc. Natl. Acad. Sci. USA* 89 (1992) 8651.
- [256] S. Brown, M. Sarikaya, E. Johnson, *J. Mol. Biol.* 299 (2000) 725.
- [257] J.L. Kulp, M. Sarikaya, J.S. Evans, *J. Mater. Chem.* 14 (2004) 2325.
- [258] R.R. Naik, S.J. Stringer, G. Agarwal, S.E. Jones, M.O. Stone, *Nat. Mater.* 1 (2002) 169.
- [259] M. Sarikaya, C. Tamerler, A.Y. Jen, K. Schulten, F. Baneyx, *Nat. Mater.* 2 (2003) 577.
- [260] P.R. Sajanlal, T. Pradeep, *Adv. Mat.* 20 (2008) 980.
- [261] E. Leontidis, K. Kleitou, T. Kyprianidou, V. Bekiaris, P. Lianos, *Langmuir* 18 (2002) 3659.
- [262] J.A. Dahl, B.L.S. Maddux, J.E. Hutchison, *Chem. Rev.* 107 (2007) 2228.
- [263] C.L. Nehl, J.H. Hafner, *J. Mater. Chem.* 18 (2008) 2415.
- [264] M.A. El-Sayed, *Acc. Chem. Res.* 34 (2001) 257.
- [265] Y. Xia, Y. Xiong, B. Lim, S.E. Skrabalak, *Angew. Chem. Int. Ed.* 47 (2008) 2.
- [266] Z. Peng, H. Yang, *Nanotoday*, 4 (2009) 143.
- [267] S. Link, M.B. Mohamed, M.A. El-Sayed, *J. Phys. Chem. B* 103 (1999) 3073.
- [268] Y.-Y. Yu, S.-S. Chang, C.-L. Lee, C.R.C. Wang, *J. Phys. Chem. B* 101 (1997) 6661.
- [269] X. Huang, I.H. El-Sayed, W. Qian, M.A. El-Sayed, *J. Am. Chem. Soc.* 128 (2006) 2115.
- [270] M.B. Mohamed, V. Volkov, S. Link, M.A. El-Sayed, *Chem. Phys. Lett.* 317 (2000) 517.
- [271] T.S. Sreepasad, A.K. Samal, T. Pradeep, *Langmuir* 24 (2008) 4589.
- [272] V.R. Rajeev Kumar, A.K. Samal, T.S. Sreepasad, T. Pradeep, *Langmuir* 23 (2007) 8667.
- [273] J.A. Dahl, B.L.S. Maddux, J.E. Hutchison, *Chem. Rev.* 107 (2007) 2228.
- [274] C.N.R. Rao, G.U. Kulkarni, P.J. Thomas, Peter P. Edwards, *Chem. Eur. J.* 8 (2002) 28.
- [275] W.P. Halperin, *Rev. Mod. Phys.* 58 (1986) 533.
- [276] R. Kubo, *J. Phys. Soc. Jpn.* 17 (1962) 975.
- [277] J.A.A.J. Perenboom, P. Wyder, F. Meier, *Phys. Rep.* 78 (1983) 173.
- [278] H. Frohlich, *Physica (Utr.)* 4 (1937) 406.
- [279] C. Kittel, *Einführung in die Festkörperphysik*, R. Oldenbourg Verlag München, Wien, 1989 (in German).
- [280] N.W. Ashcroft, N.D. Mermin, *Solid State Physics*, Saunders College, Philadelphia, 1976.
- [281] J.-H. Chen, C. Jang, S. Xiao, M. Ishigami, M.S. Fuhrer, *Nat. Nanotech.* 3 (2008) 206.
- [282] F. Miao, S. Wijeratne, Y. Zhang, U. Coskun, W. Bao, C.N. Lau, *Science* 317 (2007) 1530.
- [283] W.F. Banholzer, R.I. Masel, *J. Catal.* 85 (1984) 127.
- [284] N. Hoshi, S. Kawatani, M. Kudo, Y. Hori, *J. Electroanal. Chem.* 467 (1999) 67.
- [285] L.M. Falicov, G.A. Somorjai, *Proc. Natl. Acad. Sci. USA* 82 (1985) 2207.
- [286] N. Tian, Z.Y. Zhou, S.G. Sun, Y. Ding, Z.L. Wang, *Science* 316 (2007) 732.
- [287] R. Narayanan, M.A. El-Sayed, *Nano Lett.* 4 (2007) 1343.
- [288] K.M. Brattlie, H. Lee, K. Komvopoulos, P. Yang, G.A. Somorjai, *Nano Lett.* 7 (2007) 3097.
- [289] D. Ferrer, D.A. Blom, L.F. Allard, S. Mejia, E.P. Tijerina, M.J. Yacaman, *J. Mater. Chem.* 18 (2008) 2442.
- [290] A. Zecchina, E. Groppo, S. Bordiga, *Chem. Eur. J.* 13 (2007) 2440.
- [291] H. Lee, S. Habas, S. Kweskin, D. Butcher, G.A. Somorjai, P. Yang, *Angew. Chem. Int. Ed.* 45 (2006) 7824.
- [292] S. Schimpf, M. Lucas, C. Mohr, U. Rodemerck, A. Bruckner, J. Radnik, H. Hofmeister, P. Claus, *Catal. Today* 72 (2002) 63.
- [293] S. Panigrahi, S. Basu, S. Praharaj, S. Pande, S. Jana, A. Pal, S.K. Ghosh, T. Pal, *J. Phys. Chem. C* 111 (2007) 4596.
- [294] N.R. Jana, T.K. Sau, T. Pal, *J. Phys. Chem. B* 103 (1999) 115.
- [295] G.C. Bond, in: G. Ertl, H. Knozinger, J. Weitkamp (Eds.), *Handbook of Heterogeneous Catalysis*, vol. 2, Weinheim, VCH, 1997, p. 752.
- [296] M. Haruta, *Catal. Today* 36 (1997) 153.
- [297] Role of activated carbon as a support for the removal of pesticides from drinking water using noble metal nanoparticles, T. Pradeep et al. (Unpublished)
- [298] H. Hofmeister, P.T. Miclea, M. Steen, W. Morke, H. Drevs, *Top. Catal.* 46 (2007) 11.
- [299] S. Padtare, V.P. Vinod, K. Mukhopadhyay, A. Kumar, M. Rao, R.V. Chaudhari, M. Sastry, *Biotechnol. Bioeng.* 85 (2004) 629.
- [300] P. Serp, R. Freurer, Y. Kihn, P. Kalck, J.L. Faria, J.L. Figueiredo, *J. Mater. Chem.* 11 (2001) 1980.
- [301] P. Sabatier, *Catalysis in Organic Chemistry*, D. Van Nostrand Company, 1922, p. 64, 71-72, 135-136, 251-256.

- [302] M. Qian, M.A. Liauw, G. Emig, *Appl. Catal. A: Gen* 238 (2003) 211.
- [303] G.H. Twigg, *Proc. Roy. Soc. Lond. Math. Phys. Sci.* 188 (1946) 92.
- [304] G.H. Twigg, *Proc. Roy. Soc. Lond. Math. Phys. Sci.* 188 (1946) 105.
- [305] D. Astruc, *Nanoparticles and Catalysis*, Wiley-VCH, Weinheim, 2007.
- [306] R.M. Crooks, M. Zhao, L. Sun, V. Chechik, L.K. Yeung, *Acc. Chem. Res.* 34 (2001) 181.
- [307] M.M. Mañas, R. Pleixats, *Acc. Chem. Res.* 36 (2003) 638.
- [308] T. Yonezawa, N. Toshima, in: H.S. Nalwa (Ed.), *Advanced Functional Molecules and Polymers*, vol. 2, OPA, N.V., 2001, p. 65.
- [309] T. Senzaki, Y. Kumagai, *Kogyo Yosui* (1988) 2 (in Japanese).
- [310] T. Senzaki, Y. Kumagai, *Kogyo Yosui* (1989) 19 (in Japanese).
- [311] F.H. Rhodes, J.T. Carty, *Ind. Eng. Chem.* 17 (1925) 909.
- [312] X.-qin Li, D.W. Elliott, W.-xian Zhang, *Crit. Rev. Solid State Mater. Sci.* 31 (2006) 111.
- [313] W.-xian Zhang, *J. Nanoparticle Res.* 5 (2003) 323.
- [314] F. He, D. Zhao, C. Roberts, in: N. Savage, M. Diallo, J. Duncan, A. Street, R. Sustich (Eds.), *Nanotechnology Applications for Clean Water*, William Andrew Publication, USA, 2009.
- [315] 490 S.M.C. Ritchie, in: N. Savage, M. Diallo, J. Duncan, A. Street, R. Sustich (Eds.), *Nanotechnology Applications for Clean Water*, William Andrew Publication, USA, 2009.
- [316] K.M. Cross, Y. Lu, T. Zheng, J. Zhan, G. McPherson, V. John, in: N. Savage, M. Diallo, J. Duncan, A. Street, R. Sustich (Eds.), *Nanotechnology Applications for Clean Water*, William Andrew Publication, USA, 2009.
- [317] T. Boronina, K.J. Klabunde, G. Sergeev, *Environ. Sci. Technol.* 29 (1995) 1511.
- [318] A. Henglein, *Chem. Mater.* 10 (1998) 444.
- [319] A. Henglein, D. Meisel, *J. Phys. Chem. B* 102 (1998) 8364.
- [320] A.S. Nair, T. Pradeep, *Curr. Sci.* 84 (2003) 1560.
- [321] A.S. Nair, R.T. Tom, V.R. Rajeev Kumar, C. Subramaniam, T. Pradeep, *Cosmos* 3 (2007) 103.
- [322] A.S. Nair, R.T. Tom, T. Pradeep, *J. Environ. Monit.* 5 (2003) 363.
- [323] A.S. Nair, T. Pradeep, *J. Nanosci. Nanotechnol.* 7 (2007) 1871.
- [324] T. Pradeep, A.S. Nair, *Indian Patent No.* PCT/IN2005/000022, 2 June 2006.
- [325] T. Pradeep, A.S. Nair, *PCT Application No.* PCT/IN2005/000022, 19 Jan. 2005.
- [326] T. Pradeep, A.S. Nair, *Indian Patent Application No.* 879/CHE/2007, 10 Dec 2007.
- [327] A.S. Nair, R.T. Tom, V. Suryanarayanan, T. Pradeep, *J. Mater. Chem.* 13 (2003) 297.
- [328] V. Suryanarayanan, A.S. Nair, R.T. Tom, T. Pradeep, *J. Mater. Chem.* 14 (2004) 2661.
- [329] M.J. Rosemary, I. Mac Laren, T. Pradeep, *Carbon* 42 (2004) 2352.
- [330] M.J. Rosemary, V. Suryanarayanan, I. MacLaren, T. Pradeep, *J. Chem. Sci.* 118 (2006) 375.
- [331] M.J. Rosemary, I. MacLaren, T. Pradeep, *Langmuir* 22 (2006) 10125.
- [332] D.L. Illman, *Anal. Chem.* 78 (2006) 5266.
- [333] S.D. Richardson, *Anal. Chem.* 79 (2007) 4295.
- [334] J. Slobodnik, B.L.M. van Baar, U.A.T. Brinkman, *J. Chromatogr. A* 703 (1995) 81.
- [335] S. Andreescu, J.L. Marty, *Biomol. Eng.* 2 (2006) 1.
- [336] X.-J. Huang, Y.-K. Choi, *Sensor. Actuator. B Chem.* 122 (2007) 659.
- [337] P.K. Sudeep, S.T.S. Joseph, K.G. Thomas, *J. Am. Chem. Soc.* 127 (2005) 6516.
- [338] S.S.R. Dasary, U.S. Rai, H. Yu, Y. Anjaneyulu, M. Dubey, P.C. Ray, *Chem. Phys. Lett.* 460 (2008) 187.
- [339] D.J. Lewis, T.M. Day, J.V. MacPherson, Z. Pikramenou, *Chem. Commun.* (2006) 1433.
- [340] J.D.S. Newman, J.M. Roberts, G.J. Blanchard, *Anal. Chem.* 79 (2007) 3448.
- [341] J.D.S. Newman, J.M. Roberts, G.J. Blanchard, *Anal. Chim. Act.* 602 (2007) 101.
- [342] S.-Q. Hua, J.-W. Xie, Q.-H. Xu, K.-T. Rong, G.-Li Shen, *Talanta* 61 (2003) 769.
- [343] D.P. Dumas, H.D. Durst, W.G. Landis, F.M. Raushel, *Arch. Biochem. Biophys.* 277 (1999) 155.
- [344] V. Pavlov, Y. Xiao, I. Willner, *Nano Lett.* 5 (2005) 649.
- [345] D. Du, J. Ding, Y. Tao, X. Chen, *Sensor. Actuator. B Chem.* 134 (2008) 908.
- [346] J.M. Pingarron, P.Y. Sedeno, A.G. Cortes, *Electrochim. Acta* 53 (2008) 5848.
- [347] K.A. Hassal, *The Biochemistry and Use of Pesticides: Structure, Metabolism, Mode of Action and Uses in Crop Protection*, VCH Publishers Inc., New York, 1990.
- [348] T.-J. Lin, K.-T. Huang, C.-Y. Liu, *Biosens. Bioelectron.* 22 (2006) 513.
- [349] Rajan, S. Chand, B.D. Gupta, *Sensor. Actuator. B Chem.* 123 (2007) 661.
- [350] X. Sun, K. Xia, B. Liu, *Talanta* 76 (2008) 747.
- [351] K.P. Lisha, Anshup, T. Pradeep, *J. Environ. Sci. Health B.* (in press).
- [352] C. Burns, W.U. Spindel, S. Puckett, G.E. Pacey, *Talanta* 69 (2006) 873.
- [353] S.T. Dubas, V. Pimpan, *Mater. Lett.* 62 (2008) 2661.
- [354] K. Kneipp, H. Kneipp, I. Itzkan, R.R. Dasari, M.S. Feld, *Chem. Rev.* 99 (1999) 2957.
- [355] M. Moskovits, *Rev. Mod. Phys.* 57 (1985) 783.
- [356] K. Kneipp, Y. Wang, H. Kneipp, L.T. Perelman, I. Itzkan, R.R. Dasari, M.S. Feld, *Phys. Rev. Lett.* 78 (1997) 1667.
- [357] S. Nie, S.R. Emory, *Science* 275 (1997) 1102.
- [358] V.S. Tiwari, T. Oleg, G.K. Darbha, W. Hardy, J.P. Singh, P.C. Ray, *Chem. Phys. Lett.* 446 (2007) 77.
- [359] A. Tao, F. Kim, C. Hess, J. Goldberger, R. He, Y. Sun, Y. Xia, P. Yang, *Nano Lett.* 3 (2003) 1229.
- [360] A.J. Bonham, G. Braun, I. Pavel, M. Moskovits, N.O. Reich, *J. Am. Chem. Soc.* 129 (2007) 14572.
- [361] R.A.A. Puebla, D.S. dos Santos Jr., R.F. Aroca, *Analyst* 132 (2007) 1210.
- [362] A. Henglein, P. Mulvaney, T. Linnert, A. Holzwarth, *J. Phys. Chem.* 96 (1992) 2411.
- [363] C. Namasivayam, K. Periasamy, *Water Res.* 27 (1993) 1663.
- [364] R.R. Navarro, K. Sumi, N. Fujii, M. Matsumura, *Water Res.* 30 (1996) 2488.
- [365] V. Smuleac, D.A. Butterfield, S.K. Sikdar, R.S. Varma, D. Bhattacharyya, *J. Mem. Sci.* 251 (2005) 169.
- [366] D.M. Manohar, K.A. Krishnan, T.S. Anirudhan, *Water Res.* 36 (2002) 1609.
- [367] S.M. Evangelista, E. DeOliveira, G.R. Castro, L.F. Zara, A.G.S. Prado, *Surf. Sci.* 601 (2007) 2194.
- [368] K.P. Lisha, Anshup, T. Pradeep, *Gold Bull.* (Article in press).
- [369] X.-qin Li, W.-xian Zhang, *Langmuir* 22 (2006) 4638.
- [370] Galvanic etching-alloying with silver nanoparticles: Sequestration of toxic heavy metals in drinking water, Anshup, K.P. Lisha, T. Pradeep (submitted for publication).
- [371] T. Morris, H. Copeland, E. McLinden, S. Wilson, G. Szulcowski, *Langmuir* 18 (2002) 7261.
- [372] L. Katsikas, M. Gutierrez, A. Henglein, *J. Phys. Chem.* 100 (1996) 11203.
- [373] J.A. Creighton, D.G.J. Eadon, *Chem. Soc., Faraday Trans.* 87 (1991) 3881.
- [374] A. Henglein, C. Brancewicz, *Chem. Mater.* 9 (1997) 2164.
- [375] L. Li, Y.-J. Zhu, *J. Colloid Interf. Sci.* 303 (2006) 415.
- [376] J. Chen, B. Wiley, J. McLellan, Y. Xiong, Z.-Y. Li, Y. Xia, *Nano Lett.* 5 (2005) 2058.
- [377] E.M. Nolan, S.J. Lippard, *Chem. Rev.* 108 (2008) 3443.
- [378] D. Melamed, *Anal. Chim. Act.* 532 (2005) 1.
- [379] M. das Gracas, A. Korn, J.B. de Andrade, D.S. de Jesus, V.A. Lemos, M.L.S.F. Bandeira, W.N.L. dos Santos, M.A. Bezerra, F.A.C. Amorim, A.S. Souza, S.L.C. Ferreira, *Talanta* 69 (2006) 16.
- [380] P.A.M. Boss, S.H. Lieberman, *Appl. Spectro.* 57 (2003) 1129.
- [381] J.J. Storhoff, A.A. Lazarides, R.C. Mucic, C.A. Mirkin, R.L. Letsinger, G.C. Schatz, *J. Am. Chem. Soc.* 122 (2000) 4640.
- [382] C.M. Niemeyer, *Angew. Chem. Int. Ed.* 40 (2001) 4128.
- [383] T. Pradeep et al. (Unpublished).
- [384] Y. Lu, J. Liu, *Acc. Chem. Res.* 40 (2007) 315.
- [385] A. Ono, H. Togashi, *Angew. Chem. Int. Ed.* 43 (2004) 4300.
- [386] J.-S. Lee, M.S. Han, C.A. Mirkin, *Angew. Chem. Int. Ed.* 46 (2007) 4093.
- [387] J.-S. Lee, C.A. Mirkin, *Anal. Chem.* 80 (2008) 6805.
- [388] J. Liu, Y. Lu, *J. Am. Chem. Soc.* 125 (2003) 6642.
- [389] J. Liu, Y. Lu, *J. Am. Chem. Soc.* 126 (2004) 12298.
- [390] J. Liu, Y. Lu, *J. Am. Chem. Soc.* 127 (2005) 12677.
- [391] Z. Wang, J.H. Lee, Y. Lu, *Adv. Mater.* 20 (2008) 3263.
- [392] J.M. Slocik, J.S. Zabinski Jr., D.M. Phillips, R.R. Naik, *Small* 4 (2008) 548.
- [393] S. Si, M. Raula, T.K. Paira, T.K. Mandal, *ChemPhysChem* 9 (2008) 1578.
- [394] B. Cuenoud, J.W. Szostak, *Nature* 375 (1995) 611.
- [395] S.W. Santoro, G.F. Joyce, K. Sakthivel, S. Gramatikova, C.F. Barbas III, *J. Am. Chem. Soc.* 122 (2000) 2433.
- [396] K. Yoosaf, B.I. Ipe, C.H. Suresh, K.G. Thomas, *J. Phys. Chem. C* 111 (2007) 12839.
- [397] N. Shao, J.Y. Jin, S.M. Cheung, R.H. Yang, W.H. Chan, T. Mo, *Angew. Chem. Int. Ed.* 45 (2006) 4948.
- [398] Y. Kim, R.C. Johnson, J.T. Hupp, *Nano Lett.* 1 (2001) 165.
- [399] M. Rex, F.E. Hernandez, A.D. Campiglia, *Anal. Chem.* 78 (2006) 445.
- [400] C.-J. Yu, W.-L. Tseng, *Langmuir* 24 (2008) 12717.
- [401] C.-C. Huang, H.-T. Chang, *Chem. Commun.* (2007) 1215.
- [402] C.-C. Huang, Z. Yang, K.-H. Lee, H.-T. Chang, *Angew. Chem. Int. Ed.* 46 (2007) 6824.
- [403] G.K. Darbha, A.K. Singh, U.S. Rai, E. Yu, H. Yu, P.C. Ray, *J. Am. Chem. Soc.* 130 (2008) 8038.
- [404] A. Campion, P. Kambhampati, *Chem. Soc. Rev.* 27 (1998) 241.
- [405] A.M. Michaels, J. Jiang, L. Brus, *J. Phys. Chem. B* 104 (2000) 11965.
- [406] H. Wang, Y. Wang, J. Jin, R. Yang, *Anal. Chem.* 80 (2008) 9021.
- [407] H. Li, L. Rothberg, *Proc. Natl. Acad. Sci. U. S. A.* 101 (2004) 14036.
- [408] X. Xue, F. Wang, X. Liu, *J. Am. Chem. Soc.* 130 (2008) 3244.
- [409] V.M. Zamarion, R.A. Timm, K. Araki, H.E. Toma, *Inorg. Chem.* 47 (2008) 2934.
- [410] S. Tan, M. Erol, S. Sukhishvili, H. Du, *Langmuir* 24 (2008) 4765.
- [411] P. Jain, T. Pradeep, *Biotechnol. Bioengin.* 90 (2005) 59.
- [412] V. Sambhy, M.M. MacBride, B.R. Peterson, A. Sen, *J. Am. Chem. Soc.* 128 (2006) 9798.
- [413] I. Sondi, B.S. Sondi, *J. Colloid Interf. Sci.* 275 (2004) 177.
- [414] C. Aymonier, U. Schlotterbeck, L. Antonietti, P. Zacharias, R. Thomann, J.C. Tiller, S. Mecking, *Chem. Commun.* (2002) 3018.
- [415] T.J. Berger, J.A. Spadaro, S.E. Chapin, R.O. Becker, *Antimicrob. Agent. Chemother.* 9 (1976) 357.
- [416] Y. Lia, P. Leung, L. Yao, Q.W. Song, E. Newton, *J. Hosp. Infect.* 62 (2006) 58.
- [417] S.T. Dubas, P. Kumlangduksana, P. Potiyaraj, *Colloid. Surface. A Physicochem. Eng. Aspect.* 289 (2006) 105.
- [418] T. Maneerung, S. Tokura, R. Rujiravanit, *Carbohydr. Polymer.* 72 (2008) 43.
- [419] S. Silver, *FEMS Microbiol. Rev.* 27 (2003) 341.
- [420] S. Silver, L.T. Phung, G. Silver, *J. Ind. Microbiol. Biotechnol.* 33 (2006) 627.
- [421] J.L. Clement, P.S. Jarrett, *Metal-Based Drugs* 1 (1994) 467.
- [422] A.L. Neal, *Ecotoxicology* 17 (2008) 362.
- [423] M. Rai, A. Yadav, A. Gade, *Biotechnol. Adv.* 27 (2009) 76.
- [424] V.K. Sharma, R.A. Yngard, Y. Lin, *Adv. Colloid Interface Sci.* 145 (2009) 83.
- [425] J.R. Morones, J.L. Elechiguerra, A. Camacho, K. Holt, J.B. Kouri, J.T. Ramirez, M.J. Yacaman, *Nanotechnology* 16 (2005) 2346.
- [426] S. Pal, Y.K. Tak, J.M. Song, *Appl. Environ. Microbiol.* 73 (2007) 1712.
- [427] C.-N. Lok, C.-M. Ho, R. Chen, Q.-Y. He, W.-Y. Yu, H. Sun, P.K.-H. Tam, J.-F. Chiu, C.-M. Che, *J. Biol. Inorg. Chem.* 12 (2007) 527.
- [428] J.L. Elechiguerra, J. L. Burt, J.R. Morones, A.C. Bragado, X. Gao, H.H. Lara, M.J. Yacaman, *J. Nanobiotechnol.* 3 (2005) 6.
- [429] L. Nover, K.D. Scharf, D. Neuman, *Mol. Cell. Biol.* 3 (1983) 1648.
- [430] Q.L. Feng, J. Wu, G.Q. Chen, F.Z. Cui, T.N. Kim, J.O. Kim, *J. Biomed. Mater. Res.* 52 (2000) 662.
- [431] A.L. Lehninger, D.L. Nelson, M.M. Cox, *Principles of biochemistry*, Worth, New York, 1993.
- [432] S.Y. Liu, D.C. Read, W.J. Pugh, J.R. Furr, A.D. Russell, *Lett. Appl. Microbiol.* 25 (1997) 279.
- [433] T. Hamouda, J.R. Baker Jr., *J. Appl. Microbiol.* 89 (2000) 397.
- [434] I.E. Wachs, R.J. Madix, *Surf. Sci.* 76 (1978) 531.
- [435] R.I. Davies, S.F. Etris, *Catal. Today* 36 (1997) 107.

- [436] H. Nikaido, M. Vaara, *Microbiol. Rev.* 49 (1985) 1.  
 [437] M. Vaara, *Microbiol. Rev.* 56 (1992) 395.  
 [438] S.K. Gorgoi, P. Gopinanth, A. Paul, A. Ramesh, S.S. Ghosh, A. Chattopadhyay, *Langmuir* 22 (2006) 9322.  
 [439] Q. Chang, L. Yan, M. Chen, H. He, J. Qu, *Langmuir* 23 (2007) 11197.  
 [440] V.R. Rajeev Kumar, T. Pradeep, *J. Mater. Chem.* 16 (2006) 837.  
 [441] A. Kumar, P.K. Vemula, P.M. Ajayan, G. John, *Nat. Mater.* 7 (2008) 236.  
 [442] V.V. Tarabara, in: N. Savage, M. Diallo, J. Duncan, A. Street, R. Sustich (Eds.), *Nanotechnology Applications for Clean Water*, William Andrew Publication, USA, 2009.  
 [443] Z. Li, H. Huang, T. Shang, F. Yang, W. Zheng, C. Wang, S.K. Manohar, *Nanotechnology* 17 (2006) 917.  
 [444] W.L. Chou, D.G. Yu, M.C. Yang, *Polym. Advan. Technol.* 16 (2005) 600.  
 [445] W.K. Son, J.H. Youk, T.S. Lee, W.H. Park, *Macromol. Rapid Commun.* 25 (2004) 1632.  
 [446] K. Zdrow, L. Brunet, S. Mahendra, D. Li, A. Zhang, Q. Li, P.J.J. Alvarez, *Water Res. Res.* 43 (2009) 715.  
 [447] K. Jayaraman, *Chem. World* 4 (2007).  
 [448] T.M. Benn, P. Westerhoff, *Environ. Sci. Technol.* 42 (2008) 7025.  
 [449] C.T. Yavuz, J.T. Mayo, W.W. Yu, A. Prakash, J.C. Falkner, S. Yean, L. Cong, H.J. Shipley, A. Kan, M. Tomson, D. Natelson, V.L. Colvin, *Science* 316 (2006) 964.  
 [450] Y.-C. Chang, D.H. Chen, *J. Colloid Interf. Sci.* 283 (2005) 446.  
 [451] W. Yantasee, C.L. Warner, T. Sangvanich, R.S. Addleman, T.G. Carter, R.J. Wiacek, G.E. Fryxell, C. Timchalk, M.G. Warner, *Environ. Sci. Technol.* 41 (2007) 5114.  
 [452] M.S. Mauter, M. Elimelech, *Environ. Sci. Technol.* 42 (2008) 5843.  
 [453] E. Dujardin, T.W. Ebbesen, H. Hiura, K. Tanigaki, *Science* 265 (1994) 1850.  
 [454] K.K.S. Lau, J. Bico, K.B.K. Teo, M. Chhowalla, G.A.J. Amaratunga, W.I. Milne, G.H. McKinley, K.K. Gleason, *Nano Lett.* 3 (2003) 1701.  
 [455] M. Majumder, N. Chopra, R. Andrews, B.J. Hinds, *Nature* 438 (2005) 44.  
 [456] G. Hummer, J.C. Rasaih, J.P. Noworyta, *Nature* 414 (2001) 188.  
 [457] Z. Wang, L. Ci, L. Chen, S. Nayak, P.M. Ajayan, N. Koratkar, *Nano Lett.* 7 (2007) 697.  
 [458] A. Srivastava, O.N. Srivastava, S. Talapatra, R. Vajtai, P.M. Ajayan, *Nat. Mater.* 3 (2004) 610.  
 [459] N.M. Nagy, J. Konya, M. Beszed, I. Beszed, E. Kalman, Zs. Keresztes, K. Papp, I. Cserny, *J. Colloid Interface Sci.* 263 (2003) 13.  
 [460] A. Fujishima, T.N. Rao, D.A. Tryk, *J. Photochem. Photobiol. C Photochem. Rev.* 1 (2000) 1.  
 [461] B.K. Hordern, *Adv. Colloid Interface Sci.* 110 (2004) 19.  
 [462] F. Tepper, *Filtr. Sep.* 39 (2002) 16.  
 [463] X.B. Ke, H.Y. Zhu, X.P. Gao, J.W. Liu, Z.F. Zheng, *Adv. Mater.* 19 (2007) 785.  
 [464] X.B. Ke, Z.F. Zheng, H.W. Liu, H.Y. Zhu, X.P. Gao, L.X. Zhang, N.P. Xu, H. Wang, H.J. Zhao, J. Shi, K.R. Ratinac, *J. Phys. Chem. B* 112 (2008) 5000.  
 [465] M.K. Paknikar, *PCT Application No. WO/2005/120173*, 12 May 2005.  
 [466] T. Pradeep, P. Jain, *Indian Patent No. 20070608*.  
 [467] Anti-microbial compositions and methods of making and using the same, B. Kepner, E. Mintz, *PCT application*, WO 2006/050477.  
 [468] D.J. Kim, *European Patent No. EP20070005960*, 22 Mar. 2007.  
 [469] B. Dubertret, M. Calame, A. Libchaber, *PCT Application No. WO/2002/18951*, 29 Aug. 2001.  
 [470] F.E. Hernandez, A. Campiglia, *US Patent No. 20080081376*, 22 Aug. 2007.  
 [471] Y. Hirata, Y. Ueda, H. Takase, K. Suzuki, *PCT Application No. WO/2002/068342*, 26 Feb. 2002.  
 [472] A.D. Maynard, R.J. Aitken, T. Butz, V. Colvin, K. Donaldson, G. Oberdörster, M.A. Philbert, J. Ryan, A. Seaton, V. Stone, S.S. Tinkle, L. Tran, L.J. Walker, D.B. Warheit, *Nature* 444 (2006) 267.  
 [473] C.M. Goodman, C.D. McCusker, T. Yilmaz, V.M. Rotello, *Bioconjugate Chem.* 15 (2004) 897.  
 [474] F.F. Larese, F. D'Agostin, M. Crosera, G. Adami, N. Renzi, M. Bovenzi, G. Maina, *Toxicology* 255 (2009) 33.  
 [475] C.A. Poland, R. Duffin, I. Kinloch, A. Maynard, W.A.H. Wallace, A. Seaton, V. Stone, S. Brown, W. MacNee, K. Donaldson, *Nat. Nanotech.* 3 (2008) 423.  
 [476] A. Takagi, A. Hirose, T. Nishimura, N. Fukumori, A. Ogata, N. Ohashi, S. Kitajima, J. Kanno, *J. Toxicol. Sci.* 33 (2008) 105.  
 [477] J.E. Hutchison, *ACS Nano* 2 (2008) 395.

<b>EU:</b>	European Union
<b>TCE:</b>	Trichloroethylene, a chlorination byproduct commonly found in water
<b>TTHM:</b>	Total Trihalomethane
<b>FDA:</b>	Food and Drug Administration
<b>RDX:</b>	Research and Development Explosive (1,3,5-Trinitroperhydro-1,3,5-triazine)
<b>NPA:</b>	Asparagine-Proline-Alanine
<b>TDS:</b>	Total Dissolved Solids
<b>VOC:</b>	Volatile Organic Compound
<b>UV:</b>	Ultraviolet
<b>SERS:</b>	Surface-Enhanced Raman Spectroscopy
<b>TEM:</b>	Transmission Electron Microscopy
<b>AOT:</b>	Sodium bis(2-ethylhexyl) sulfosuccinate
<b>EDTA:</b>	Ethylenediaminetetraacetic acid
<b>IR/FTIR:</b>	Infra Red/Fourier Transform Infra Red
<b>NIR:</b>	Near Infra Red
<b>XPS:</b>	X-Ray Photoelectron Spectroscopy
<b>MPC:</b>	Monolayer Protected Cluster
<b>TOAB:</b>	Tetraoctylammonium Bromide
<b>PAMAM:</b>	Polymidoamine
<b>PPI:</b>	Poly(propylene imine)
<b>SANS:</b>	Small Angle Neutron Scattering
<b>AFM:</b>	Atomic Force Microscopy
<b>CTAB:</b>	Cetyl trimethylammonium Bromide
<b>TMAOH:</b>	Tetra-methyl Ammonium Hydroxide
<b>CVD:</b>	Chemical Vapor Deposition
<b>ZVI:</b>	Zerovalent Iron
<b>XRD:</b>	X-ray Diffraction
<b>OPH:</b>	Organophosphorus Hydrolase
<b>AChE:</b>	Acetylcholine Esterase
<b>SEM:</b>	Scanning Electron Microscopy
<b>EDAX:</b>	Energy Dispersive X-Ray Analysis
<b>MCL:</b>	Maximum Contaminant Level
<b>HOMO:</b>	Highest Occupied Molecular Orbital
<b>LUMO:</b>	Lowest Unoccupied Molecular Orbital
<b>LB:</b>	Langmuir-Blodgett
<b>LPS:</b>	lipopolysaccharide
<b>HAADF:</b>	High Angle Annular Dark Field
<b>ZPC:</b>	Zero Point Charge
<b>CNT:</b>	Carbon Nanotube
<b>MWNT:</b>	Multi-walled Nanotube



**T. Pradeep** is a professor of Chemistry at the Indian Institute of Technology, Madras. He received his PhD from the Indian Institute of Science, Bangalore and had post doctoral training at the University of California, Berkeley and Purdue University, Indiana. He held visiting positions in Purdue University, USA; Leiden University, Netherlands; EPFL, Switzerland; Institute of Chemistry, Taiwan; Pohang Institute of Science and Technology, South Korea; Institute of Molecular Science, Okazaki, Japan and Hyogo University, Japan. He has 190 research papers and 12 patents to his credit. He is the author of 'Nano: The Essentials', McGraw-Hill and one of the authors of 'Nanofluids: Science and Technology', Wiley Interscience. He is an elected fellow of the Indian Academy of Sciences. One of the dreams of his research group is to develop an affordable all-inclusive drinking water purifier using nanotechnology. For more details please visit, <http://www.dstuns.iitm.ac.in/pradeep-research-group.php>.



**Anshup** holds a B. Tech. degree from IIT Madras and is currently working with Professor T. Pradeep at the DST Unit on Nanoscience, Indian Institute of Technology Madras, Chennai, India. He studies application of nanomaterials in drinking water purification and desalination. He is also part of a team working on the development of nanomaterials-based affordable drinking water purifier. He is working with Professor Pradeep to establish InnoNano Research Private Limited, an organization focusing on nanomaterials research for commercial applications.

## List of acronyms and their definitions

<b>USPHS:</b>	United States Public Health Service
<b>USEPA:</b>	United States Environmental Protection Agency
<b>CCL:</b>	Candidate Contaminant List (Published by USEPA)
<b>WHO:</b>	World Health Organization